Transfer of Surface Finish from Roll to Strip in the Temper Rolling of Steel

by

David Alan Stephenson

S.B.M.E., Massachusetts Institute of Technology (1981)

SUBMITTED TO THE DEPARTMENT OF

MECHANICAL ENGINEERING

IN PARTIAL FULFILLMENT OF THE

REQUIREMENTS OF THE

DEGREE OF

MASTER OF SCIENCE IN

MECHANICAL ENGINEERING

at the

MASSACHUSETTS INSTITUTE OF TECHNOLOGY

February 1983

Signature of Author _____
Department of Mechanical Engineering
November 16, 1982

Certified by _____
Dr. Ernest Rabinowicz
Thesis Supervisor

Accepted by _____
Chairman, Department Committee on Theses

TRANSFER OF SURFACE FINISH FROM ROLL TO STRIP IN THE TEMPER ROLLING OF STEEL

by

David Alan Stephenson

Submitted to the Department of Mechanical Engineering on November 17, 1982
in partial fulfillment of the requirement of the
Degree of Master of Science in Mechanical Engineering

ABSTRACT

The transfer of surface finish from roll to strip in the temper rolling of steel was examined from an experimental and theoretical point of view. The transfer process was modeled as an indentation process in which the roughness peaks of the roll are pressed into the strip surface. It was argued that complete roll-strip surface matching can occur only if the surface of the strip flows plastically and molds itself around the roughness peaks of the rolls, and that this strip surface deformation is most easily accomplished in shear, since, due to material constraint considerations like those encountered in the analysis of hardness indentations, the surface asperities of the strip can transmit surprisingly large normal stresses without deforming markedly.

These arguments indicated that transfer efficiency (the degree of roll-strip surface matching) should increase with increasing maximum roll-bite shear stress, and, therefore, with plastic arc length and the slope of the roll-bite pressure distribution. Theoretical considerations thus predicted on increase in transfer efficiency with increasing extension, roll diameter, and strip yield stress and decreasing average tension and strip thickness under otherwise constant conditions. Theoretical arguments additionally indicated that transfer efficiency should increase with increasing mill speed and remain constant with typical variations in roll roughness in dry-temper rolling, and that transfer efficiency should decrease with increasing mill speed and lubricant viscosity in wet-temper rolling. Extensive data supporting all of these predictions was obtained on two laboratory mills. Mechanical and surface transfer data from a production mill was also obtained, and is tabulated in an appendix.

A method of calculating the ratio of final strip to roll roughness from rolling conditions was developed from an analysis of the mechanics of the temper rolling process and tested against a limited amount of data. Measured and calculated transfer values agreed rather well in this comparison; however, extensive material testing is presently required to use this method, and further development is required before it can be applied to practical situations.

Thesis supervisor: Dr. Ernest Rabinowicz

Title: Professor of Mechanical Engineering

Acknowledgements

It is a pleasure to acknowledge the assistance of a large number of people in the production of this thesis. This work was supported by the United States Steel Corporation Research Laboratory through its master's degree cooperative education program; thanks are due to many individuals at U. S. Steel Research, including R. J. Bentz and E. J. Patula, whose advice, supervision, encouragement, and wealth of contacts were invaluable, W. G. Miller and P. A. Shearer, who operated the laboratory mills through many early tests, T. G. Nilan, who advised the author on surface metrology and commercial temper-rolling practice, H. M. Alworth and G. F. Carpenter, who provided valuable advice on heat treatment and annealing, J. I. Tokar, who patiently typed the manuscript, and especially to J. K. Slagle, who operated the mills during the bulk of the experiments, and to W. L. Roberts, with whom the author had many long and fruitful discussions on rolling theory.

The author would also like to express thanks to several individuals at U. S. Steel Irvin Works, particularly to F. J. McMaster and L. E. Chopp, who arranged production trials on Irvin's No. 7 temper mill, and also to M. J. Murcek, who arranged for the heat treatment of laboratory coils in Irvin's batch annealing furnaces.

Finally, the author wishes to thank Professor Ernest Rabinowicz of M.I.T. for his guidance and encouragement in this project, and for his sustained interest in and contributions to the author's technical education.

CONTENTS

I INTRODUCTION

I.1 Motivation

No solid surface is infinitely smooth; on a microscopic scale, all consist of a series of asperities and depressions superimposed on the macroscopic contours of the substrate. The distribution of these irregularities, both spacially and in size and shape, constitutes the finish of the surface in question. Surface finish is important from an engineering point of view because it affects the visual appearance of an object, and because it can influence machining tolerances and lubrication and friction in forming operations. For these reasons, surface textures have been studied widely since the advent of modern machine tools for the mass production of interchangeable parts, and quantitative measures of surface finish have been developed to allow designers and manufacturers to specify desired surface properties for both finished products and incoming raw materials.

This thesis explores the mechanics of producing steel sheet with surface properties suitable for exposed, painted applications. Large amounts of such sheet are used in the automotive and appliance industries for the manufacture of items such as (for example) car hoods and refrigerator doors; its surface texture must, therefore, be adequate for both painting and press-forming. The surface properties required for these operations, though not entirely mutually exclusive, are different enough for compromise to be necessary.[1)]* For painting, a smooth, uniform, and a kneaded or

*See References.

porous surface is required for an acceptable final appearance; for press-forming, on the other hand, a rougher surface is necessary to insure proper lubrication and, thus, prevention of buckling, breakage, and die galling.[2,3,4] The roughness asperities must consequently have a high density per unit surface area and an average height within specified upper and lower bounds. One large automaker, for example, currently requires an average roughness height between 20 and 50 microinches, and a minimum 50-microinch peak count (a measure of peak density) of 5.3 times the roughness height minus 104, for Class I autobody sheet. These standards are changed periodically, and are generally growing more stringent with the increasing use of thinner, water-base paint systems, which require a lower average roughness height for acceptable appearance than traditional hydrocarbon-base paints.[5]

The general trend toward more restrictive sheet-surface requirements has been accompanied by increasing complexity in the methods employed to produce these surfaces. Surface finish is imparted to steel sheet by temper rolling, a processing step in which annealed stock is given a light rolling reduction using specially textured work rolls. Temper mills have traditionally been operated without rolling lubricants; the high friction produced by dry contact simplifies the control of the reduction given (e.g., reduction increases comparatively slow with increasing roll force), and with no lubricant to be removed, the temper-rolled product can be shipped to the customer without an additional cleaning

step.[6] "Dry" temper mills, however, tend to generate metallic dust by abrasion of the work rolls and strip; over a period of time, this dust can build up in the mill and eventually fall between the rolls and strip, causing a decrease in both roll life and product quality. For this reason, there has been an increasing trend toward commercial "wet" temper rolling in recent years. The rolling solutions used in wet-temper mills are generally poor from the standpoint of lubrication; they consist basically of dilute aqueous solutions of detergents and are intended, primarily, to keep the mill relatively free of dust without leaving a substantial residual film on the finished sheet.[6] Nonetheless, they do have a noticealbe effect on the mechanics of the process[7] and particularly on the relation between the roll texture used and final strip texture produced.[5,8] This can present the wet-temper mill operator, whose understanding of this relation is derived largely from experience in dry-temper rolling, with serious problems in producing sheet of acceptable surface quality.

In view of the increasing importance of consistently controlling the surface texture of cold-rolled steel sheet, an increased understanding of the mechanisms involved in transferring surface finish from work roll to strip in wet- and dry-temper rolling would be of some interest. This document examines these mechanisms from a theoretical and experimental point of view.

II.2 Measurement of Surface Finish

Surface finish was discussed in very subjective

terms in Section I.1, and, in fact, some of the properties which it influences and for which it is studied (such as visual or as-painted appearance) are themselves rather subjective and aesthetic. A meaningful, scientific investigation of the subject, however, requires well-defined, reasonably objective, and (preferably) quantitative measures of surface texture. In this section, the measures currently accepted by virtually all sheet producers, consumers, and researchers are defined and briefly discussed.

A variety of methods exist for the evaluation of surface topography and quality; these include taper sectioning, adsorption, and numerous optical techniques.[9] As a class, however, these methods are time consuming and painstaking. In situations in which a large number of surfaces must be measured and compared routinely, surface finish is virtually always evaluated by profilometry. This method employs a device called a profile meter, which consists of a very hard, blunt stylus (quite similar to a phonograph needle), a motor to draw the stylus across the surface, and electronic circuity to record the stylus' motions during its traverse. The profile meter produces an amplified cross section of a surface from which parameters indicative of surface character can be deduced, or (more commonly) automatically calculated values of these parameters alone.

The parameters most commonly used to characterize surface topography are best defined with reference to a typical surface profile, as, for example, that shown in Figure 1.1. The most common (and perhaps most natural and

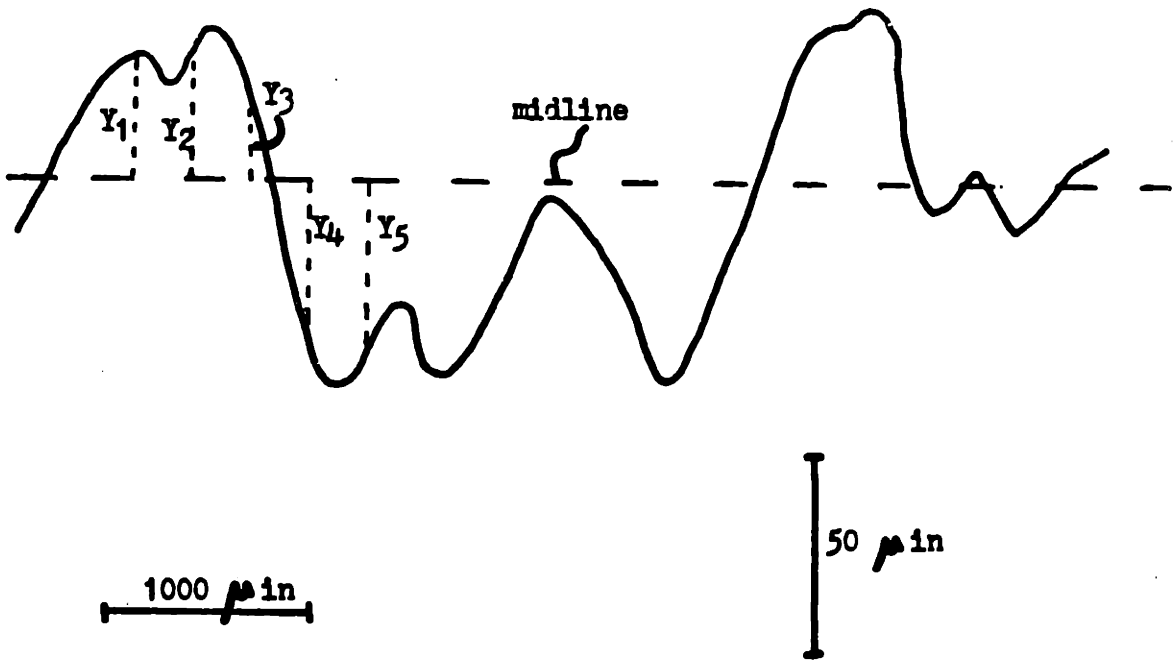

Fig. 1.1 Typical surface profile from a profile meter

obvious) parameter extracted from a surface profile is the arithmetic average roughness peak height, or (more compactly) the average roughness. This is the deviation in height from an electronically determined centerline of equally spaced points on a surface:

$$\text{average roughness} = \frac{\sum_{i}^{n} Y_i}{n}$$

The notation for arithmetic-average roughness is R_a, usually given in millimeters or microinches. For example, an arithmetic average roughness of 11 microinches is written 11 μin.R_a. A second parameter frequently inferred from surface profiles is the peak count. This is a measure of peak density, defined as the number of peaks encountered by the stylus per unit length of its traverse. The value of this parameter, of course, depends on what is regarded as a peak. Two definitions are now in common use. One (used in Surfaccount units and similar instruments) defines a peak as two changes in elevation of opposite sign of magnitude greater than some minimum cutoff; in the second (used in Profilometer-type devices), a peak is defined as two deviations larger than a preset minimum value above and below an electronically determined centerline. These two definitions are illustrated, and shown to not always give equivalent results for the same surface, in Figure 1.2, adapted from Reference 4. Peak count is usually reported in peaks per inch, abbreviated ppi; a subscript is often added to indicate what minimum peak height was used in counting. For example, a peak count of 150 peaks per inch based on a 50 microinch minimum height is written 150 ppi_{50}.

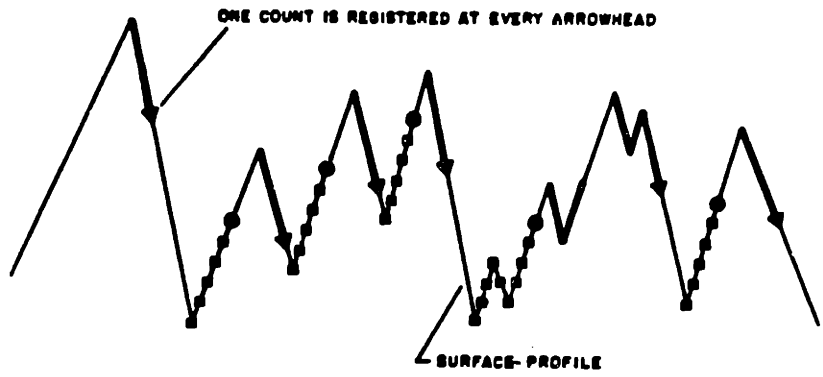

(a)

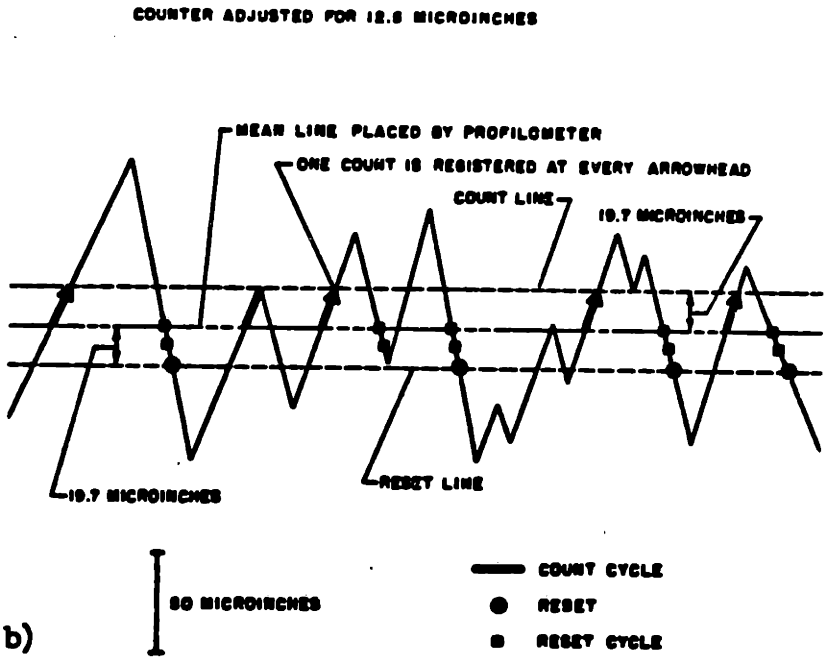

(b)

Fig. 1.2 Peak definitions in current use

(a) Surfacount-type instruments

(b) Profilometer-type instruments

(adapted from reference 4)

A number of other parameters are occasionally computed from surface profiles; Average roughness and peak count, however, are the only parameters for which required ranges are routinely specified by sheet consumers. Profilometry, it should be emphasized, has a number of shortcomings. A very minute fraction of the surface is directly sampled during a stylus trace, which can lead to very misrepresentative characteristics being ascribed to a surface, particularly if (as is frequently the case on the shop floor) only one trace is taken. There is, in fact, some question as to whether a two-dimensional, random array of roughness peaks can ever be adequately characterized by a finite set of numbers. Considerable dissatisfaction exists with current methods of surface characterization,[2,5] and there is every reason to expect that new methods and new parameters will be proposed and accepted in the future to either replace or supplement current techniques. At present, however, average roughness and peak count seem to give a reasonable indication of how a surface will perform in press-working and in the paint shop; and, since they are both easily and quickly measured (with, it might be added, equipment already widely manufactured and in use), they are likely to be with us for some time. In this document, therefore, these parameters will be taken as adequate measures of surface quality for purposes of comparison between two or more surfaces. Because of the minimum peak height used in its definition, however, peak count is a difficult quantity to work with mathematically; consequently, all quantitative expressions developed

will involve only the average roughness.

I.3 Rolling Terminology and Nomenclature

From the point of view of tonnage of material annually produced, rolling is predominant by far among all manufacturing processes. This tremendous economic importance has long made it the subject of extensive research, which has spawned a very large literature. As a natural byproduct of these activities, a very specialized and, to nonspecialists, very confusing rolling terminology has developed. In this section, those portions of rolling terminology that will be extensively used in this document are defined, and, additionally, the corresponding symbols and nomenclature used subsequently in quantitative expressions are listed.

Much of rolling terminology relates to rolling mills themselves, which are generally classed according to the size and arrangement of the rolls they employ. The most common type of roll arrangement for cold rolling is the four high; the overall layout of a typical four-high, single-stand mill is shown in Figure 1.3. In this arrangement, the incoming strip is uncoiled and threaded through an entry bridle and between two work rolls, where deformation occurs; once processed, the strip is threaded through an exit bridle and recoiled. The entry and exit bridles are used primarily to apply tensions to the strip on each side of the mill, which may differ greatly from desired coiling and uncoiling tensions. The work rolls are supported by two larger backup

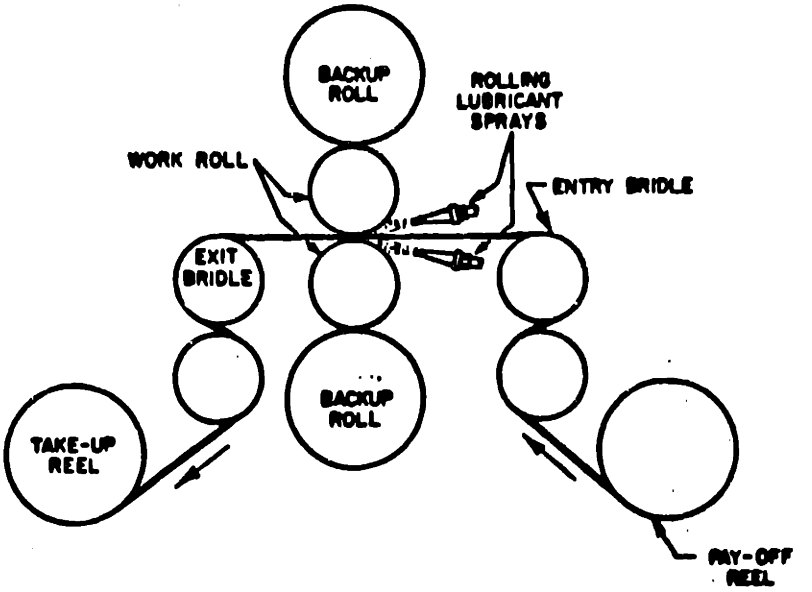

Fig. 1.3 General layout of a single-stand, four-high rolling mill. Arrows indicate direction of strip travel.

(adapted from reference 10)

rolls which add rigidity and give rise to the term "four-high." In most cold mills (though not usually in sheet-temper mills) more than one set of work and backup rolls, or stands, are included between the entry and exit bridle; such tandem mills, in fact, often consist of five or six stands, each contributing to the cummulative deformation imparted to the strip. Sheet-rolling mills are generally referred to by the face width (or axial length) of the work rolls employed, since this determines the maximum width of the sheet they can produce. For example, an 84-inch sheet-temper mill can process sheet up to about 80 inches wide.

The actual zone of deformation between the work rolls is too small to be seen in Figurel.3; a distorted but informative view is given in Figure 1.4. This zone, referred to as the roll bite, is bounded by the entry and exit planes, where deformation begins and ends, and by the arcs of contact between the rolls and strip surfaces. Due to its continuously changing thickness, the surface speed of the strip in the roll bite is continuously changing (ignoring, for now, the possibility of sticking friction); near the entry plane, it is less than the peripheral speed of the rolls, while near the exit plane it is greater than this speed. In principle, the strip surface speed should thus be equal to the peripheral roll speed at some position in the roll bite; this position is designated the neutral point or plane, and serves to divide the roll bite into two parts, the entry and exit regions. As will be seen, the friction force should be acting in opposite directions in these regions, a

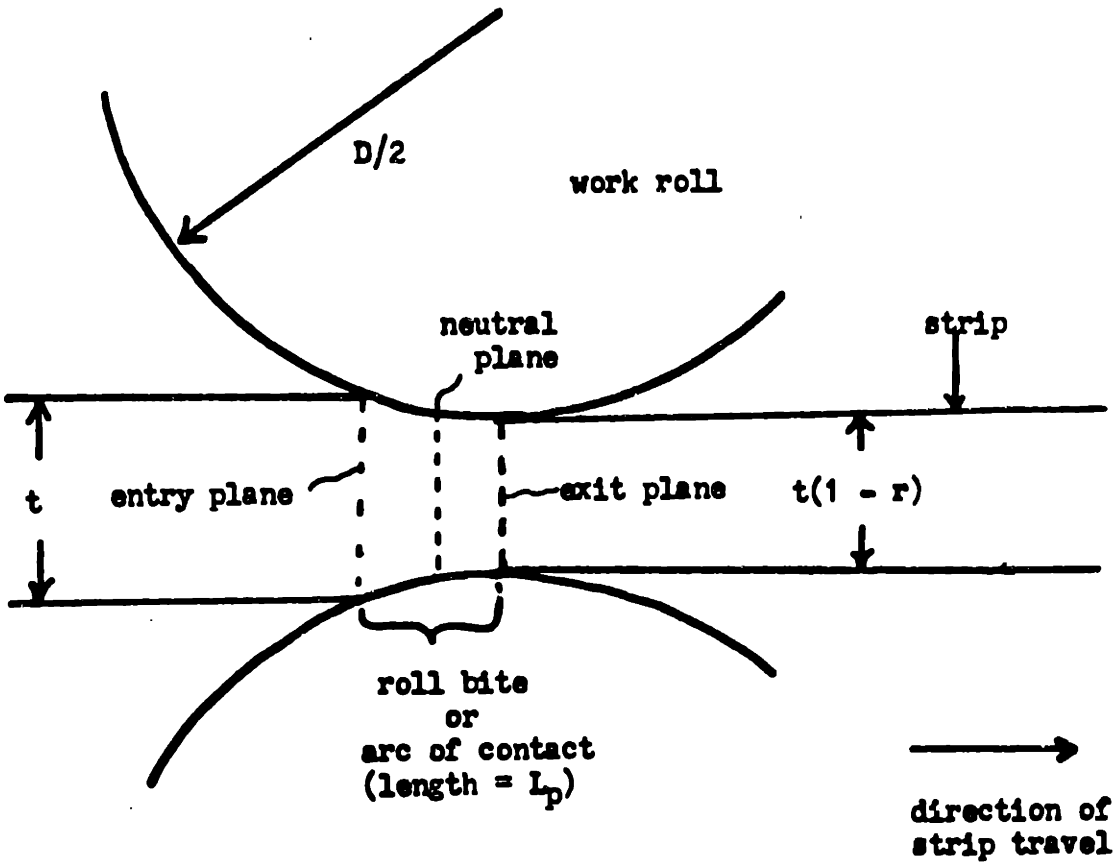

Fig. 1.4 Simplified view of roll bite

fact which greatly complicates the examination of stresses along the arc of contact. In temper rolling, the plastic strain imparted to the strip in the roll bite is often referred to as extension rather than reduction, since in the case of small strains it is easier to measure changes in length (over a large gage length) than changes in thickness. These terms will be used interchangably in this thesis. Not shown in Figure 1.4 are zones of elastic contact between the roll and strip located at the beginning and end of the roll bite.

Several schools of rolling nomenclature have developed as numerous mathematical models of the process have been proposed and refined. The nomenclature used in this thesis is based primarily on that favored by Roberts in his book, "Cold Rolling of Steel." Some of this nomenclature is given in Figure 1.4; a more complete list is given in Table I.1.

Table I.1

Nomenclature

Symbol	Units	Description
A_r, A_a	$Inch^2$	Real and apparent areas of contact
a	None	Constant, $= \frac{2\mu L_p}{rt}$
α	None	Constant between 1 and 2
D	Inches	Work-roll diameter
$\dot{\varepsilon}$	1/seconds	Average strain rate
E	psi	Elastic modulus of rolls
f	lbs/inch	Specific rolling force; force per inch strip width
f_p, f_e	lbs/inch	Plastic and elastic components of f
H	Kg/mm^2	Penetration hardness
h(x)	Inches	Thickness of strip in roll bite
K	None	Factor in arc length equation
L	Inches	Length of the arc of contact
L_s	Inches	Length of sticking zone
L_e, L_p	Inches	Elastic and plastic portions of L
L_N	Kg	Normal load
μ	None	Effective coefficient of sliding friction
n	None	Constant ≥ 1
$P_i(x)$, $p_o(x)$	psi	Normal pressure in entry and exit portions of roll bite

Table I.1 (continued)

r	Percent or decimal fraction	Reduction or extension
ρ_r	μin.R_a	Work-roll roughness
ρ_i , ρ_f	μin.R_a	Initial and final strip roughness
σ_c	psi	Effective average compressive yield strength of strip
$\bar{\sigma}_c$	psi	Average normal pressure in roll bite
σ_s	psi	Interfacial shear stress
σ_Y	psi	Yield stress in uniaxial compression
τ_m, τ_c	inch-lbs/inch	Measured and corrected specific total spindle torque
τ_Y	psi	Yield stress in shear
τ_L	inch-lbs/inch	Torque or bearing loss
T_1, T_2	Pounds	Entry and exit strip tensions
t	inches	Initial strip thickness
t_r	None	Roughness transfer ratio = $\frac{\rho_f}{\rho_r}$
X	Inches	Distance from exit plant (inside roll bite)
X_1, X_2	Inches	Boundaries of sticking zone
X_n	Inches	Position of neutral plane
$Z(X)$	Inches	Elastic roll deformation at point X

II THEORY

II.1 Nature of the Problem

To the author's knowledge, the mechanisms involved in transferring surface finish from roll to strip in temper rolling have never been the primary subject of formal study, despite their economic importance. Peripheral references to these mechanisms in papers on roll preparation and strip quality indicate that they are apparently quite complex, and seem to depend on roll-bite friction and lubricity, roll and strip roughnesses, strip tensions, strip grade, reduction, mill speed, and rolling force.[11,12] Since this list includes, directly or indirectly, virtually every process variable in temper rolling, we must concur that, at first glance, the mechanisms of surface transfer are, indeed, extremely complex.

If, however, we reflect on what is actually being accomplished by these mechanisms, we find that this is rather straightforward. Mill experience has shown that, although the surface properties of a sheet temper rolled under given conditions cannot, a priori, be predicted with any great certainty, it can be said that these properties will depend directly on the texture of the work rolls used; with other conditions held constant, rougher rolls will invariably produce a rougher sheet. This indicates that, not surprisingly, temper rolling involves the pressing or coining of the roll surface into the strip. The degree of coining achieved may depend on rolling conditions in a complicated manner; the

overall process of transferring surface texture can, nonetheless, be viewed as a process of achieving conformity between two surfaces under a given type and geometry of loading. Such problems of surface conformity are encountered in many engineering situations (as, for example, in solid-phase welding and in the calculation of electrical and thermal contact resistances), and extensive experiments have been carried out to determine the degree of conformity achieved as a function of loading for certain simple geometries. The results of these experiments are of little direct value in indicating how specific variables should influence the transfer process in temper rolling, but do give some very clear insights into the nature of the interactions of surfaces under high contact pressures. These insights will be examined in the next section as a preliminary to analyses more specific to temper rolling.

II.2 Conformity of Surfaces Under High Contact Pressures

Figure 2.1 shows a rather familiar microscopic view of two surfaces in contact under a moderate normal load L_N. Note that, because of the finite roughnesses of the surfaces, contact is not continuous across the interface, but is confined to isolated sites. The net area of these sites, the real area of contact A_r, can be estimated by the equation[13)]

$$A_r = \alpha \frac{L_N}{H} \qquad (2.1)$$

where H is the penetration hardness of the softer surface and α is a constant traditionally taken as unity[13)] but possibly closer to 2.[14)] A quantity of interest in the present

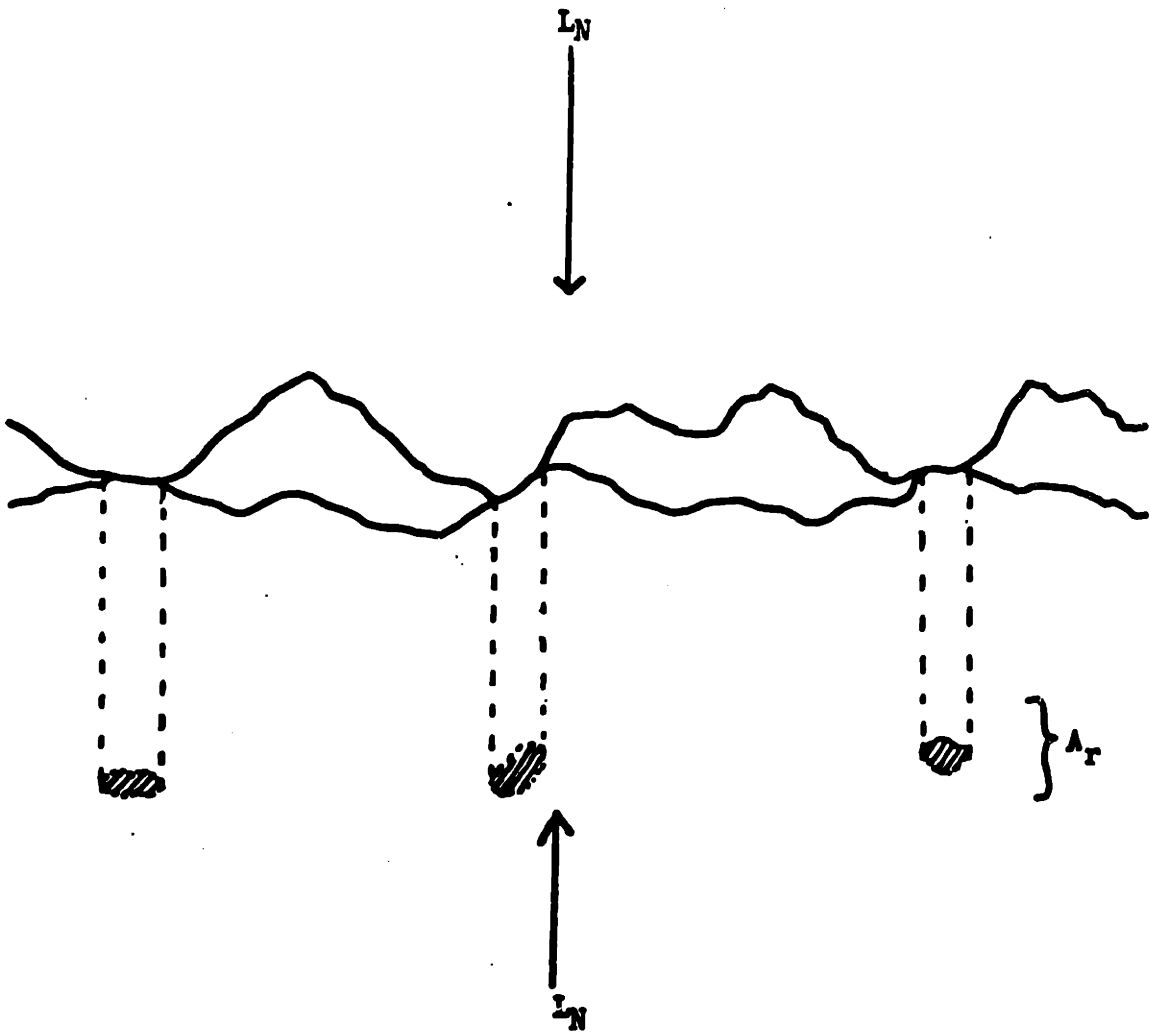

Fig. 2.1 Microscopic view of surfaces in contact under a moderate normal load L_N. Shaded regions are the projected real area of contact.

context is the normal load required for a real area of contact equal to the apparent area of contact, e.g., for complete surface mating. Denoting this load L_{NC} and the apparent area A_a, Equation 2.1 gives

$$\frac{L_{NC}}{A_a} = \frac{H}{\alpha} \qquad (2.2)$$

It is well known that, for most pure metals and alloys (and a large class of nonmetals), hardness is equal to roughly three times the yield stress in uniaxial tension or compression, σ_y.[15] Substituting $H = 3\sigma_y$ into Equation 2.2, and denoting L_{NC}/A_a as the contact pressure σ, we find that the pressure which must be applied to achieve complete conformity falls in the range

$$1.5\sigma_y \leq \sigma \leq 3\sigma_y \qquad (2.3)$$

In the absence of large hydrostatic pressures, the softer body will not support such pressures. We therefore conclude that the two surfaces can never be made to conform completely under most conditions.

The above, well-known analysis is hardly exact, but illustrates a striking property of the surface layers of solids: their ability to transmit surprisingly high normal stresses without deforming markedly. This property was first noted experimentally by Moore,[16] who cut a series of fine grooves in an annealed copper surface and then deformed the specimen with a hard cylindrical indenter. He found that, although he could induce considerable deformation in the bulk of the specimen, he was unable to make the grooves disappear under purely normal loading, no matter how highly he loaded

the indenter. Similar experiments were later conducted by Williamson[17] using an aluminum cylinder embedded in a steel jacket and axially pressed against a hardened steel cylinder. Under these constraints, Williamson found that he could eventually obliterate the roughness peaks of the aluminum surface, but only if extremely high pressures were applied. Figure 2.2, adapted from Williamson's paper, illustrates this point rather graphically. A third set of early experiments in this area were conducted by Greenwood and Rowe.[18] In these tests, aluminum cylinders of varying height-to-diameter ratios with roughened ends were compressed axially against a hard steel cylinder. Relatively tall cylinders, it was found, tended to "barrel" during deformation, producing a dead zone of undeformed material near the surface; in these cases the surface asperities were little changed by the bulk deformation. For shorter, penny-like specimens, however, no barrelling or dead zone developed; plastic deformation extended to the tool-workpiece interface, and the roughness asperities were readily flattened.

Two key concepts are evident from these experiments. The first is that complete conformity (e.g., mating or matching) of two surfaces requires the plastic flow of one surface at the interface. Referring again to Figure 2.1, we can easily see why this is the case. The surfaces pictured will obviously match completely only if the softer one flows plastically into the existing voids and molds itself around the roughness peaks of the harder one. The second concept evident from these experiments is that it is difficult to

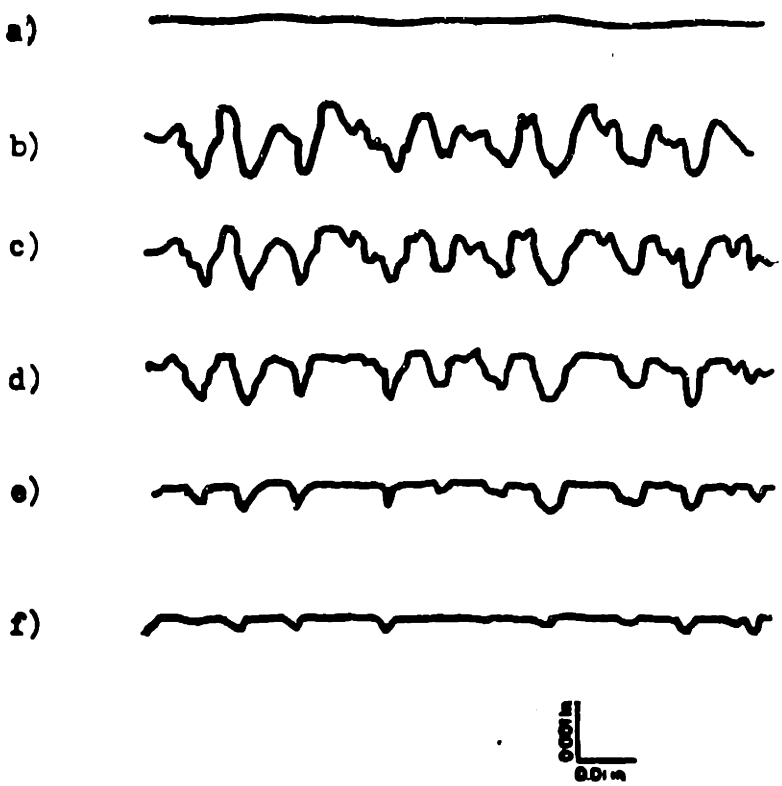

FIGURE 2.2 —Profiles showing progressive deformation of asperities in high pressure experiment. (a) Virgin surface. (b) Bead-blasted to 200μ in. CLA. (c) After loading to 200 lb (1800 psi). (d) After loading to 1000 lb (9000 psi). (e) After loading to 3800 lb (34 200 psi). (f) After loading to 8000 lb (72 000 psi). The pressures stated are the apparent pressures; the real pressure on the contact spots is much greater.

(adapted from paper by Williamson, ref. 17. The yield strength of the surface in uniaxial compression is approximately 9000 psi)

induce the surface deformation necessary for complete conformity through purely normal loading, because roughness asperities are capable of transmitting stresses easily sufficient to initiate yield in subsurface regions without deforming themselves. The reasons why this is true are much less clear. They appear, however, to be related to interactions between adjacent asperities. It has been shown, by simple theoretical arguments[19] and by experiments and slip line solutions,[20] that an array of asperities acting together can support a much greater load than the same number of isolated asperities acting independently. The compression of one asperity, loosely speaking, seems to impose a hydrostatic pressure on its neighbors, increasing their effective yield strengths much in the way that constraint from neighboring material apparently triples the yield stress of a surface during a hardness test indentation[21] (cf. p. 14). Referring once again to Figure 2.1, we see that at very light loads the actual contact sites may be very isolated and act independently, but that at high contact pressures, when A_r/A_a is, say, one-half, adjacent sites are almost certain to influence each other.

The conditions prevailing in the experiments described above differed from temper-rolling conditions in two important ways. First, these experiments were generally conducted using a hard, flat indenter in contact with a rough, soft workpiece. In sheet-temper rolling, the harder surface (the roll) is usually roughened, while the workpiece (strip), although never perfectly smooth, generally has a

lower roughness. Experiments analogous to those described above, however, have been carried out using a roughened tool and a smooth workpiece with virtually identical results;[22,23] it seems likely, therefore, that the qualitative properties of surface interactions deduced from these tests are largely independent of tool and workpiece roughnesses. A more critical difference arises from the loading geometry used in the experiments. For the most part, the results discussed above were obtained under purely normal loading. In temper rolling, however, the strip surface is subjected to significant shear stresses arising form relative slip between the roll and strip. The mechanisms cited to explain the resistance of surface asperities to purely normal deformation, which involve an increase in an asperity's effective yield strength due to hydrostatic pressures exerted by its neighbors, should not be effective for cases in which appreciable shear stresses act on the asperities; hydrostatic pressure increases a material's resistance to deformation in uniaxial compression, but has a negligible effect on its yield strength in pure shear.[24] We would, therefore, not expect surface asperities to resist deformation in shear to the surprising extent that they resist normal deformation. Moore, in fact, found that he could easily flatten the otherwise persistent grooves on his test specimens by introducing relative sliding (e.g., shear stress) between the specimen and indenter.[16] Similar results have been obtained in other indentation tests, and in experiments in cold pressure welding.[25,26,27] This point, although generally

ignored in most papers on the subject, is of great importance when applying indentation test results to practical situations in which significant interfacial sliding occurs. Although it is mentioned apparently only in passing in this discussion, it will serve as one of the more important qualitative considerations motivating further analysis, as will be seen starting with the next section.

II.3 Importance of Reduction in Surface Transfer

The experimental results reviewed in the previous section indicate that the transfer of surface finish in temper rolling is governed by the stresses and corresponding deformation arising at the roll-strip interface. Complete transfer, or complete matching between the roll and strip surfaces, can occur only if the surface layer of the strip flows plastically and molds itself around the roughness peaks of the rolls. The transfer level achieved under given rolling conditions thus depends on both the deformation imparted to the strip and the distribution of this deformation within the strip under these conditions. Because the surface asperities of the strip can transmit surprisingly large normal stresses without significantly deforming themselves, the strip surface deformation necessary for roll-strip surface matching is probably most easily produced by shear stresses (rather than normal stresses) at the roll-strip interface.

These considerations indicate that surface transfer in temper rolling should depend more strongly on reduction than on any other process variable. In the first place,

reduction is a direct measure of the deformation imparted to the strip; an increase in overall strip deformation should increase strip surface deformation, and thus roll-strip surface matching. Moreover, it will be shown (in the next section) that an increase in reduction increases the maximum shear stress occuring at the roll- strip interface; when this stress reaches the yield stress of the strip material in shear, the entire strip surface will flow plastically in shear, leading to complete roll-strip surface matching. Summarizing, the degree to which the final strip and roll surface match should increase gradually with increasing reduction until some critical reduction (which varies with rolling conditions) is reached, above which plastic flow invariably occurs at the strip surface and matching is uniformly complete. For roughness transfer, this qualitative statement can be expressed quantitatively by designating the ratio of final strip to roll roughness t_r and assuming that t_r varies linearly with r up until a cricital reduction R (depending on the rolling conditions) is reached, after which t_r remains constant and equal to unity;

$$t_r = \frac{\rho_f}{\rho_r} = \frac{\rho_i}{\rho_r} + \frac{\rho_r - \rho_i}{\rho_r}\frac{r}{R}, \quad r < R \qquad (2.4)$$

$$t_r = 1 \qquad r \geq R$$

At this point, this equation may appear to have been pulled out of thin air, and, although the overall qualitative behavior of transfer with varying reduction expressed by Equation 2.4 can be readily explained, no theoretical reason

has in fact yet been given to expect a linear relationship between t_r and r. This equation, however, seemed to fit early experimental data rather well (when a suitable vaue of R was used); it was moreover later noticed that some factors which seem to be linearly related to surface conformity on the basis of data from indentation tests, such as average (calculated) roll-bite pressure, increase linearly with reduction in many rolling situations. Equation 2.4 may thus be regarded as an empirical relation that is qualitatively consistent with theoretical reasoning.

At this point, Equation 2.4 is of relatively limited value. It illustrates the two most obvious qualitative trends discussed thusfar——namely that a rougher roll will invariably produce a rougher strip, and that the degree to which roll and strip surfaces match increases with increasing reduction——but is of otherwise dubious utility without an expression for the critical reduction R. This parameter represents the smallest reduction at which, under the given rolling conditions, the maximum shear stress at the roll-strip interface equals or exceeds the yield strength of the strip in shear. A priori, it is not clear how various rolling variables affect this stress, and thus exactly how R varies with rolling conditions. The stresses at the roll-strip interface, however, can be calculated with reasonable effort, provided a number of simplifying assumptions ae made in the analysis. While the expression for R obtained through such an exercise will of course be only as accurate as the assumptions made, it seems reasonable to expect that a relatively

tractable analysis will yield an expression which reflects, at least, the qualitative influences of the various rolling variables on R, and thus on transfer. The next section will therefore be devoted to an analysis of the mechanics of the temper-rolling process. Even with a number of simplifying assumptions, this analysis will be fairly long and complicated, and will apparently take us rather far from the subject of this thesis. It should be borne in mind, however, that the understanding of the interfacial stresses and deformations developed in the course of this digression will be of great value in later considering the effects of various rolling variables on transfer, and, as will be seen in Part III, will lead to quantitative expressions for roughness transfer that agree quite well with experimental data.

II.4 Mechanics of Temper Rolling

II.4.1 Basic Assumptions

Rolling theory is a large subject, and many mathematical models of the rolling process have been published in the last sixty years.[28] Surprisingly, only three (to the author's knowledge) have dealt at any length with the specialized process of temper rolling[29,30,31,32,33]; the small reductions taken and usual lack of applied lubricants make temper rolling mathematically the simplest, although economically not the most important, type of rolling from the point of view of modeling. Existing theories, both of temper rolling and cold rolling in general, have in any event established the validity of a number of frequently made simplifying assumptions. The present analysis will differ from

previous treatments primarily in the frictional assumptions made (of subsection II.4.2). The assumptions made regarding other aspects of the process, which for the most part are in line with most modern treatments of the problem, are listed below.

1) It is assumed that the strip constitutes a continuous medium undergoing homogeneous deformation in compression. It is further assumed that the strip possesses an average effective compressive yield strength, σ_c, that is constant across the roll bite. These assumptions are probably the most questionable made in the entire analysis; temper-rolled sheets are known to yield inhomogeneously,[34,35] and the yield stress of the strip probably varies somewhat across the roll bite, due to variations in strain rate and (possibly) slight work hardening. For cold rolling, however, Bland and Ford have shown that the error arising from an assumption of homogeneous deformation is probably smaller than that associated with specifying the material properties of the strip.[36] Due to the small reductions and comparatively small pressures involved, moreover, any variation in yield stress across the roll bite is likely to be gradual, so that the assumed average yield stress will probably be fairly close to the actual yield stress at most points along the arc of contact.
2) The lateral spread of the strip in roll bite is assumed negligible, so that the process can be

modeled as a plane-strain compression problem. This is probably an excellent approximation, provided the ratio of strip thickness to width is small.

3) The angle of contact between roll and strip is assumed to be small. For the small reductions typical of temepr rolling, this is clearly a valid assumption.

4) The arc of contact between the rolls and strip is assumed to be planar in shape. While this is probably not actually the case, such an assumption greatly simplifies the mathematics of the analysis. Moreover, it has been shown by Keller that, for a fixed arc length, the assumed shape of the arc of contact has little effect on the calculated rolling force.[37] In Subsection II.4.3, pressure distribution equations will be derived for both planar and nonplanar arc shapes and compared to demonstrate this point for the case of temper rolling.

5) Thermal effects are assumed negligible, as are inertial effects arising from the acceleration of the strip in the roll bite.

II.4.2 Frictional Assumptions

Rolling theorists have generally (but not always) assumed that Amonton's law of friction is valid along the arc of contact in rolling, and that the frictional stress σ_s at any point along the roll-strip interface is given by the product of the normal pressure, p, at that point and some effective coefficient of friction, μ. While this is not a

particularly bad assumption for rolling situations in which lubrication is good and the reduction is small, for the case of dry-temper rolling, which requires a fairly large coefficinet of friction, this assumption frequently yields frictional stresses significantly larger than the yield stress ofthe strip in shear, i.e., much larger than can actually occur. Since this analysis is concerned primarily with accurately estimating the stresses (particularly the shear stress) acting at the roll-strip interface, the assumption of a constant friction coefficient will not be made.

A limited amount of theoretical and experimental work has been carried out to determine the relationship between normal pressure and friction stress at contact pressures up to those encountered in metalworking processes.[27,38,39,40] Figure 2.3, taken from Reference 38, shows the pressure-friction relation usually obtained for dry sliding. As can be seen, the nature of this relation changes as normal pressure is increased. At low pressures, Amonton's law holds, and the ratio of friction stress developed to normal pressure applied is constant. As pressure is increased, however, this ratio begins to decrease. When a large enough pressure is applied, the friction stress reaches the yield stress of the softer material in shear; since this is the largest shear stress that can exist at the interface, the friction stress remains constant at this value as pressure is further increased. Since this condition is accompanied by plastic flow of the softer surface in shear, an expression for the critical reduction R in Equation 2.4 can

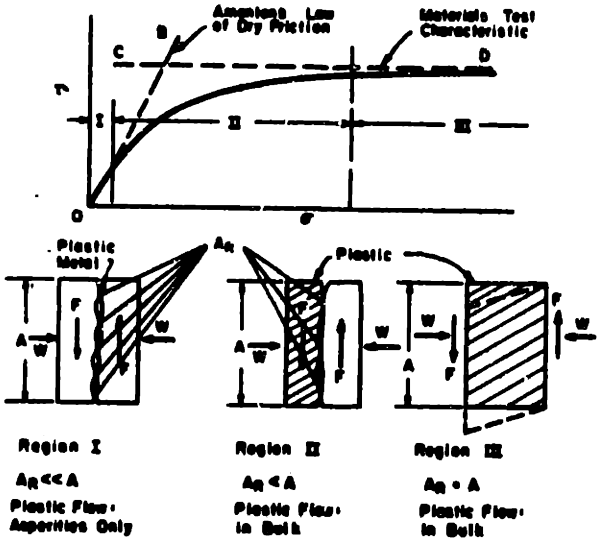

Fig. 2.3 The three regions of solid friction

Variation of frictional shear stress with normal pressure

Region I: low pressure, Amonton's law valid.

Region II: moderate pressure; ratio of friction stress to normal pressure decreases with increasing pressure.

Region III: plastic flow of one surface in shear, or "sticking" friction. Friction stress constant.

(taken from paper by Shaw, Ber, and Mamin, reference 38)

probably be obtained if the criteria for its occurrence in temper rolling can be determined.

From Figure 2.3 and the accompanying experimental data given by Shaw et al.[38] (which is consistent with the data of Wanheim et al.[27,39,40]), the most appropriate quantitative frictional stress-pressure relation would be one in which the frictional stress σ_s approaches the yield stress in shear τ_y asymptotically with increasing pressure p; although these investigators do not postulate an expression, their data seems to fit an equation of the form

$$\sigma_s = \tau_y\left(1 - e^{-\frac{\mu p}{\tau_y}}\right) \tag{2.5}$$

As can be seen, this relation reduces to Amonton's law for small p and gives an asymtotic value of τ_y for σ_s as p becomes infinite. However, such an asympototic friction model does not give a sharp division between regions of elastic and plastic surface stress; i.e., it does not predict the point at which plastic flow in shear will ensue in the softer surface. For this reason, a more approximate friction model, first proposed by Orowan,[41] will be used in this analysis. Figure 2.4, adapted from Reference 40, illustrates the differences between this model and that described above. Quantitatively, Orowan shows that the yield stress in shear is equal to half the compressive yield stress:

$$\tau_y = \sigma_{c/2} \tag{2.6}$$

using this relation, he proposed a friction-pressure relation which assumes Amonton ("slipping") friction until σ_s reaches τ_y, and "sticking" (i.e., constant shear) friction thereafter:

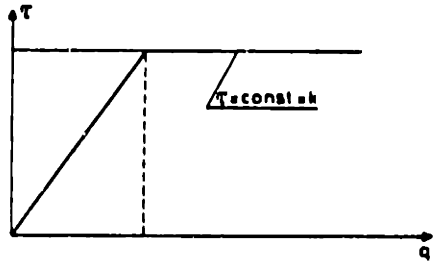

1. Orowan's friction model.

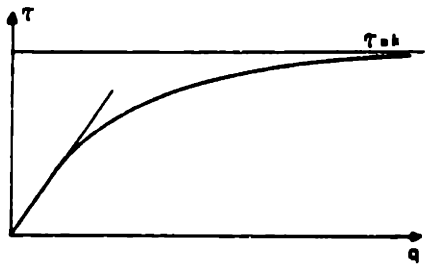

2. Shaw's friction model.

Fig. 2.4 Comparison of Shaw and Orowan friction models.

horizontal axes: normal pressure

vertical axes: friction stress

K is the yield stress of the softer material in shear.

(Adapted from paper by Wanheim, Bay, and Peterson, reference 40)

$$\sigma_s = \mu p \ , \ \mu p \leq \frac{\sigma_c}{2}$$
$$\sigma_s = \frac{\sigma_c}{2} \ , \ \mu p > \frac{\sigma_c}{2} \qquad (2.7)$$

This relation gives a sharp division between regions of elastic and plastic surface stress, which is necessary in the present analysis to obtain an expression for R in Equation 2.4. The available experimental data indicates that such a sharp division probably does not occur in nature; the transition to plastic surface flow is probably a gradual one. However, if an appropriate value of μ is chosen (one corresponding to region II, rather than region I, in Figure 2.3; from the data of Dokos,[42] probably in the range of 0.2 to 0.25 for dry-temper rolling), this model shcuild give reasonable values both of the overal contribution of friction to rolling force and of the pressure required to produce significant plastic surface flow. In the next subsection, this model will be used to calculate the stresses at the roll-strip interface, the reduction required to initiate plastic flow in the strip surface, and the plastic contribution to rolling force in temper rolling.

II.4.3 Interfacial Stresses and Plastic Roll Force

Figure 2.5 shows the roll bite geometry and stress state used in this analysis. Note that the coordinate X is measured from the exit plane, and that two stresses are assumed to act at any point along the roll-strip interface, a normal stress p(X) and a shear stress $\sigma_s(X)$. Since, from Equation 2.7, a knowledge of p(X) is required to calculate

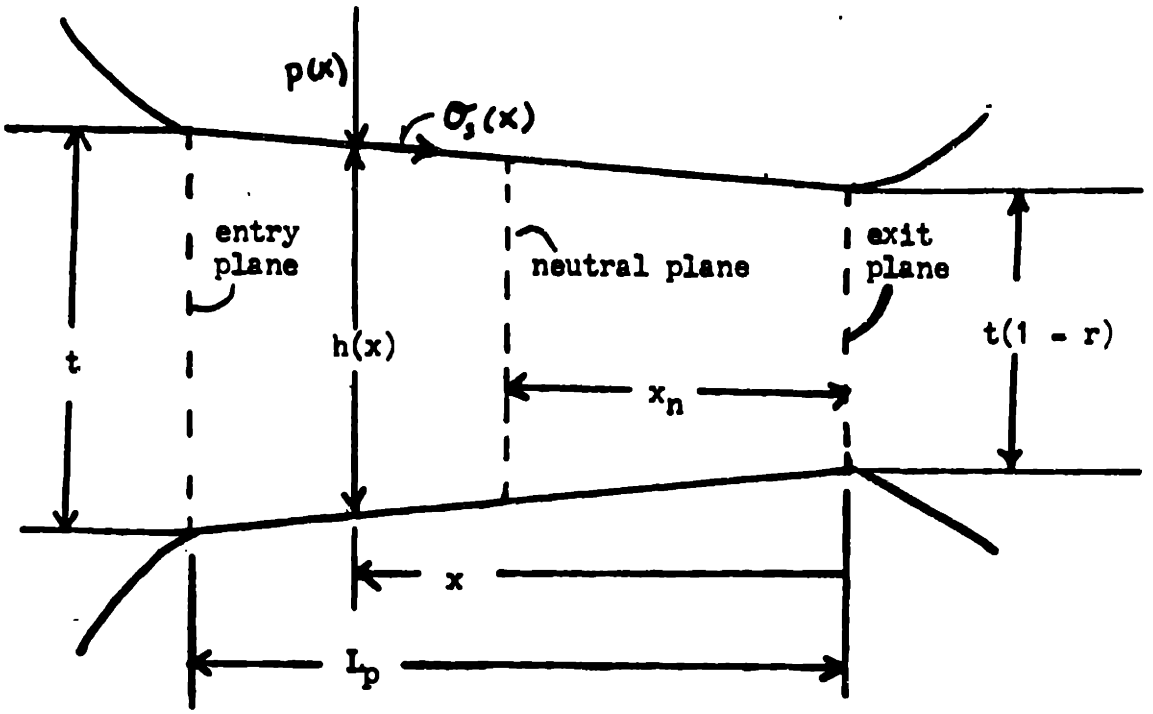

Fig. 2.5 Roll bite geometry and nomenclature used in stress analysis.

$\sigma_s(X)$, we will first consider the distribution of normal pressure along the arc of contact.

A balance of forces on a differential roll-bite element yields a differential equation for the pressure distribution in terms of the compressive yield stress, σ_c, the thickness of the strip, h(X), and the shear stress:

$$\frac{p(X)}{2}\frac{dh(X)}{dx} \mp \sigma_s(X) = \frac{d\left(\frac{h(X)}{2}(p(X)-\sigma c)\right)}{dX} \qquad (2.8)$$

The ambiguous sign of the shear stress term occurs because the friction force acts in opposite directions in the entry and exit zones; the minus sign applies to the entry pressure, while the plus sign applies to the exit zone. This equation is a form of Von Karman's equation, first derived by Von Karman in 1925.[43] Its derivation is now classical; an argument leading to the form quoted above, based on a derivation published by Roberts[44] but employing less restrictive assumptions, is given in Appendix I.

Substituting the assumed combined slipping-sticking friction model, Equation 2.7, into Equation 2.8, gives four differential equations applicable to the four types and/or directions of roll-bite shear stress.

$$p(X)\left(\frac{dh(X)}{dX} \mp 2\mu\right) = \frac{d[h(X)(p(X) - \sigma_c)]}{dX} \quad \text{(slipping friction)}$$

$$p(X)\frac{dh(X)}{dX} \mp \sigma_c = \frac{d[h(X)(p(X)) - \sigma_c]}{dX} \quad \text{(sticking friction)} \qquad (2.9)$$

if the arc of contact is assummed planar,

$$h(X) = t\left(1 - r + \frac{X r}{L_p}\right) \qquad (2.10)$$

these equations reduce to (with $\frac{d\sigma_c}{dx} = 0$)

$$\frac{dp(X)}{dX} \pm \frac{2\mu}{h(X)}\, p(X) = \frac{\sigma_c rt}{L_p h(X)} \qquad \text{(slipping friction)}$$

$$\frac{dp}{dX} = \frac{\sigma_c}{h(X)}\left[\frac{tr}{L_p} \mp 1\right] \qquad \text{(sticking friction)} \tag{2.11}$$

These are all first-order differential equations, and thus solvable (exactly for a planar arc) by standard methods.[45] For the case of slipping friction, the solution of Equation 2.11 yields the result

$$p_i(X) = \sigma_c\left[\frac{1}{a} + \left(1 - \frac{1}{a}\right)\left(\frac{t}{h(X)}\right)^a\right] \qquad \text{(entry region)}$$

$$p_o(X) = \sigma_c\left[\left(1 + \frac{1}{a}\right)\left(\frac{h(X)}{t(1-r)}\right)^a - \frac{1}{a}\right] \qquad \text{(exit region)} \tag{2.12}$$

where $a = 2\mu L_p/(rt)$ and the boundary conditions $p_i(L_p) = p_o(0) = \sigma_c$ have been used. The derivation of Equation 2.12 is given in Appendix I. To check the validity of assumption 4 of subseccion 2.4.1, the derivation and solution of an equation corresponding to Equation 2.9 for a nonplanar arc shape of the form

$$h(X) = t\left[1 - r + \left(\frac{X}{L_p}\right)^n r\right] \tag{2.13}$$

where n is arbitrary (but greater than or equal to unity), is also given in Appendix I. The resulting solution is approximate and involves slowly convergent infinite series:

$$p_i(X) = \sigma_c\left\{nr(1+r)\left[\left(\frac{X}{L_p}\right)^n S_1(bX) - S_1(bL_p)\right] + e^{b(L_p - X)}\right\} \qquad \text{(entry region)}$$

$$p_o(X) = \sigma_c e^{bX}\left[1 + nr(1+r)\left(\frac{X}{L_p}\right)^n S_2(bX)\right] \qquad \text{(exit region)} \tag{2.14}$$

where $b = \frac{2\mu(1 + r)}{t}$

$$S_1(bX) = \sum_{k=0}^{\infty} \frac{(bX)^k}{k!(n + k)}$$

$$S_2(bX) = \sum_{k=0}^{\infty} \frac{(-bX)^k}{k!(n + k)}$$

and, again, the boundary conditions $P_i(L_p) = P_o(0) = \sigma_c$ have been used. As asserted in subsection II.4.1, the influence of the shape factor n on these expressions is negligible; if the terms involving n are neglected, in fact, Equation 2.14 reduces to Roberts' approximate temper-rolling pressure distribution.[29,30] Pressure distributions calculated from Equations 2.12 and 2.14 (for values of n of 1, to check the accuracy of the approximations made, 1.5 and 2) are plotted in Figure 2.6 for typical laboratory conditions (specimen 20 of Table III.8, $\mu = 0.24$) to demonstrate that the assumed shape of the arc of contact has little effect on the calculated pressure distribution for a fixed arc length.

Two points of interest are easily calculated from Equation 2.12: the points in the entry and exit regions where the interfacial shear stress (as calculated from Equation 2.7) reaches $\sigma_c/2$. Designating these points X_1 and X_2 respectively, by definition $p_i(X_1) = p_o(X_2) = \sigma_c/2\mu$, which yields

$$\frac{X_1}{L_p} = \frac{1}{r}\left\{ r - 1 + \left[\left(\frac{1}{1 - \frac{1}{a}}\right)\left(\frac{1}{2\mu} - \frac{1}{a}\right)\right]^{-\frac{1}{a}}\right\}$$

$$\frac{X_2}{L_r} = \frac{1}{r}\left\{ r - 1 + (1 - r)\left[\left(\frac{1}{1 + \frac{1}{a}}\right)\left(\frac{1}{2\mu} + \frac{1}{a}\right)\right]^{\frac{1}{a}}\right\} \qquad (2.15)$$

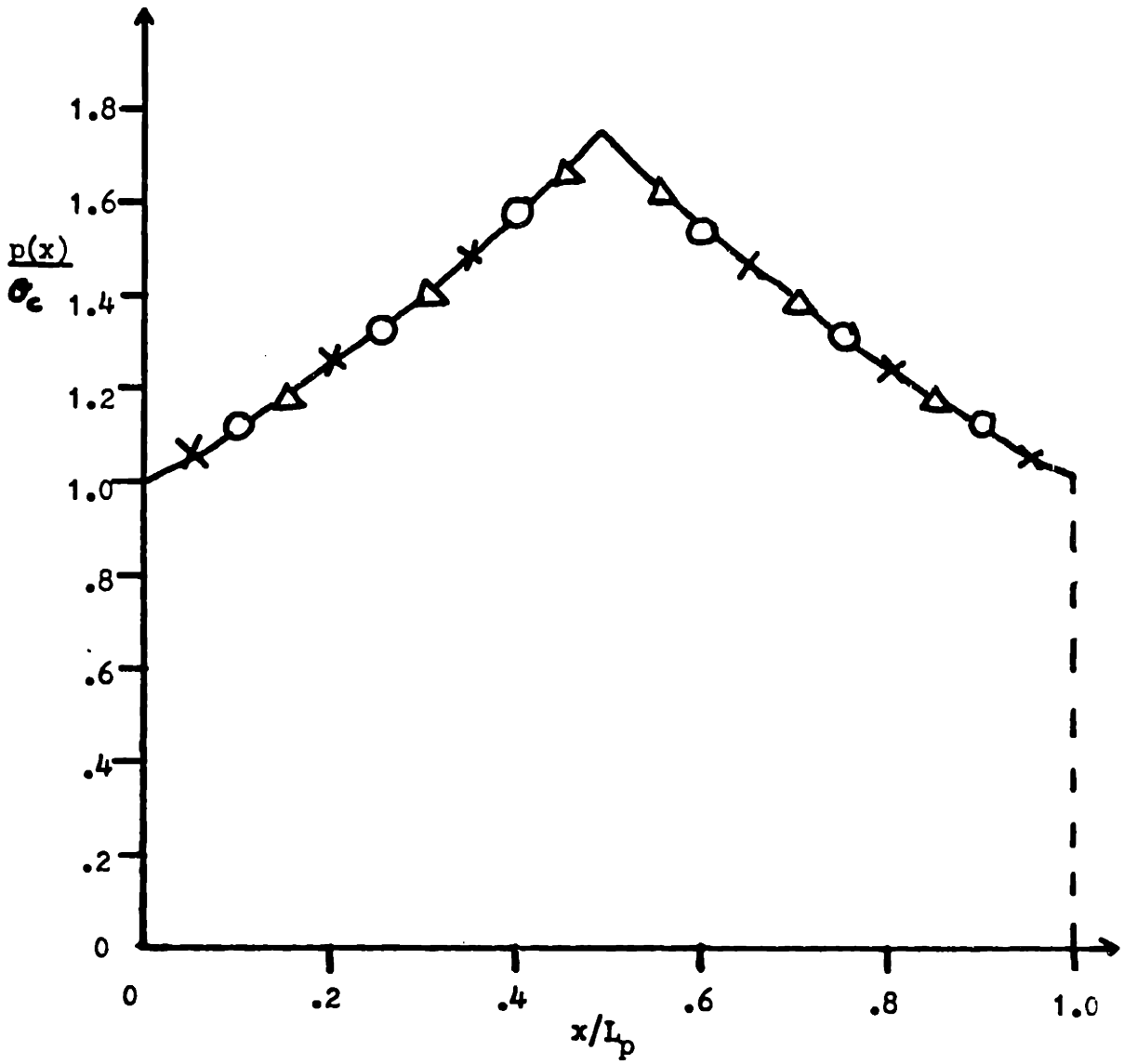

Fig. 2.6 Comparison of pressure distributions calculated for specimen 20 of Table 3.8 assuming planar and nonplanar arc shapes.

— Equation 2.12 (planar)

X Equation 2.14, n = 1 (planar)

O Equation 2.14, n=1.5 (planar-cylindrical)

△ Equation 2.14, n = 2 (cylindrical)

For light reductions, sticking friction may not occur; the maximum shear stress in the roll bite may be less than $\sigma_c/2$, in which case Equation 2.15 will yield $X_2 > X_1$. Equation 2.15 can thus be used to determine a condition for sticking friction; the calculated length of the sticking zone, defined as the difference between X_1 and X_2, must be greater than or equal to 0 for sticking friction to arise:

$$L_s = X_1 - X_2, \quad X_1 - X_2 > 0$$

$$L_s = 0, \quad X_1 - X_2 \leq 0 \tag{2.16}$$

$$X_1 - X_2 = \frac{L_p}{r}\left\{\left[\left(\frac{1}{1 - \frac{1}{a}}\right)\left(\frac{1}{2\mu} - \frac{1}{a}\right)\right]^{-\frac{1}{a}} - (1 - r)\left[\left(\frac{1}{1 + \frac{1}{a}}\right)\left(\frac{1}{2\mu} + \frac{1}{a}\right)\right]^{\frac{1}{a}}\right\}$$

The occurrence of sticking friction in the roll bite is equivalent to the occurrence of plastic flow at the strip surface; thus Equation 2.16 also gives the desired expression for the critical reduction R in Equation 2.4. Specifically, R is the smallest r satisfying $X_1 - X_2 \geq 0$. An evaluation of the influences of various rolling variables on Equation 2.16 is given in Section 2.5.

If Equation 2.16 returns a value of 0 for L_s, the pressure distribution in the roll bite is given completely by Equation 2.12. If a nonzero L_s is returned, however, then the pressure distribution for $X_2 < X < X_1$ must satisfy the sticking friction version of Equation 2.11. Exact solutions of these Equations are given in Appendix I. Using the

boundary conditions $p_i(X_1) = p_o(X_2) = \sigma_c/2$ the pressure distribution for the sticking region is given by

$$p_i(X) = \sigma_c \left[\frac{1}{2\mu} + \left(1 - \frac{a}{2\mu}\right) \ln \left\{ \frac{h(X)}{t\left[\left(\frac{1}{1 - \frac{1}{a}}\right)\left(\frac{1}{2\mu} - \frac{1}{a}\right)\right]^{-\frac{1}{a}}} \right\} \right] \quad \text{(entry region)}$$

$$p_o(X) = \sigma_c \left[\frac{1}{2\mu} + \left(1 + \frac{a}{2\mu}\right) \ln \left\{ \frac{h(X)}{t(1 - r)\left[\left(\frac{1}{1 + \frac{1}{a}}\right)\left(\frac{1}{2\mu} + \frac{1}{a}\right)\right]^{\frac{1}{a}}} \right\} \right] \quad \text{(exit region)} \tag{2.17}$$

(valid only for $X_2 < X < X_1$)

A plot of the pressure distribution for a typical case in which calculated sticking friction occurs (Specimen 24 of Table III.8, $\mu = 0.24$) is given in Figure 2.7.

Equations 2.12 and 2.17 can be integrated across the arc of contact to give expressions for plastic rolling force. Since these expressions will be useful in testing the theoretical arguments of Section II.5 empirically, the results of these integrations are quoted below. The integrations themselves are, again, carried out in Appendix I.

$$f_p = \frac{\sigma_c L_p}{r} \left\{ \frac{\left(1 - \frac{1}{a}\right)}{(a - 1)} \left[\left(1 - \frac{r}{2}\right)^{-a + 1} - 1 \right] + \frac{\left(1 + \frac{1}{a}\right)}{(1 - r)^a \ (a + 1)} \left[\left(1 - \frac{r}{2}\right)^a - (1 - r)^a \right] \right\} ; \ L_s = 0 \tag{2.18}$$

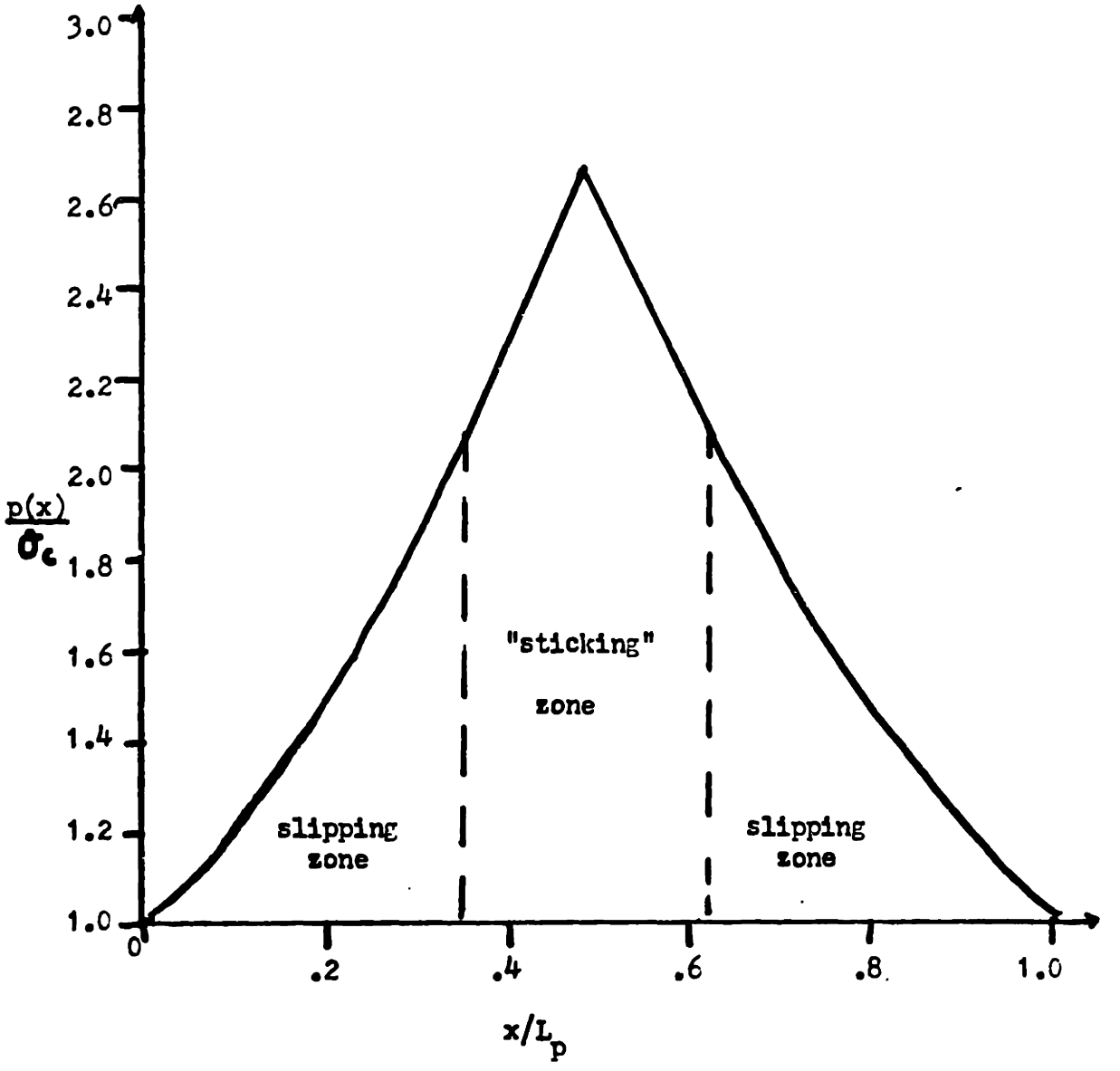

Fig. 2.7 Pressure distribution calculated for specimen 24 of Table 3.8. According to Equation 2.15, sticking friction occurs for x/L_p between .35 and .62. Equations 2.12 and 2.17 were used to calculate p(x).

$$f_p = \frac{\sigma_c L_p}{r}\left\{\left(\frac{2-r}{a}\right)\left(\frac{1}{2\mu}-1\right)+\frac{1}{2}\left[\frac{(2\mu)^{\frac{1}{a}}+\frac{(1-r)}{(2\mu)^{\frac{1}{a}}}}{}\right]\left[\frac{1}{\mu}+\left(1-\frac{a}{2\mu}\right)\ln\left(\frac{\left(1-\frac{r}{2}\right)}{(2\mu)^{\frac{1}{a}}}\right)\right]\right\};\ L_S > 0$$

As a byproduct of these integrations (i.e., in setting the bounds on the integrals), expressions for X_n, the position of the neutral plane, are found in Appendix 1. Due to the symetry between $p_i(X)$ and $p_o(X)$ for small reductions, X_n is invariably approximately equal to $L_p/2$ in temper rolling.

II.4.4 Plastic Arc Length and Constrained Yield Stress

The expressions given in the previous subsection for the pressure distribution along the arc of contact, the plastic contribution to rolling force, and the reduction required to initiate strip surface yield (Equations 2.12, 2.14, 2.16, 2.17, and 2.18) were all directly dependent on the length of the arc of plastic contact, L_p, and the effective compressive yield strength of the strip, σ_c. These expressions are thus of limited value without further expressions relating L_p and σ_c to input rolling variables. At the present time, no such expressions have been developed. In this subsection, the expected qualitative behavior of these quantities with varying rolling conditions is examined, and empirical methods for estimating L_p and σ_c from torque and tension measurements are described. These methods are employed in Section III.11 to produce a limited amount of

empirical data to test the equations presented above.

The determination of the length of the arc of contact is one of the more important, and difficult, problems in rolling theory. This length cannot be measured directly, at least not without great difficulty and (consequently) uncertainty (cf methods used and assumptions made by Siebel and Leug,[46] Van Rooyen and Backofen,[47] Kobasa and Schultz,[48] and Kannel and Dow,[49] for example). Previous treatments have, therefore, generally relied on theoretical or semiempirical (i.e., determined by fitting data to a given roll-force equation) arc length formulas. The author has used a number of these methods with equation 2.18, including those of Hitchcock,[50] Roberts,[30,51] and Jortner,[52] and compared the resulting caculated roll forces with empirical values. The calculated roll force returned by Equation 2.18 is extremely sensitive to arc length, however, and even the relatively small differences between these calculated arc lengths and those eventually inferred (cf. Figure 3.41) from torque data produced large variations in calculated rolling force.

A number of expected qualitative trends in the behavior of the plastic arc length with varying rolling conditions can be deduced from the geometric constraints of the roll bite. As shown in Figure 2.8, the vertical-roll deformation at the entry and exit planes ($Z(0)$ and $Z(L_p)$, respectively), roll curvature, $\frac{L_p^2}{D}$, and half draft, $tr/2$, must satisfy the relation

$$\frac{L_p^2}{D} + Z(L_p) - Z(0) = \frac{tr}{2} \qquad (2.19)$$

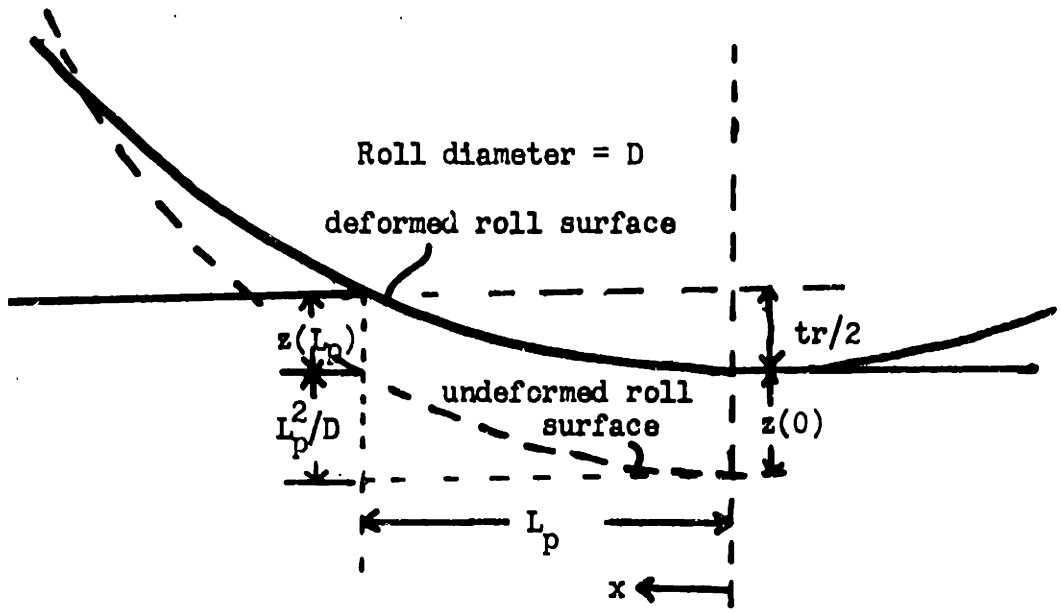

Fig. 2.8 Geometry of roll bite illustrating relationship between roll curvature, L_p^2/D, half draft, tr/2, and entry and exit plane roll deformations, $z(L_p)$ and $z(0)$:

$$\frac{L_p^2}{D} + z(L_p) - z(0) = \frac{tr}{2}$$

The basic unknowns in Equation 2.19 are the roll deformations, $Z(L_p)$ and $Z(0)$. The author has calculated (via microprocessor) the plastic contribution to these deformations, using the pressure distributions given in Subsection II.4.3 and influence functions derived by Jortner,[52] for a number of rolling situations, and has found that, due to the symetry of the pressure distributions given by Equations 2.12 and 2.17, this calculation invariably yields

$$Z(0) \approx Z(L_p), \quad \text{(plastic contributions)} \tag{2.20}$$

giving the "rigid roll" arc length,

$$L_p \approx \sqrt{\frac{Dtr}{2}} \qquad \text{(if Equation 2.20 holds)} \tag{2.21}$$

Such a calculation, however, ignores the contributions of the elastic entry and exit zones to roll deformation. Figure 2.9 illustrates the expected nature of these contributions at two reductions. As will be discussed in the next subsection, the pressure distribution arising from purely elastic contact between rolls and strip (i.e., a state in which rolls and strip are in contact but reduction is zero) is likely to be roughly elliptical and symetric. At extremely low reductions, this distribution is effectively split in half, with the relatively short plastic pressure distribution interposed between the two halves. Under these conditions, as shown (in a distorted view) in Figure 2.9(a), symetry is maintained between the elastic entry and exit zones, and Equations 2.20 and 2.21 hold for the elastic contributions to $Z(0)$ and $Z(L_p)$ as well. As reduction is increased, however, the gap between the entry and exit zones grows, and symetry is destroyed; as

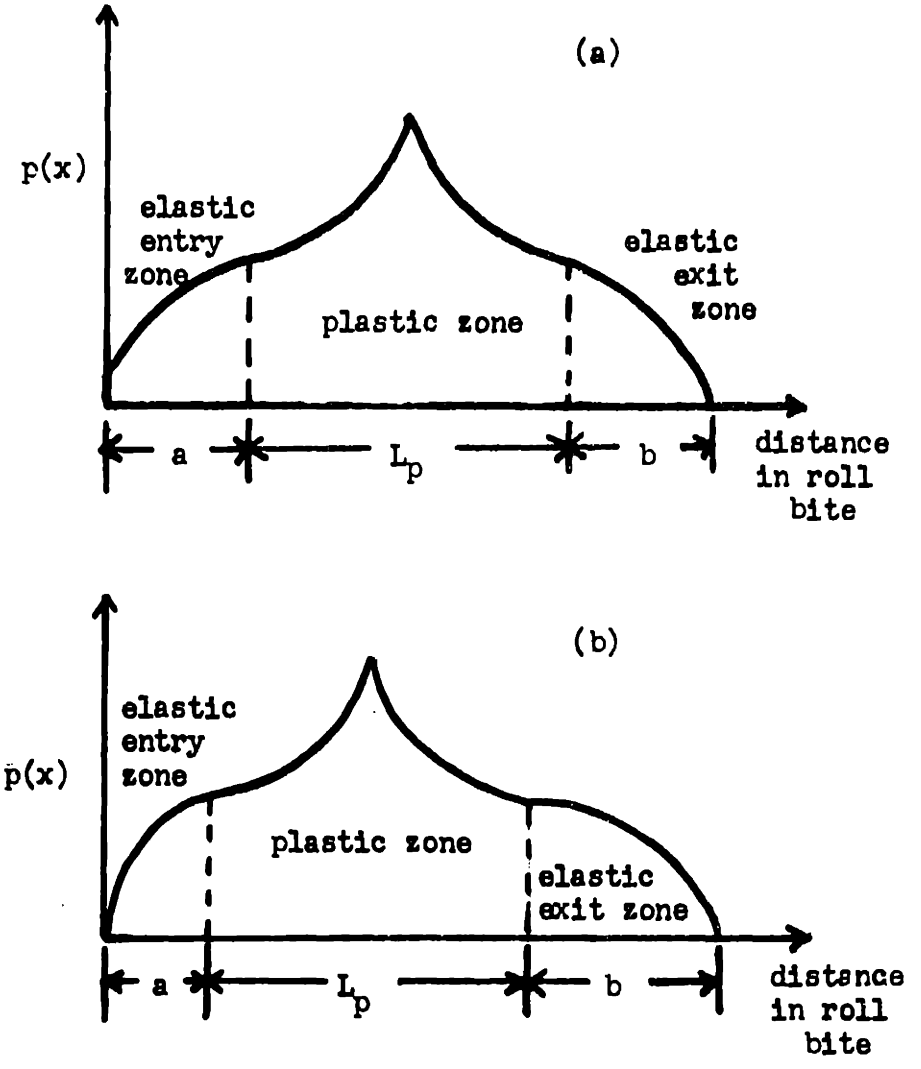

Fig. 2.9 Comparison of elastic entry and exit zone lengths, a and b, at low and high reductions.

(a) extremely small reduction;

$$a \cong b \text{ and } z(L_p) - z(0) \cong 0$$

(b) higher reduction;

$$a < b \text{ and } z(L_p) - z(0) < 0$$

shown in Figure 2.9(b), the elastic exit zone becomes larger than the entry zone, and the plastic arc length grows in relation to the corresponding rigid roll estimate. At present, this arc length appears to obey a relation of the form

$$L_p = K \sqrt{\frac{Dtr}{2}} \tag{2.22}$$

where K is a factor (not a constant) which approaches unity as r approaches 0. K increases with increasing reduction and compressive yield stress, since these contribute (in the case of r) to the separation (e.g., inbalance) between the entry and exit zones, and (in the case of σ_c) to the numerical difference between Z(0) and $Z(L_p)$ produced by a given degree of imbalance. These qualitative trends are evident in the limited amount of inferred arc length data given in Section III.11; it should be emphasized, however, that the above discussion, and Equation 2.22, represent a very rudimentary analysis of the problem, and that further work (e.g., an analysis of stresses in the elastic zone comparable to the plastic zone analysis of Subsection II.4.3) is necessary before the influences of various rolling variables on plastic arc length can be established with adequate confidence.

The effective compressive yield stress of the strip is less subject to analysis than the plastic arc length, since this stress is a material property which must be measured under conditions near those of interest to be known with any certainty. In the present analysis, the problem is further complicated by the fact that the assumed constant yield stress is not, strictly speaking, a physically real

quantity; the actual yield stress of the strip probably varies somewhat across the arc of contact. Nonetheless, the assumption of a constant yield stress is commonly made in rolling theory, and extensive previous research has established the most important qualitative influences on this parameter. The effective strip yield stress is directly related to the tensile strength of the strip (as measured in a low speed tensile test) and should additionally increase with increasing strain rate,[53] $\dot{\varepsilon}$, and decreasing average tension, $\frac{1}{2tw}(T_1 + T_2)$. The average roll-bite strain rate can be estimated by dividing the total strain, r, by the time required to achieve this strain, L_p/V:

$$\dot{\varepsilon} = \frac{rV}{L_p} \tag{2.23}$$

The effective strip yield stress most likely obeys a relation of the form

$$\sigma_c = 1.155\ (\text{tensile strength} + f\ [\dot{\varepsilon}]) - \frac{T_2 + T_1}{2tw}$$

where $f(\dot{\varepsilon})$ is a slowly increasing function of $\dot{\varepsilon}$ (for example, some data indicates that $f(\dot{\varepsilon}) = a \log[1000\ \dot{\varepsilon} + 1]$ is a reasonable choice). Qualitatively, the inferred yield stress values reported in Section III.11 seem to increase with reduction (which increases $\dot{\varepsilon}$) and to vary somewhat with the ratio D/t (for unclear reasons). Once again, it should be emphasized that the above discussion represents a zeroeth-order analysis, and that additional work and data are necessary to develop a reasonably accurate method of calculating σ_c. It should also be noted that a vast literature on this subject exists, although most investigators have (understandably) concerned themselves with strains much larger than

those typical of temper rolling. A brief review of this literature can be found in Reference 4, Sections 8-25 to 8-34.

Although neither σ_c or L_p can be calculated at this point, both can be inferred from experimental data. σ_c can be estimated directly from roller-die drawing tests; in this process, the roll drive spindles of the mill are disconnected, and all deformation energy is supplied to the strip through entry and exit tensions. The deformation energy per unit volume of strip material is given in terms of σ_c by the relation[54]

$$\frac{\text{deformation energy}}{\text{unit volume}} = \sigma_c \ln\left(\frac{1}{1-r}\right) \tag{2.25}$$

Using this relation, as shown in Figure 2.10, an energy balance on the roller-die drawing process yields

$$\sigma_c \approx \frac{T_2 - T_1(1-r) - \tau_L}{tw(1-r)\ln\left(\frac{1}{1-r}\right)} \tag{2.26}$$

The average roll-bite pressure, $\bar{\sigma}_c$, can be estimated from measured spindle-torque data in rolling tests. As illustrated in Figure 2.11, a force balance and the definition of torque give

$$\bar{\sigma}_c \approx \frac{2\tau_c}{Dtr} \tag{2.27}$$

where

$$\tau_c \approx \tau_m - \tau_L + \frac{D}{2w}\left(T_2 - T_1(1-r)\right) \tag{2.28}$$

using the further relation

$$\bar{\sigma}_c \approx \frac{f_p}{L_p} \tag{2.29}$$

the plastic arc length can be estimated by matching the measured average roll-bite stress and rolling force with values

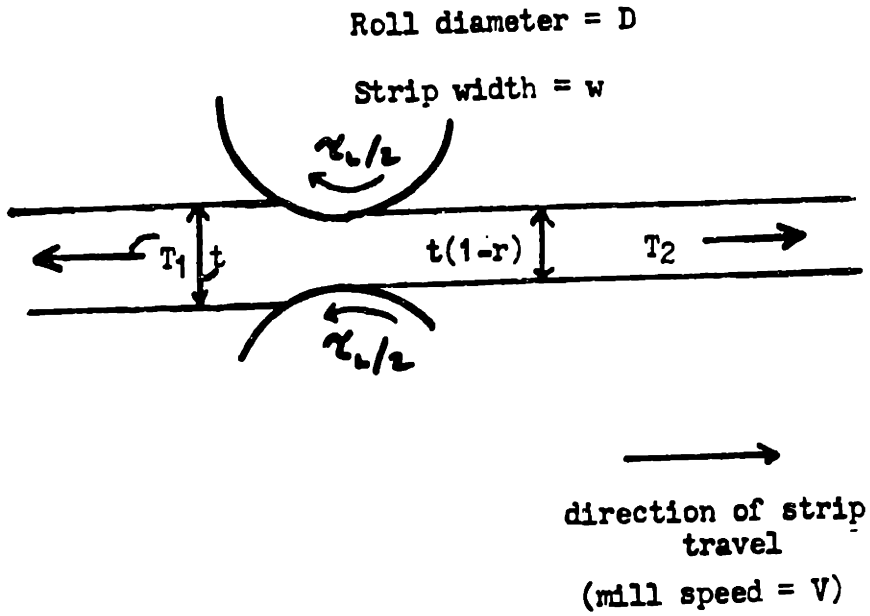

Fig. 2.10 Estimation of effective yield stress, σ_c, from energy balance on roller die drawing process.

Energy balance gives (with consistent units)

tension energy - bearing loss = deformation energy

$$T_2V - T_1(1-r)V - \tau_L V \cong (1-r)Vtw\,\sigma_c \ln\left(\frac{1}{1-r}\right)$$

or

$$\sigma_c \cong \frac{T_2 - T_1(1-r) - \tau_L}{tw(1-r)\ln\left(\frac{1}{1-r}\right)}$$

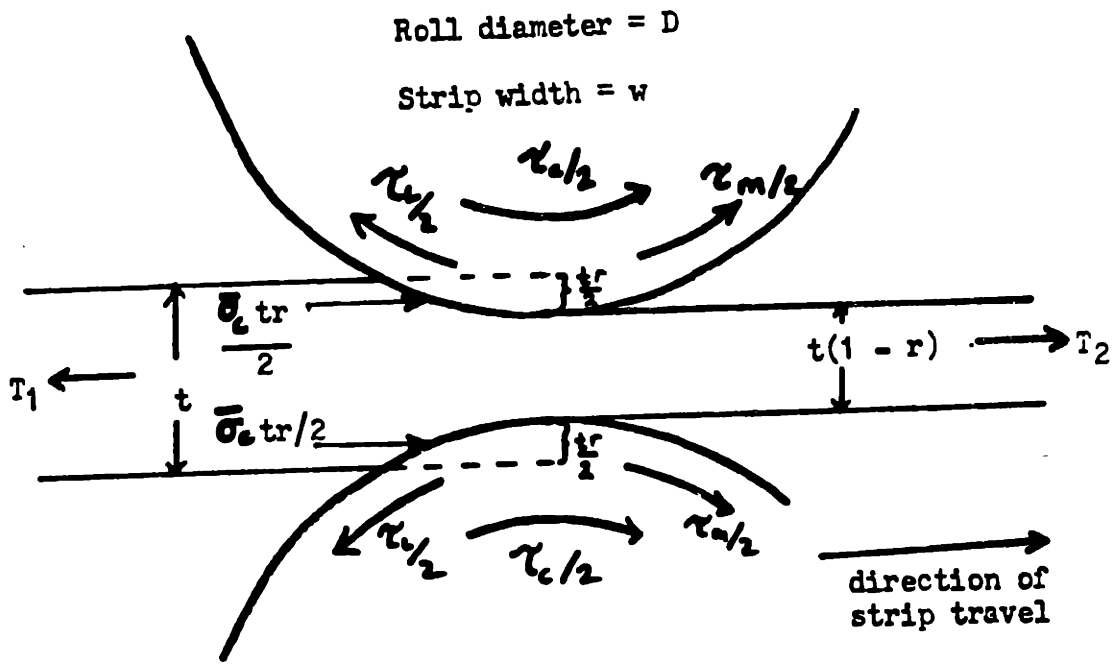

Fig. 2. 11 Estimation of average roll bite pressure, $\bar{\sigma}_c$, from corrected torque, τ_c. From force equilibrium and the definition of torque

$$\tau_c \cong \tau_m - \tau_i + \frac{D}{2w}\left[T_2 - T_1(1 - r)\right]$$

and

$$\frac{Dtr}{2}\bar{\sigma}_c \cong \tau_c$$

or $$\bar{\sigma}_c \cong \frac{2\tau_c}{Dtr}$$

computed from Equations 2.29, 2.18, 2.31, and 2.33, using a measured σ_c. These estimates are of limited accuracy at low speeds and extremely low reductions, conditions for which it is difficult to accurately account for bearing losses; however, as will be seen in Section III.11, the stability of these estimates improves substantially at higher reductions, to the point that they can be employed to meaningfully compare theoretical expressions with experimental data.

II.4.5 Elastic Contributions

The contributions of the elastic entry and exit zones to the specific rolling force are ignored in most theories of cold rolling. In the case of temper rolling, however, the plastic strain imposed (reduction) is frequently of magnitude comparable to elastic strains. It is therefore likely that, for small temper-rolling reductions, a considerable portion of the rolling force arises from the elastic compression of the strip, and that, consequently, the regions of elastic contact between the rolls and strip cannot be neglected in a mechanical analysis of temper rolling.

At this point, no detailed treatment of the stress distribution in the elastic region has been carried out. The elastic contributions to arc length and rolling force can be estimated, however, by assuming that, as reduction approaches zero, the roll-strip interface approximates a Hertzian contact between a cylinder (of the same diameter as the roll) and a semi-infinite plate. For such a contact, the well-known analysis of Hertz[55,56] indicates that the pressure

distribution between the cylinder and plate is elliptical, with a maximum pressure (occurring at the center of the contact) given by the equation (assuming both roll and plate have equal elastic moduli E and poisson's ratios equal to 0.3)

$$P_{max} = 0.592 \sqrt{\frac{f_e E}{D}} \tag{2.30}$$

where f_e is the contact force. Assuming $P_{max} = \sigma_c$ thus gives an estimate of the elastic contribution to rolling force:

$$f_e = 2.86 \frac{\sigma_c^2 D}{E} \tag{2.31}$$

under the same assumptions regarding elastic modulus and poisson's ratio, the Herzian contact equations give a similar expression for the elastic arc length:

$$L_e = 2.16 \sqrt{\frac{f_e D}{E}} = \frac{3.65 \sigma_c D}{E} \tag{2.32}$$

The total rolling force and arc length are obtained by superposing the elastic and plastic components:

$$f = f_p + f_e \tag{2.33}$$

$$L = L_p + L_e \tag{2.34}$$

II. 5 Effect of Specific Rolling Variables on Surface Transfer

The analysis presented in the previous two sections resulted in quantitative expressions for roughness transfer, specifically Equations 2.4 and 2.16:

$$t_r = \frac{\rho_f}{\rho_r} = \frac{\rho_i}{\rho_r} + \frac{\rho_r - \rho_i}{\rho_r}\left(\frac{r}{R}\right) \quad ; \; r \leq R$$

$$t_r = 1 \qquad\qquad r > R$$

where R is the smallest r satisfying

$$\frac{L_p}{r}\left\{\left[\frac{1}{\left(1 - \frac{1}{a}\right)}\left(\frac{1}{2\mu} - \frac{1}{a}\right)\right]^{-\frac{1}{a}} - (1 - r)\left[\left(\frac{1}{1 + \frac{1}{a}}\right)\left(\frac{1}{2\mu} + \frac{1}{a}\right)\right]^{\frac{1}{a}}\right\} \geq 0$$

Although these equations deal explicitly with a single surface parameter, it seems reasonable to expect that the degree of matching between roll and strip surfaces will increase as the final strip roughness approaches the roll roughness, and thus that conditions which promote increased roughness transfer will also lead to increased transfer of other surface parameters (such as peak count). We are thus now in a position to evaluate the expected influences of various rolling variables on transfer efficiency by examining their effects on roughness transfer values calculated using Equations 2.4 and 2.16.

Before considering the influence of any particular variable on transfer, it is helpful to consider the imortance of roll bite geometry to the interfacial stresses developed along the arc of contact. As emphasized previously, complete transfer should occur when the peak normal pressure at the center of the roll bite reaches σ_c . Referring to the "friction hill" pressure distribution shown in Figure 2.6, and to its mathematical description, Equation 2.12, it can easily be seen that, on a very basic level, two factors determine the magnitude of this peak central stress: the

slope of the pressure distribution, and the distance over which the pressure is able to build up. As a basic rule of thumb, therefore, we would expect any variation in rolling conditions that increases plastic arc length or the rate at which normal pressure increases with distance in the roll bite to increase roll-strip surface matching as well.

Differentiation of the simplest slipping-zone pressure distribution, $p_o(X)$ in Equation 2.12, gives the slope of the presure distribution across the entire roll bite (due to symetry between the exit and entry pressure functions):

$$\frac{dP_o(X)}{dX} = \sigma_c \left[\left(\frac{r}{L_p(1-r)} + \frac{2\mu}{t(1-r)} \right) \left(1 + \frac{Xr}{L_p(1-r)} \right)^{a-1} \right] \quad (2.35)$$

Although the influence of L_p on the number returned by this equation is not obvious, $\frac{dp_o(X)}{dX}$ seems to increase with plastic arc length for most situations; using data consistent with that presented in Table III.8, for example ($t = 0.0185$ inches, $\mu = 0.24$, $r = 0.03$, $\frac{X}{L_p} = 0.4$) gives values of $\frac{dp_o(X)}{dX}$ of $46.50\sigma_c$/inch for $L_p = 0.051$ inches and $45.5\sigma_c$/inch for $L_p = 0.049$ inches. Changes in rolling conditions which lead to increased plastic arc length should, therefore, concurrently lead to a more rapid buildup of pressure in the roll bite, and thus by the rule of thumb stated above should lead to a definite increase in transfer effficiency. Referring to Subsection II.4.4, therefore, the degree of roll-strip surface matching achieved under otherwise constant conditions should increase with increasing reduction, roll diameter, and

strip yield strength, and additionally with decreasing average tension, since this leads to an increase in strip yield stress. At first glance, it might also seem that increasing strip thickness, which increases arc length as well, should also increase transfer efficiency. Examination of Equation 2.35, however, indicates that the slope of the pressure distribution in the arc of contact decreases sharply with increasing strip thickness; this is reflected in the behavior of the critical reduction with increasing gage (cf. Table III.6). Although the theoretical reasoning presented thusfar predicts clearly the effects of variations of roll diameter, reduction, strip yield strength, and average tension on the transfer process, it is somewhat ambiguous concerning the influence of strip gage. Quantitatively, it predicts a decrease in transfer levels with increasing gage, although qualitatively we would expect an increase. The effect of strip gage on transfer will be considered more fully in sections III.9 and IV.1.

Equation 2.35 also indicates that the slope of the roll-bite pressure function, and thus transfer efficiency, should increase sharply with increasing friction coefficient; this is hardly surprising, in view of the emphasis placed on interfacial shear stress in the foregoing analyses. (It should also be noted that the friction coefficient probably influences plastic arc length as well.) While the coefficient of friction is not itself subject to simple and precise control in temper rolling, this observation is useful in predicting the influences of rolling variables which alter

roll-bite frictional conditions on transfer efficiency. Foremost among these is lubrication. In the foregoing treatment of the mechanics of the process, no distinction was drawn between wet- and dry-temper rolling, and it is doubtful that the relatively watery rolling soultions employed in wet-temper rolling significantly alter the nature of the roll bite as compared to unlubricated conditions. However, it is highly probable that even these relatively inviscid lubricants are entrapped to some degree between the roll and strip during deformation, particularly at production mill speeds. While it is unlikely that the degree of this entrapment would ever be such that a state of hydrodynamic lubrication is approached and metal-to-metal contact is interrupted at the center of the roll bite, inhibiting strip surface shear deformation and drastically altering transfer efficiency, any degree of entrapment is likely to reduce the effective friction coefficient in the roll bite, and thus the maximum shear stress achieved at the roll-strip interface. Since, as mentioned above, some lubricant entrapment is almost certain to occur under commercial wet-temper rolling conditions, transfer efficiency in wet-temper rolling should be less than that observed under corresponding unlubricated conditions (although this effect may be difficult to duplicate under low speed, laboratory conditions). Since the degree of entrapment occurring under given conditions should increase with increasing lubricant viscosity, we would also expect transfer efficiency to decrease with increasing lubricant viscosity in wet-temper rolling tests.

Roll-bite friction may also be influenced by work roll (and initial strip) roughness and mill speed. The nature of the influences of these variables on friction and transfer, however, differs for lubricated and unlubricated conditions. Increasing roll roughness is generally thought to increase the friction coefficient in dry rolling; however, dry-sliding tests performed under light loads have shown that roughness has very little effect on friction, if extremely rough or atomically smooth surfaces are excluded.[57] While it should be borne in mind that extrapolating this result to systems sliding under loads characteristic of temper rolling is somewhat risky, it seems likely that no significant difference in roll-bite friction arises in using a 40 microinch rather than 60 microinch roughness roll (although a significant difference may arise in going from a 3 to 60 microinch roll). The transfer process in dry-temper rolling is therefore probably independent of roll roughness in the range of roughnesses commonly encountered. In wet-temper rolling, however, roll roughness is likely to influence lubricant entrapment and thus transfer efficiency. A priori, however, the nature and significance of this influence is difficult to decipher. (At this point, it should be mentioned that changes in initial strip roughness probably effect the transfer process by influencing interfacial friction, if at all. The influence of initial strip roughness on transfer efficiency is thus probably the same as that of roll roughness). Mill speed also affects surface transfer in wet- and dry-temper rolling differently. In dry-temper rolling, an

increase in mill speed increases the average roll-bite strain rate, increasing the effective strip yield strength and plastic arc length. Transfer efficiency should therefore increase with increaseing mill speed in the unlubricated case. In wet-temper rolling, however, the increase in yield stress with increasing speed is accompanied by an attendent increase in lubricant entrapment. Since the increase in yield stress with strain rate is probably rather slow (Roberts[30] postulates a logarithmic increase), the increase in entrapment probably has a much more marked effect on the transfer process. Transfer efficiency should therefore decrease with increasing mill speed in wet-temper rolling.

A summary of the theoreticlly expected influences of various rolling variables on transfer efficiency (the degree of roll-strip surface conformity) is given in Table II.1. Also given in this table is a summary of the empirically observed influences, which will be described in Part III. (As can be seen, theory and experiment agree in every case cited.) The author realizes that this section may seem somewhat terse and dense, considering the length of the analyses carried out in preparing for it. This section was, however, primarily intended to describe the basic rules of thumb useful in evaluating the influence of a given rolling variable on the transfer process, and to state briefly the expected effect of the most basic process variables on transfer. Each trend cited in this section is reiterated, expanded upon, and supported by fairly extensive empirical data in Sections III.4 to III.10.

Table II.1

Theoretically Predicted and Empirically Observed Influences of Increasing Various Rolling Variables on Transfer Efficiency (the degree of roll-strip surface matching)

Rolling Variable Increased (other variables held constant)	Effect on Transfer Efficiency (degree of roll-strip surface matching)	
	Theory	Experiment
Reduction	Increases	Increases
Work-roll Diameter	Increases	Increases
Strip Yield Stress	Increases	Increases Slightly
Average Tension	Decreases	Decreases Slightly
Strip Thickness	Decreases	Decreases
Lubricant Viscosity	Decreases	Decreases
Mill Speed	Increases (dry)	Increases Slightly (dry)
	Decreases (wet)	Decreases (wet)
Work-roll and Strip Roughness	No Effect (dry)	No Effect (dry)
	? (wet)	No Wet Data Available
Rolling Force*	Generally Increases	Generally Increases

*The influence of rolling force on transfer is primarily due to its influence on more basic rolling variables, particularly reduction; cf. Section IV.2.

III EXPERIMENTAL PROCEDURES AND RESULTS

III.1 Rolling Mills

The data presented in the following sections was obtained primarily on two instrumented laboratory rolling mills. Both are single-stand mills with a four-high roll arrangement. The smaller of the two, referred to as the Nash mill below, has a roll face width of 5.25 inches, a work-roll diameter of 3.25 inches, and a backup-roll diameter of 8.5 inches. The larger of the mills, referred to as the Bliss mill below, uses 6.5-inch-diameter work rolls and 19-inch-diameter backup rolls with face widths of 14 inches. Both mills are instrumented to provide for continuous monitoring and recording of rolling force, spindle torque, entry and exit tensions, reduction, mill speed, and forward slip during testing. Both the mills and their instrumentation have been more fully described in previous documents.[10,58] These papers give an accurate description of the gages and transducers presently in place on the mills; however, since their publication, the eight-channel oscillograph they describe has been replaced by a microprocessor-based data acquisition system (consisting of a Hewlett-Packard 9825A microprocessor, 2241A Extender, and 2240A measurement and control processor), which permits direct digital printout of the rolling variables mentioned above.

A limited amount of production temper-rolling data was also obtained on two commercial temper mills. The bulk of this data was acquired on the No. 7 84-inch sheet temper mill at U. S. Steel Irvin plant. This is a

single-stand four-high mill designed to use work rolls with diameters between 23 and 27 inches. A sixteen-channel brush recorder connected to the operator's instrumentation produced a printout of roll force, mill speed, extension, and strip tensions for tests on this mill. A small amount of data was also obtained on the 80-inch sheet temper mill at the North Sheet Mill of U. S. Steel Gary Works. This is a four-high, single-stand mill, employing 24-inch work rolls. For this mill, no printout of rolling variables was obtainable, and mill speed and reduction were monitored during testing by watching the relevant gages in the operator's cab.

III. 2 Materials

A large variety of strip materials were used in this investigation. For the laboratory tests, the bulk of these materials were taken from a general stock. These coils were of somewhat uncertain history, but fell in two general categories: "Full hard" stock, materials which had undergone substantial (greater than 50 percent, and perhaps as much as 90 percent) prior cold reduction, and "annealed," which exhibited only slight yield points during tensile testing and were probably commercially temper rolled subsequent to annealing and prior to delivery. The mechanical properties of these coils are given in Table III.1. The yield stresses reported in this table are 0.2 percent yield stresses, as conventionally measured in a low speed, uniaxial tension test. Further laboratory tests were performed on specially prepared coils of nominally identical chemical composition.

Table III.1

Mechanical Properties of Coils From General Stock

Coil	Type	Gages (inches)	0.2 Percent Yield Strength, psi (low speed tension test)
A	Annealed	0.012	34,600
B	Annealed	0.0122	32,200
C	Full Hard	0.010	123,700

These coils were produced by rolling steel from a single, 0.047-inch-thick coil to different thicknesses, and, using heat-treatment cycles developed from small sample tests, reannealing the resulting smaller coils to obtain essentially the same steel, with the same yield stress, in three different gages. The mechanical properties of these coils are given in Table III.2, along with estimates of the temperatures at which they were soaked. The coils were annealed at the tops of two commercial box-annealing furnaces. The nominal soaking temperatures were 1100 and 1220 °F; the soaking temperatures listed in Table III.2 are approximate values based on the temperature gradients generally observed in these furnaces. The coils exhibited considerable sticking and strain-breaking problems after annealing, which may indicate that, due to their relatively small masses, they were substantially overheated in the commercial furnaces. The chemical compositions of the coils before and after annealing are given in Table III.3. As can be seen, no significant variation in either carbon or manganese content resulted from the heat treatments.

The coils used in the production trials were all commercially annealed materials. 0.036-inch-thick electrogalvanizing line stock was used in the tests at Gary Works; since no recorded roll-force data was obtained, no samples of this material were tensile tested. Both autobody sheet and appliance skirt stock were rolled at the Irvin trials. Several coils of roughly 0.030-inch thickness and 40,000 psi yield strength were used. More precise information on

Table III.2

Properties of Specially Annealed Coils
(All coils soaked 12 hours at soaking temperature; approximately 6 hours heat up and cool down periods.)

Coil	Thickness, inches	Soaking Temperature, °F	Yield Stress, psi
E1	0.0120	1300	32,200
E2	0.0185	1300	29,300
E3	0.0295	1175	27,900

Table III.3

Chemical Analyses of Coils E1, E2, and E3 After Annealing and Unannealed Parent Coil

Coil	Gage (inches)	Percent C	Percent N	Percent S	Percent Mn
Original	0.047	0.058	0.003	0.036	0.40
E3	0.0295	0.051	0.003	0.037	0.39
E2	0.0185	0.053	0.002	0.033	0.40
E1	0.012	0.047	0.001	0.023	0.37

specific coils is given in Table A.2 in Appendix II.

The roll surfaces used in the laboratory tests were all specially prepared for this investigation by commercial shot blasting, except in one instance when an existing set of Bliss mill rolls, which had apparently been rough ground and then shot blasted, was used. The textures produced covered a fairly wide range, although roll roughnesses and peak counts generally fell in the respective ranges of 60 to 90 μin.R_a and 120 to 180 ppi_{50}. More precise roll and strip textures are given in the presentation of specific data in Sections III.4 to III.11. More varied roll textures were used in the production tests. Electro-discharge textured, chrome-plated work rolls were used in the tests at Gary Works, while shot-blasted rolls with both steel and chrome-plated surfaces were used in the Irvin trials.

The lubricants used in the laboratory tests were for the most part standard wet-temper lubricants, and were usually applied in a 3 percent aqueous solution at 130°F. In some tests, however, water alone was used as a lubricant, while in others a tallow-based tandem tin mill oil was applied neat to give maximum lubricity.

III.3 Experimental Procedures

The nature of the subject under investigation required that both the surface properties of the rolls and strip and the mechanical variables of the temper rolling process be monitored during testing. This led to the development of essentially four testing procedures, one each for

surface texture and mechanical data for both laboratory and production situations.

The mechanical testing procedures involved recording the rolling conditions prevailing at various points in a coil during rolling and being able to locate these points to measure the resulting surface properties after rolling. In the laboratory this was accomplished by monitoring the rolling variables on a CRT screen until desired conditions were reached, then storing the screen contents under a given test number in a computer file, while at the same time inserting a numbered carboard tag into the take-up real of the mill. This resulted in a computer printout of rolling conditions at points which could be located by unwinding the processed coil to each of the cardboard tags. Because of the small reductions taken, the values of rolling variables displayed on the screen tended to fluctuate somewhat, and normally two sets of conditions—one just before the tag was inserted in the mill and one just after—were recorded and later averaged for each test. The procedure for the production trials at Irvin was basically the same. In this case, however, rolling variables were monitored by watching the gages in the operator's cab; at the same time, phone contact was maintained between the cab and a motor room some distance away, where the brush recording system was set up. When desired conditions were encountered, a signal was given over the telephone to record, while at the same time the reading on the operator's linear-footage meter (which indicated how many feet of the current coil had been rolled) was recorded,

along with the test number. Combined with the total footage of a coil, these linear-footage readings gave the distance from the end of the coil for each point for which rolling conditions were known. The coil was then unwound to these points on a recoil line equiped with a similar footage meter.

The procedures for surface texture measurement involved the determination of strip-surface characteristics before and after testing and the inference of the roll texture during rolling. In the laboratory, strip samples were taken from several points within a coil prior to testing and from the marked points in the coils after testing. The samples taken were of length roughly equal to the circumference of the rolls; eight profile meter traces, four on each side, were taken and averaged to compute the average roughness and peak count of each sample. The textures of both rolls were measured before and after each series of tests. A total of 12 profile meter traces were taken at 90-degree intervals around the circumference of each roll. The roll surface properties used in computing transfer levels for a particular series of tests were obtained by averaging measurements taken before and after the series. In the production trials, procedures were again basically identical, although practical considerations again dictated some differences. Strip profile readings could be taken before rolling only at the head end of the coil, since annealed coils cannot be recoiled prior to temper rolling without risk of cracking or strain breaking. After testing, samples could not be cut from a coil and profiled on both sides; final strip surface

measurements were thus made directly on the recoil line, with four traces being taken on one side of the strip only. Finally, roll surface measurements were taken across the barrel of the roll at one peripheral position only. At Gary, roll surface measurements were taken with the rolls in the mill by climbing over the mill entry table, and roll profile readings could be taken before and after each coil. At Irvin, however, the mill design was different, and the rolls had to be removed from the mill for measurement. Roll profiles could thus not be taken after each coil, and roll wear was compensated for by linearly interpolating surface measurements taken three or four coils apart.

In the laboratory tests, surface measurements were made predominately with a Bendix profilometer. In some early laboratory tests and in all production tests, measurements were made with a Rank-Taylor Hobson Surtronic 3. In the author's experience these instruments, if properly maintained, give virtually interchangeable results. All surface measurements were made in compliance with SAE standard J911.[59] Specifically, a one inch trace was taken and a 0.030-inch roughness cutoff and 50 microinch peak height definition were used. All profile meter traces were taken perpendicular to the rolling direction; however, for shot-blasted rolls at least, roll texture is fairly uniform in the axial and circumferential directions, and strip surface roughness values should be independent of the direction of measurement. The author has checked this assertion for several specimens; typical data is given in Table III.4. It should

Table III.4

Surface Roughness Measurements Parallel to and Perpendicular to Rolling Direction

Spec	Roughness, microinch Ra	
	Perpendicular to Rolling Direction	Parallel to Rolling Direction
1	52.3 ± 1.7	54.3 ± 3.2
2	57.6 ± 2.4	58.5 ± 5.8
3	83.3 ± 2.5	84.8 ± 6.2
4	97.4 ± 3.6	99.4 ± 2.8

be noted, however, that this result probably would not hold for ground rolls. Also, the transfer values quoted in the following sections were obtained by dividing average surface characteristics, measured on both sides of a sample, by corresponding average roll characteristics measured on both rolls. Since, in general, the textures of the two rolls, and of the two sides of a given strip sample, differed slightly for any given test, it might legitimately be asked if "one-sided" transfer values, obtained by dividing measurements from one side of a sample only by measurements from the corresponding roll, might differ significantly from two-sided average values. The author has also compared one- and two-sided transfer values for a limited number of samples and has found no significant differences between them. Representative data is given in Table III.5.

III.4 Effect of Reduction on Transfer

As was emphasized in Section II.3, surface transfer in temper rolling should depend more strongly on reduction than on any other easily measured and controlled process variable, since this variable reflects most directly the extent of strip surface deformation. The strength of this dependence is easily demonstrated. For example, in the dry-temper rolling of 0.012-inch-thick annealed strip, performed at 50 feet per minute with 18,000 psi entry and exit tensions applied, and employing 6-½-inch-diameter work rolls with a texture (in microinches R_a/ppi_{50}) of 70/140, strip samples rolled to approximately 0, 1, 2, 3, and 4 percent

Table III.5

Comparison of One- and Two-Sided Transfer Valves

Sample	Strip Roughness / Roll Roughness	Strip Peak Count / Roll Peak Count
1 (top)	0.473 ± 0.015	0.729 ± 0.043
1 (bottom)	0.465 ± 0.014	0.680 ± 0.041
1 (average, top and bottom)	0.469 ± 0.021	0.705 ± 0.059
2 (top)	0.880 ± 0.033	0.942 ± 0.030
2 (bottom)	0.844 ± 0.026	0.911 ± 0.036
2 (top and bottom)	0.862 ± 0.042	0.927 ± 0.047
3 (top)	0.900 ± 0.026	1.000 ± 0.071
3 (bottom)	0.920 ± 0.014	1.026 ± 0.046
3 (top and bottom)	0.910 ± 0.030	1.013 ± 0.085

reductions had measured textures of 11/33, 30/83, 37.5/97, 54/126, and 70/138, respectively. Figure 3.1 shows the surface of a strip sample taken from the roll bite following these tests; it shows (on the right) the relatively smooth, undeformed strip entering the mill, and (on the left) the abruptly roughened surface of the strip after a four percent temper-rolling reduction.

The reductions quoted for the tests above are only approximate. The almost linear relationship between roughness transfer and reduction is more clearly illustrated by more precise data, as, for example, that shown in Figure 3.2. Corresponding peak count transfer data is given in Figure 3.3. This data is from dry-temper rolling tests performed on the Nash mill at low speeds and with various levels of applied strip tension. The strong relation between transfer and reduction, however, is characteristic of all data obtained in this investigation. Slight nonlinearities in the relationship between roughness transfer and reduction, also characteristic of most of the data obtained, are evident in Figure 3.2, particularly at lower reductions; transfer is somewhat better in this region than would be expected from Equation 2.4. The least squares estimate of the ratio of initial strip to roll roughness based on the data given in Figure 3.2, for example, is about 0.34; the actual value, from roll and initial strip roughness measurements, is about 0.16. Also, there is a slight decrease in slope in going from relatively low to high reduction in the roughness transfer versus reduction graphs for most data. In Figure 3.7,

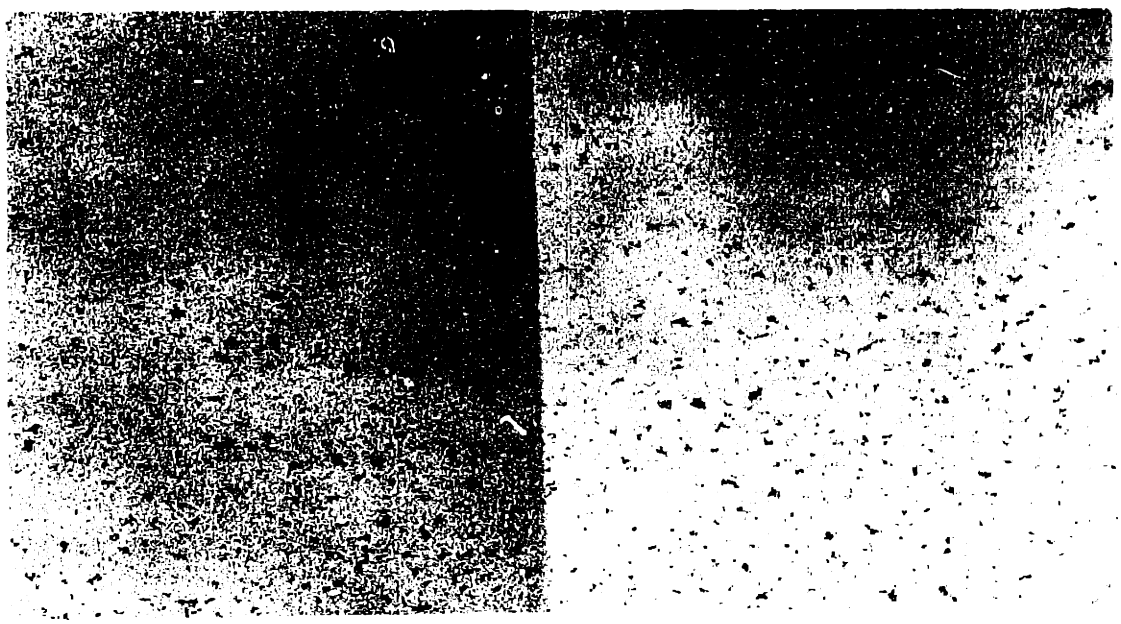

Fig. 3.1. Sample from Roll Bite of a Laboratory Temper Mill.

Right: Undeformed Strip; approximately 11-microinch roughness, 33 ppi_{s_0} Peak count.

Left: Strip Temper Rolled to approximately 4 percent reduction; 70-microinch roughness, 138 ppi_{s_0} Peak count.

Fig. 3.2 Roughness Transfer vs. Reduction

Roll Diameter (inches): 3.197
Roll Roughness: (microinches R_a): 59
Strip: Coil A
initial roughness (microinches R_a): 9.5
Mill Speed (feet/minute): 50
Lubrication: Dry

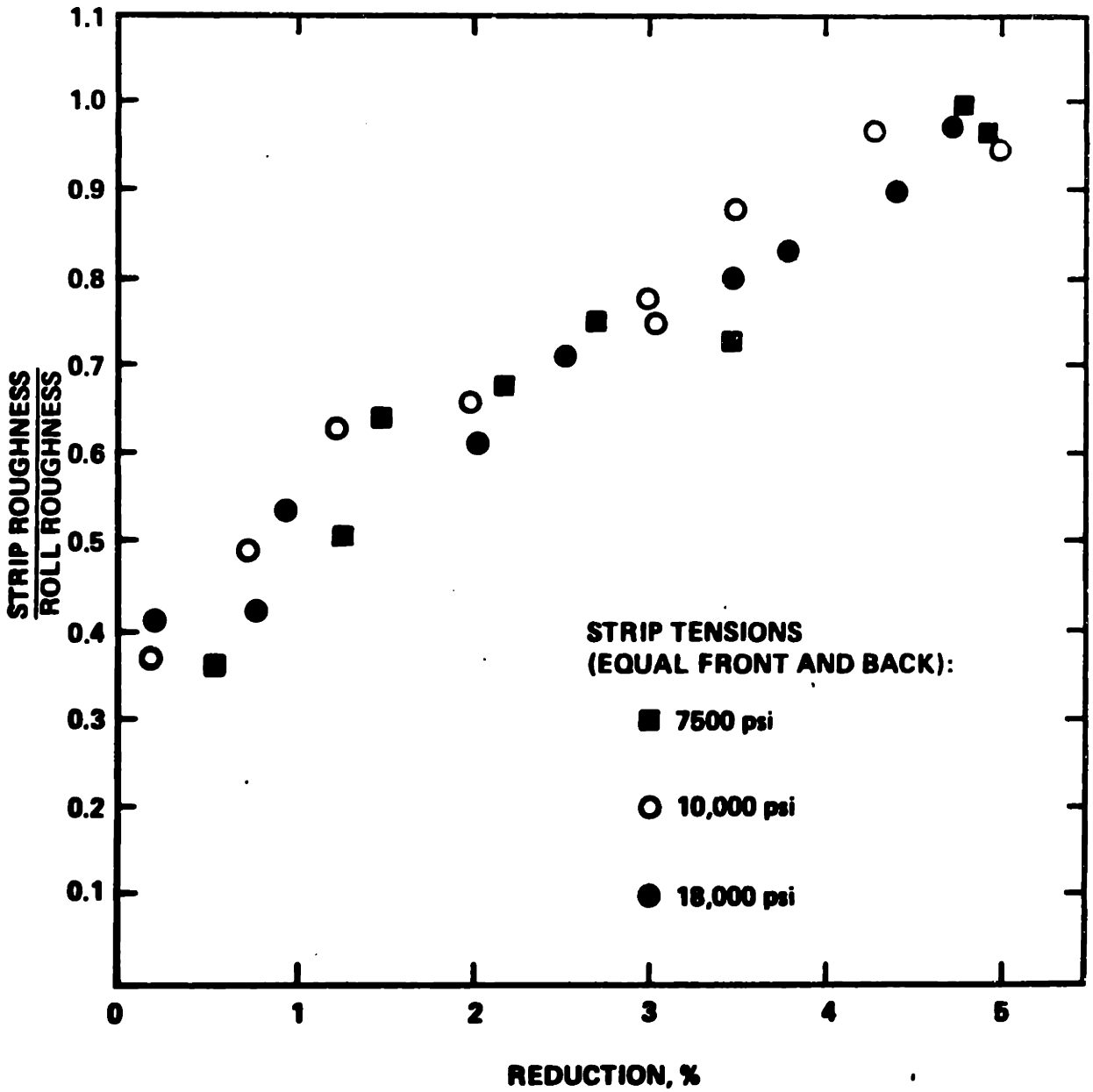

Fig. 3.3 Peak Count Transfer vs. Reduction

Roll Diameter (inches): 3.197
Roll Peak Count (ppi_{50}): 154
Strip: Coil A
Initial peak count (ppi_{50}): 26
Mill Speed (feet/minute): 50
Strip Tensions (psi): Entry x 7500 O 10000 • 18000
Exit x 7500 O 10000 • 18000
Lubrication: Dry

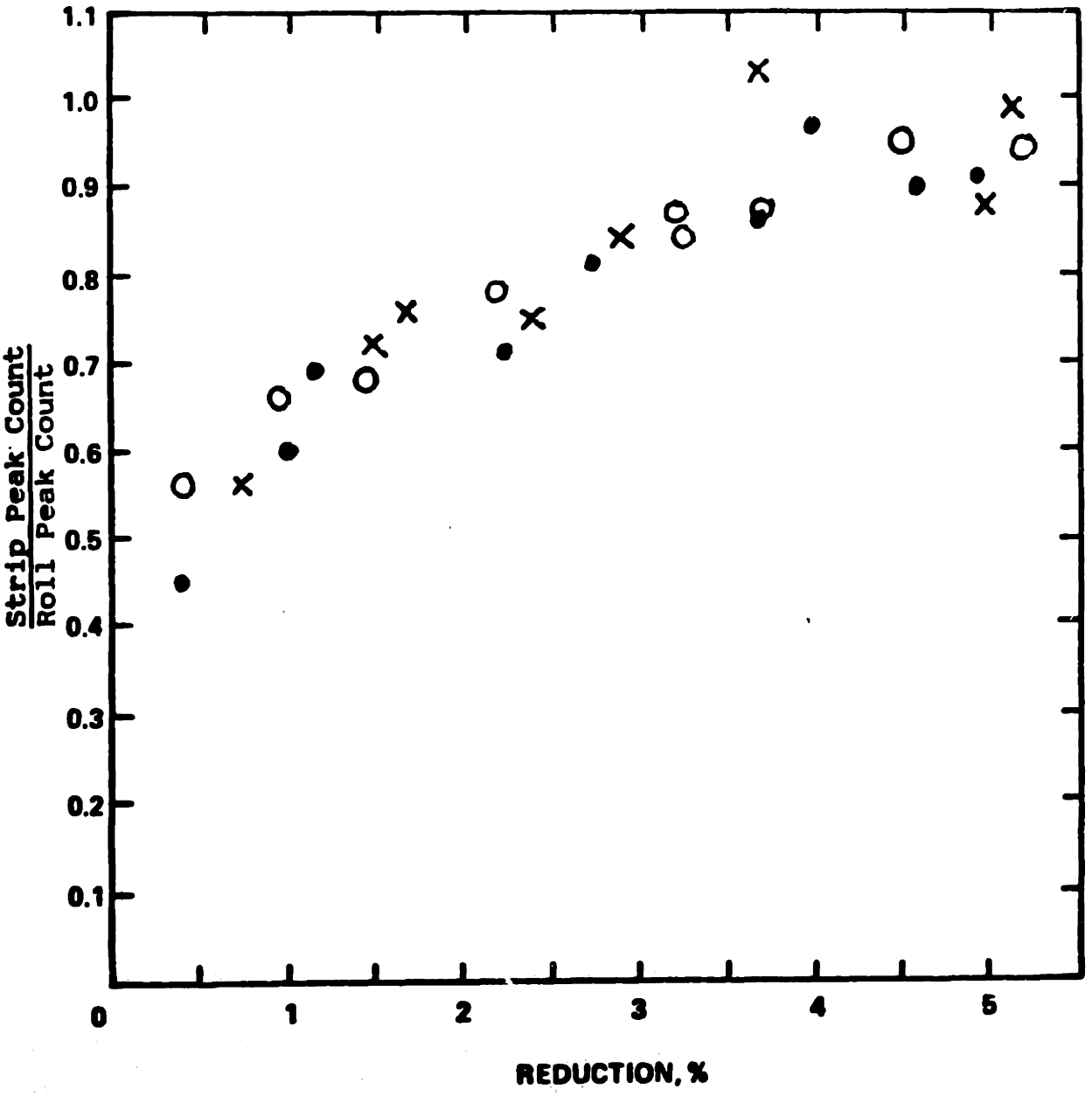

for example, the least squares estimate for the critical reduction required for complete transfer is 4.85 percent when all data for which transfer is less than 90 percent is used, but 4.45 percent for a fit based on data for which transfer is less than 70 percent. However, these departures from linearity, although noticeable in most cases, are rarely striking. In general, the linear relationship between roughness transfer and reduction postulated by Equation 2.4 was found to adequately represent the available data.

The strength of the relationship between transfer and reduction was such, in fact, that it was found convenient and natural to use this relationship as a gage to measure the effect of changing other variables on transfer. More precisely, the data cited in the following sections on the effects of other variables on transfer will be presented as a series of transfer versus reduction plots, and the slope of this plot (or, equivalently, the critical reduction required for complete transfer in a particular situation), will be used as a measure of transfer efficiency (e.g., a lower critical reduction implying more "efficient" transfer). This is by no means the only way in which this data could be presented, or even the most logical; in light of the theoretical discussion of Section II.5, it might seem more reasonable, for example, to plot transfer against a calculated arc length or maximum roll-bite pressure. The form of Equation 2.4, however, together with the ease with which reduction can be measured and controlled in both production and laboratory situations, and the difficulty of holding reduction constant

while changing other variables, makes the chosen manner of presentation by far the most practical. Moreover, the strong relationship between reduction and the more basic variables mentioned above minimizes any benefit to be gained by resorting to a less convenient method.

III.5 Effects of Roll Diameter and Roll Roughness on Transfer

With other rolling variables held constant, an increase in roll diameter should lengthen the arc of contact, increasing the maximum roll bite pressure and leading to a decrease in the reduction required for strip surface yield in shear, and thus to a decrease in the critical reduction required for complete transfer. Data in support of this conclusion is presented in Figures 3.4 to 3.7. The steel rolled in these tests came from different sections of two coils, and the inherent variation of surface properties within a single coil (e.g., the inner wraps of a coil often have a slightly different texture than the outer wraps, as will be demonstrated in Section III.13) is evident in the variation in reported initial surface properties. Nonetheless, at reductions sufficient to erase the effects of initial strip surface differences, a clear increase in transfer efficiency with increasing roll diameter is evident.

The textures of the Bliss- and Nash-mill rolls used in these tests did not match as closely as might have been desired. However, as can be seen from the data shown in Figures 3.8 and 3.9, variations in roll roughness do not seem to significantly influence the transfer process in dry-temper

Fig. 3.4 Roughness Transfer vs. Reduction
(ROLL DIAMETER VARIED)
Roll Diameter (inches): X 3.197 O 6.374
Roll Roughness: (microinches R_a): X 66 O 80.4
Strip: COIL B
initial roughness (microinches R_a): X 21.5 O 10.6
Mill Speed (feet/minute): 50
Strip Tensions (Psi): Entry X 10000 O 15000
Exit X 10000 O 15000
Lubrication: Dry

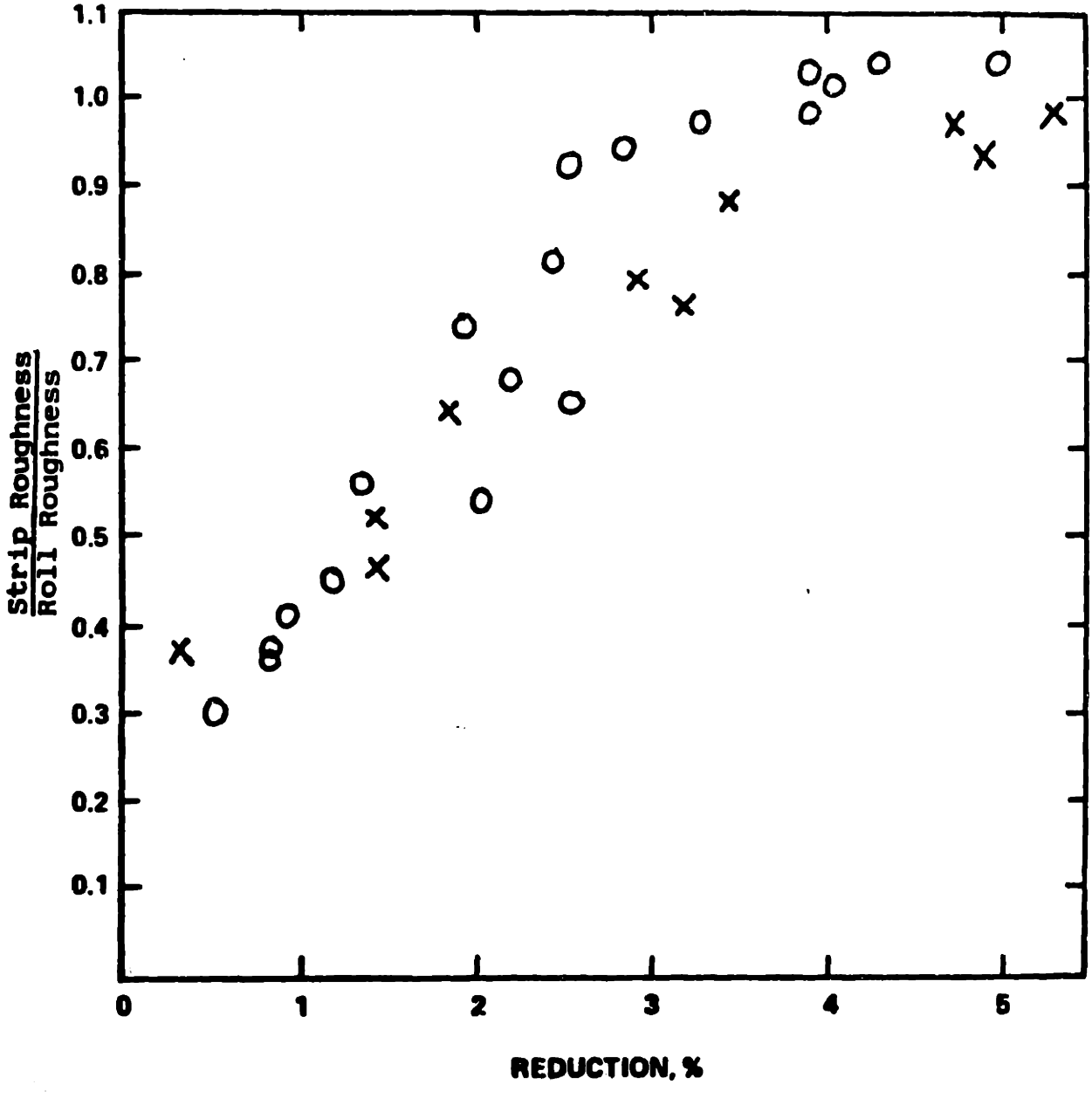

Fig. 3.5 Peak Count Transfer vs. Reduction
(ROLL DIAMETER VARIED)
Roll Diameter (inches): X 3.197 O 6.374
Roll Peak Count (ppi_{50}): X 131 O 100
Strip: COIL B
Initial peak count (ppi_{50}): X 109 O 36
Mill Speed (feet/minute): 50
Strip Tensions (psi): Entry X 10000 O 15000
Exit X 10000 O 15000
Lubrication: DRY

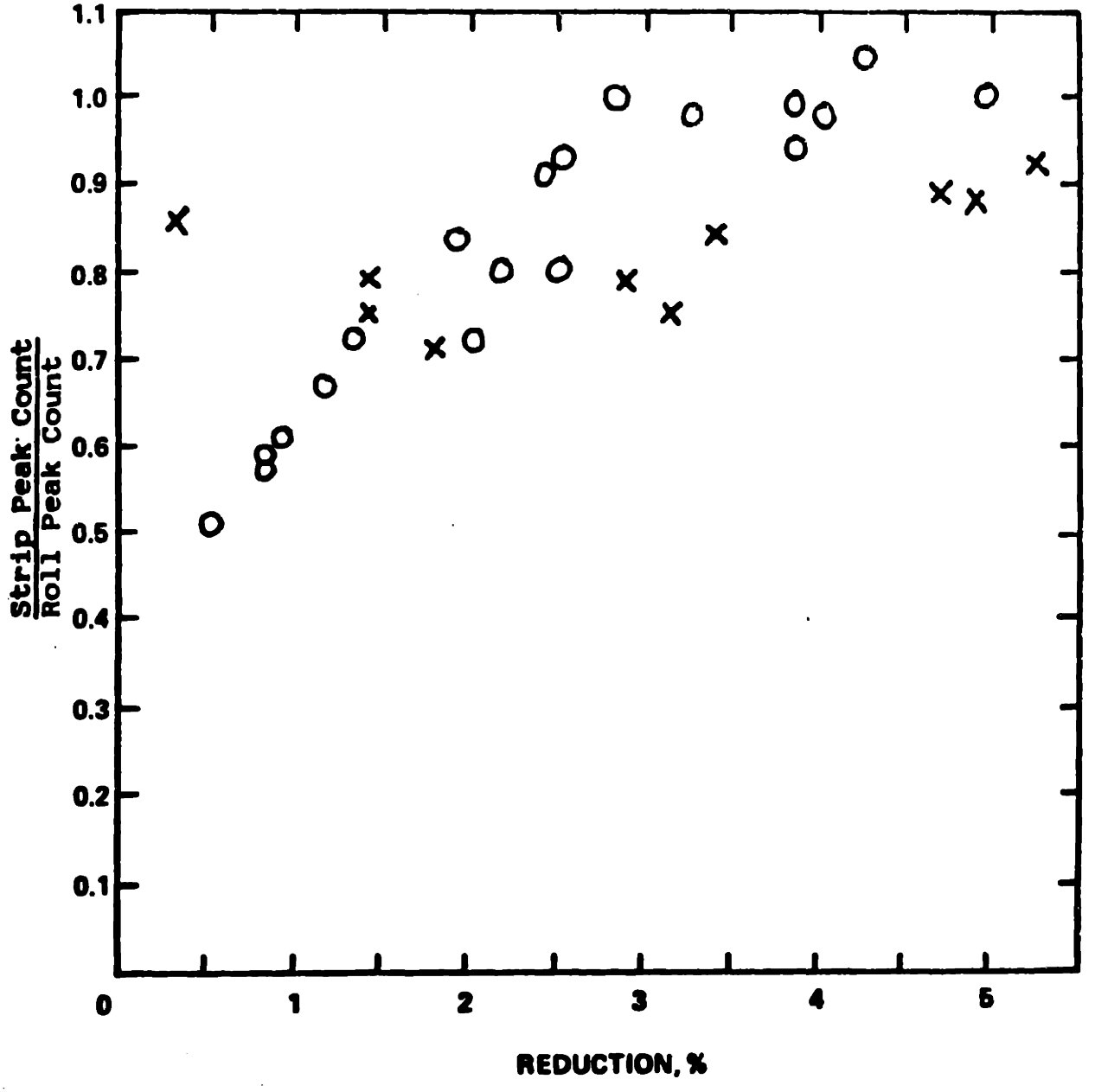

Fig. 3.6 Roughness Transfer vs. Reduction (ROLL DIAMETER VARIED)
Roll Diameter (inches): X 3.135 O 6.374
Roll Roughness: (microinches R_a): 61.2
Strip: COIL E2
initial roughness (microinches R_a): 19.6
Mill Speed (feet/minute): 100
Strip Tensions (Psi): Entry 10000
Exit 10000
Lubrication: Dry

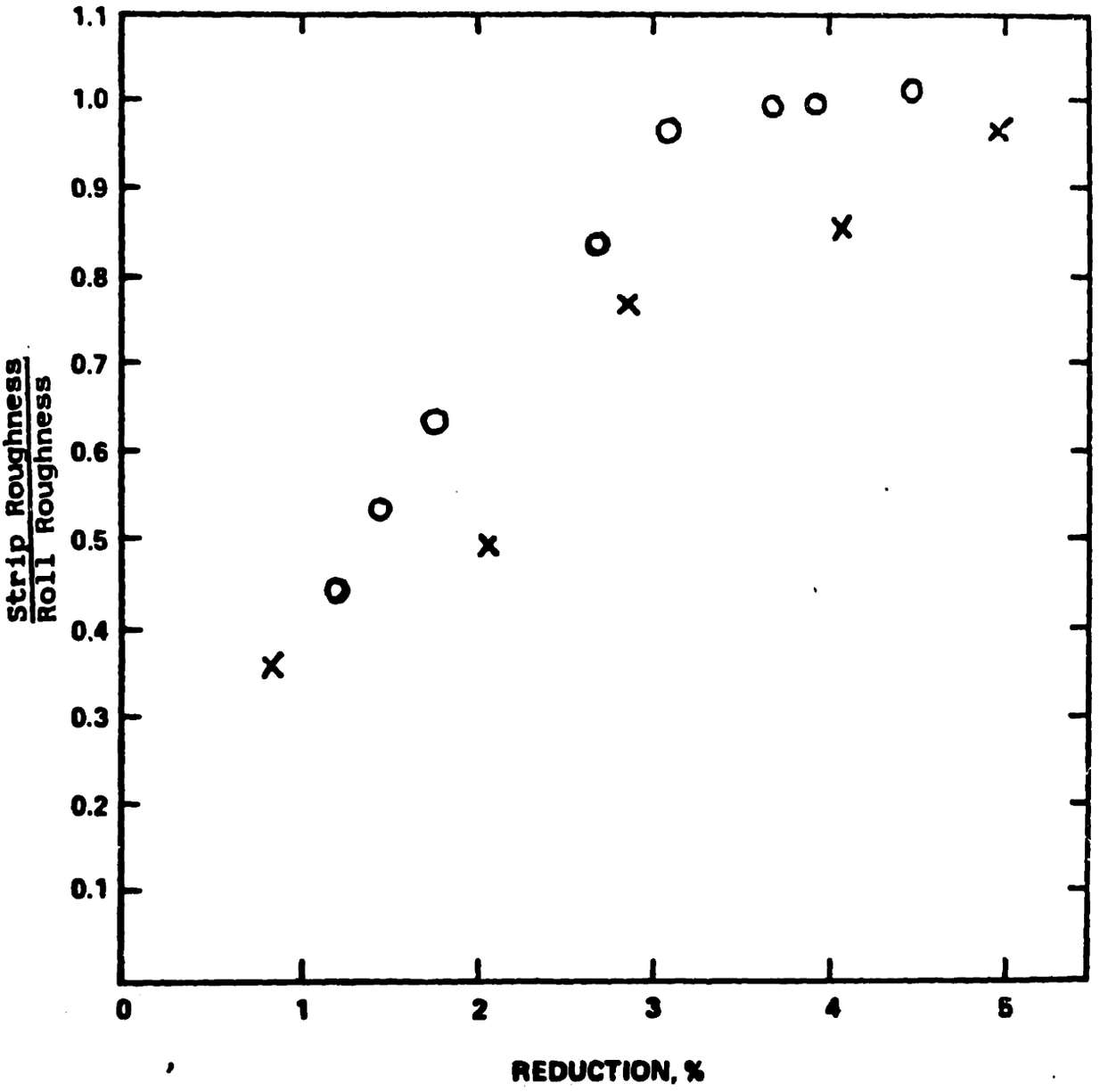

Fig. 3. 7 Peak Count Transfer vs. Reduction
(ROLL DIAMETER VARIED)
Roll Diameter (inches): X 3.135 O 6.374
Roll Peak Count (ppi_{50}): X 123.5 O 141
Strip: COIL E2
Initial peak count(ppi_{50}): X 74 O 95
Mill Speed (feet/minute): 100
Strip Tensions (psi): Entry 10000
Exit 10000
Lubrication: DRY

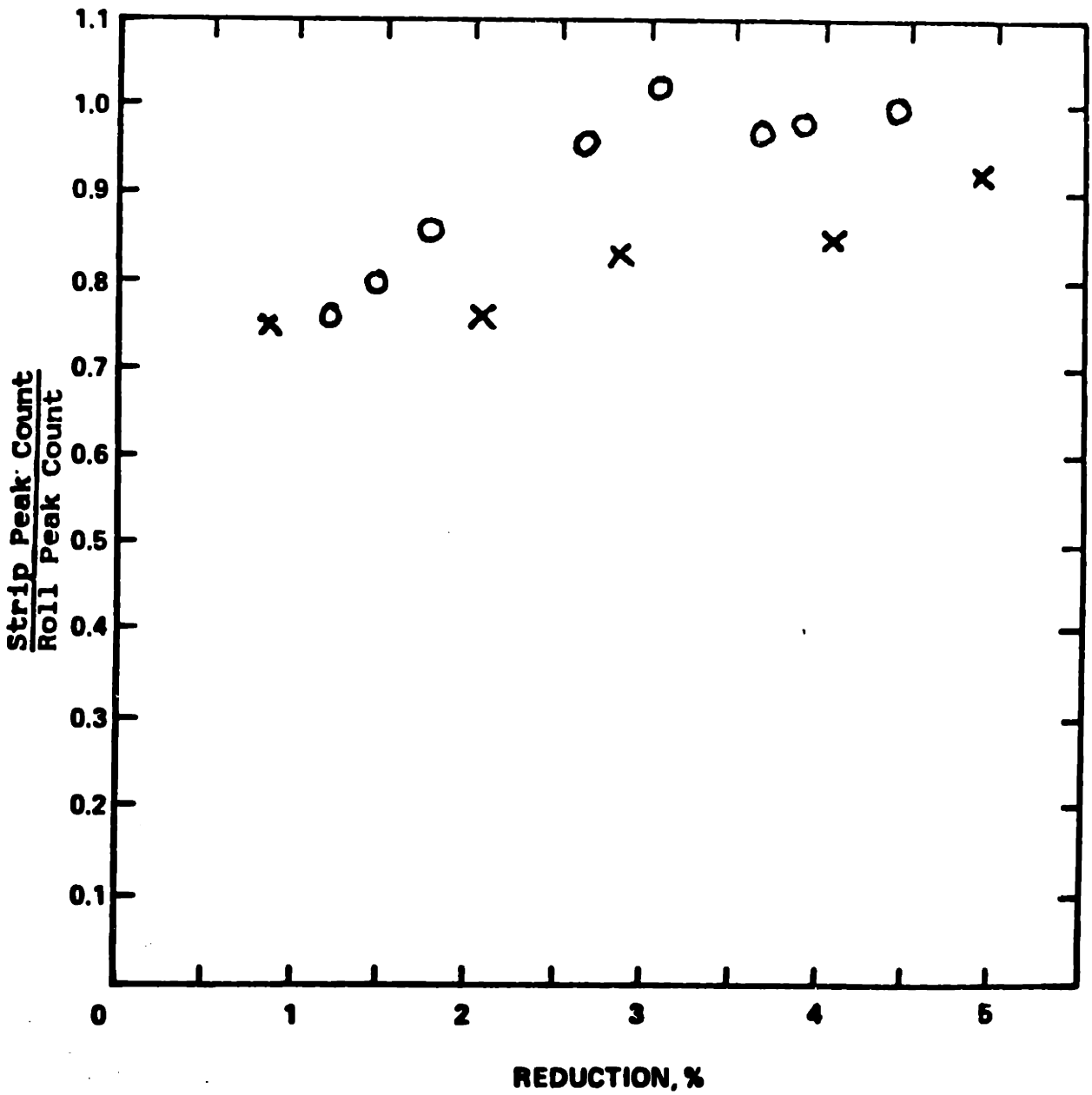

Fig. 3. 9 Roughness Transfer vs. Reduction
(ROLL ROUGHNESS VARIED)
Roll Diameter (inches): X 6.343 O 6.374
Roll Roughness: (microinches R_a): X 80.4 O 165.9 • 91.0
Strip: COIL B
initial roughness (microinches R_a): X 10.6 O 16.7 • 14.6
Mill Speed (feet/minute): 50
Strip Tensions (Psi): Entry X • 15000 O 10000
Exit X • 15000 O 10000
Lubrication: DRY

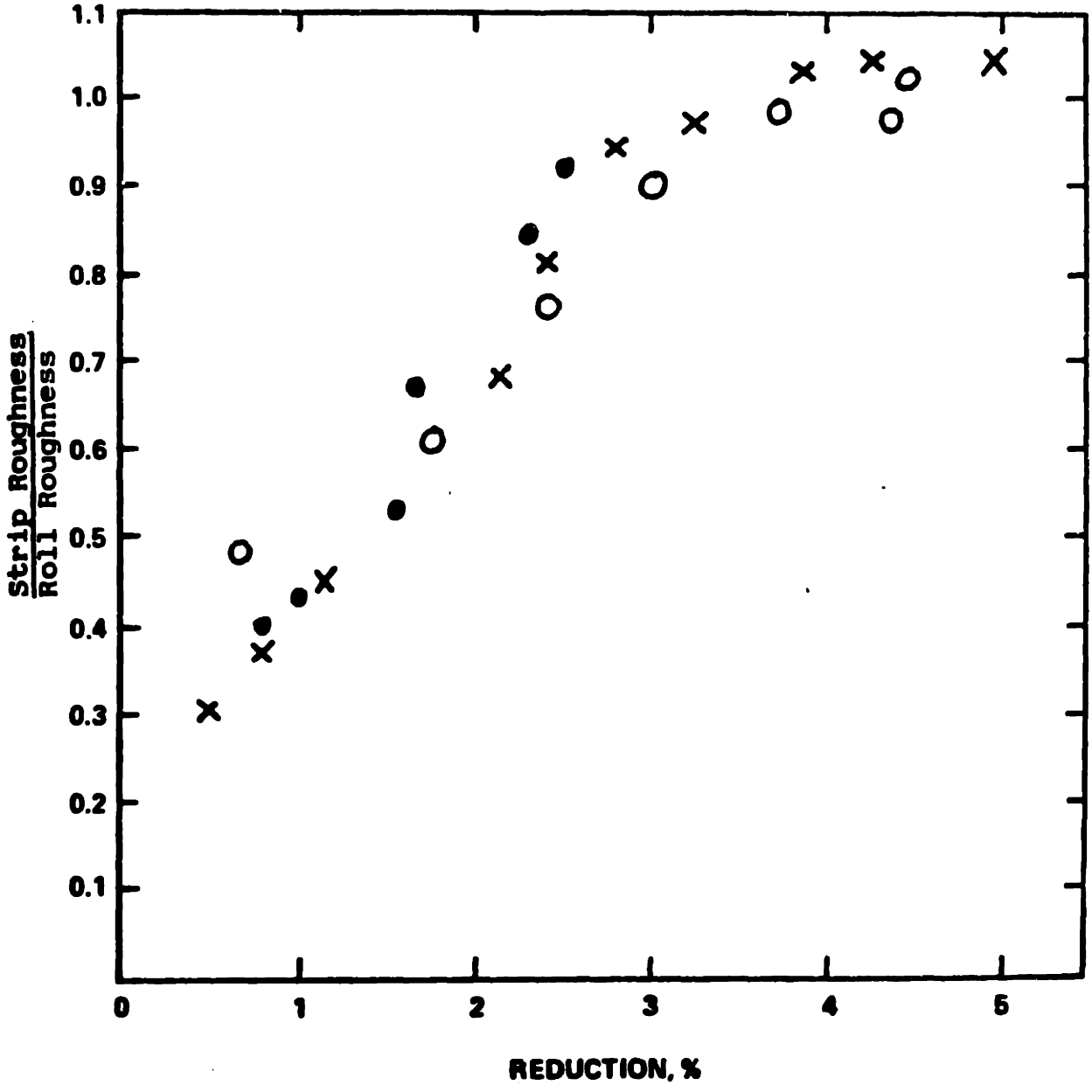

Fig. 3. 9 Roughness Transfer vs. Reduction
(ROLL ROUGHNESS VARIED)
Roll Diameter (inches): 6.374
Roll Roughness: (microinches R_a): X 58.3 O 67.6
Strip: COIL E3
initial roughness (microinches R_a): 20.7
Mill Speed (feet/minute): 100
Strip Tensions (Psi): Entry 10000
Exit 10000
Lubrication: DRY

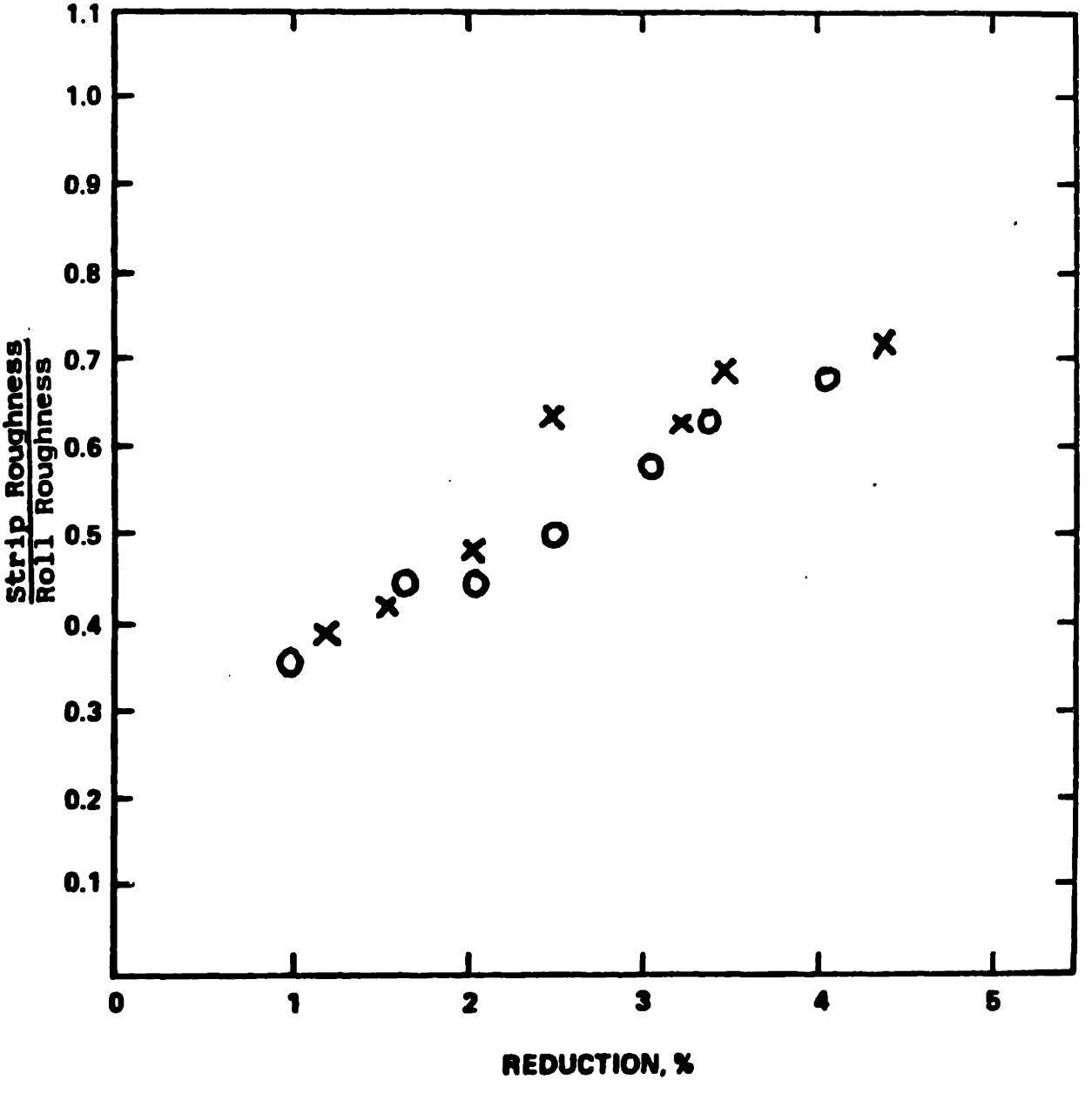

rolling. Such variations would be expected to influence surface transfer only if they give rise to corresponding variations in the coefficient of sliding friction in the roll bite, and, as discussed in Section II.5, experimental evidence (from low pressure experiments) has shown that this is generally not the case in dry sliding, if pathelogically rough or smooth surfaces are excluded.[57] This result seems to apply to the temper-rolling tests performed to produce Figures 3.8 and 3.9; the variation in roll roughness in these tests produced no variation in rolling force, indicating that the friction coefficient remained constant. Although these tests were performed at low speeds, it seems reasonable to expect this result to apply to dry-temper rolling at commercial speeds as well, (since, in dry sliding, the friction coefficient generally varies only slightly with sliding speed[60]) and to conclude that variations in roll roughness within the ranges usually encountered in production situations generally have little effect on roll bite friction and roughness transfer in commercial dry-temper rolling. It should be emphasized, however, that this conclusion is drawn from an extrapolation of the results of low speed tests. It should also be noted that a variation in roll roughness could very well alter lubricant entrapment, and thus roll bite friction and roughness transfer, in wet-temper rolling, particularly at commercial speeds. The author has conducted a limited number of tests in this area; however, these tests used materials and conditions identical (except for the presence of a lubricant) to those of the tests used to construct Figure 3.9,

and, due to the low mill speed and consequent lack of significant entrapment, produced virtually identical results. Data on the variation of rolling force with roll roughness in commercial wet-temepr rolling would give an indirect indication of the influence of roll roughness on roll-bite friction, and thus on transfer, in this area; such data, however, is not presently available.

Peak count transfer data corresponding to Figures 3.8 and 3.9 is not given, because the minimum peak height used to define a peak makes this parameter extremely sensitive to absolute roughness values. A roll with a roughness of 90 microinches, for instance, will transfer all of its peaks at a lower reduction than one with a roughness of 40 microinches (if a peak height definition of 50 microinches is used), even if the variation in percent roughenss transfer with reductuion is identical between the two cases. Finally, some of the data compared in Figures 3.4 to 3.9 was taken from tests in which slightly different levels of strip tension were used. The effect of tension on transfer will be discussed in Section III.10; in these tests, however, the changes in tension were small compared to the compressive yield stress of the strip in the roll bite, and consequently, as will be shown, probably had little effect on transfer (cf. also Figures 3.2 and 3.3).

III.6 Effect of Strip Grade on Transfer

As was noted in Section II, the plastic arc length in temper rolling should, in general, increase with compressive yield strength of the strip. Consequently, transfer

efficiency should increase with increasing strip yield strength, the difference being most marked when comparing annealed strip with strip that has undergone substantial prior cold work. This trend is illustrated by Figures 3.10 and 3.11. The materials tested in this instance were from different coils, but in general the author has found that full-hard strip gives complete transfer at a significantly lower reduction than annealed or temper-rolled stock; typical values are 3 percent for full-hard material versus 4 to 5 percent for comparable annealed material. This result is of limited practical benefit, since commercial sheet-temper rolling is generally carried out only on annealed (or, in the case of the second stand of a tandem temper mill, lightly reduced) strip. The result is, however, of some theoretical value, since it is consistent with the theoretical discussion given in Part II, but somewhat contrary to intuition; a priori, one would probably expect that it would be more difficult to press the asperities of the roll into a hard, strong surface than into a softer one.

III.7 Effect of Lubrication on Transfer

As was discussed in Section II.5, the introduction of a lubricant into the roll bite in temper rolling would significantly affect the mechanics of the process only if significant lubricant entrapment within the roll bite itself occurred. Such entrapment would reduce the friction coefficient at the roll-strip interface; this, in turn, would increase the critical reduction required for complete transfer and reduce transfer efficiency as compared to

Fig. 3.10 Roughness Transfer vs. Reduction
(Strip grade Varied)
Roll Diameter (inches): 3.197
Roll Roughness: (microinches R_a): X 66 059
Strip: X COIL C (FULL HARD) O COIL A (Annealed)
initial roughness (microinches R_a): X 14.3 O 10
Mill Speed (feet/minute): 50
Strip Tensions (Psi): Entry 10000
Exit 10000
Lubrication: Dry

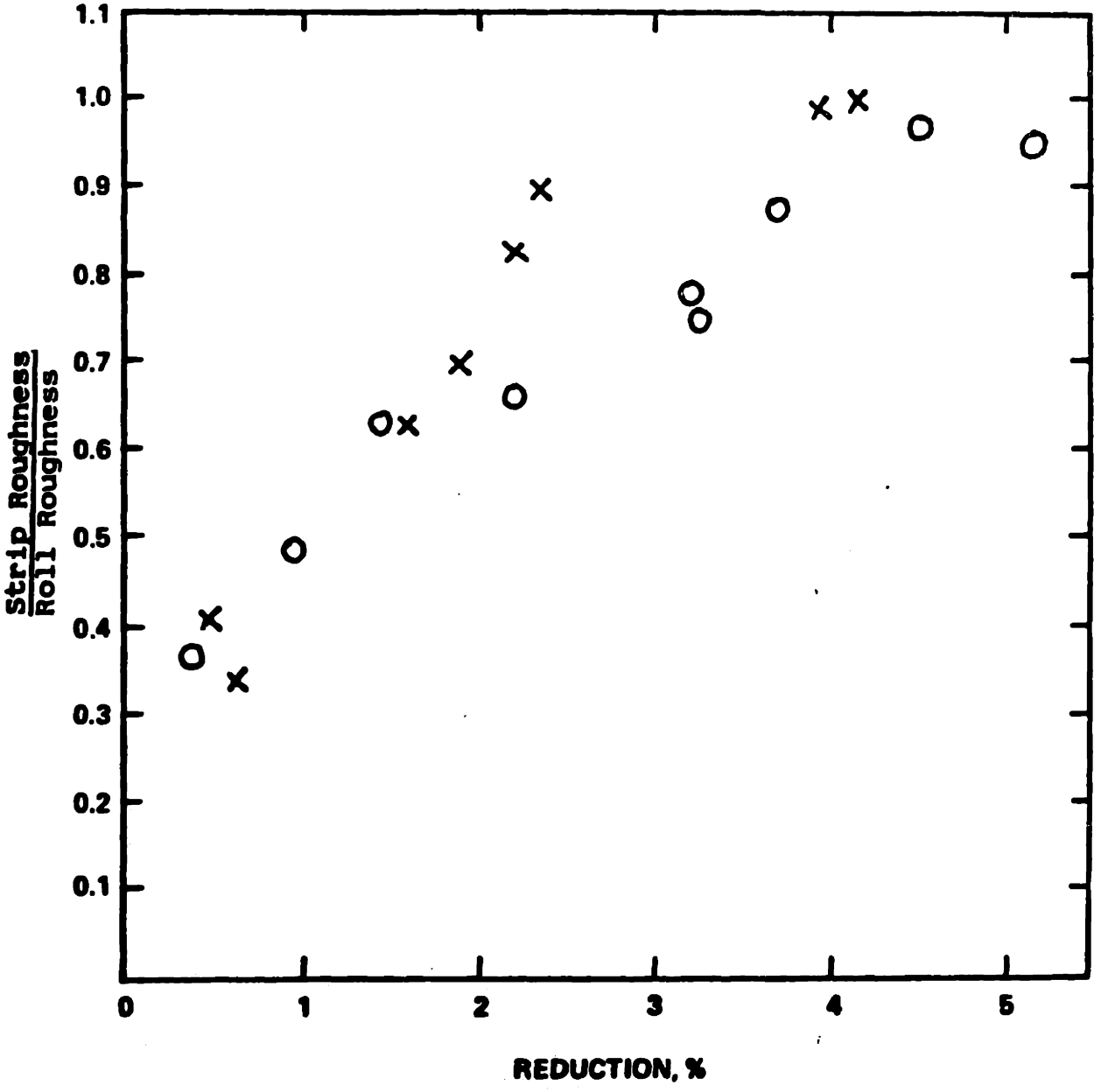

Fig. 3.11 Peak Count Transfer vs. Reduction
(STRIP GRADE VARIED)

Roll Diameter (inches): 3.197
Roll Peak Count (ppi_{50}): X 131 O 154
Strip: X COIL C (FULL HARD) O COIL A (Annealed)
Initial peak count (ppi_{50}): X 92 O 28
Mill Speed (feet/minute): 50
Strip Tensions (psi): Entry 10000
Exit 10000
Lubrication: DRY

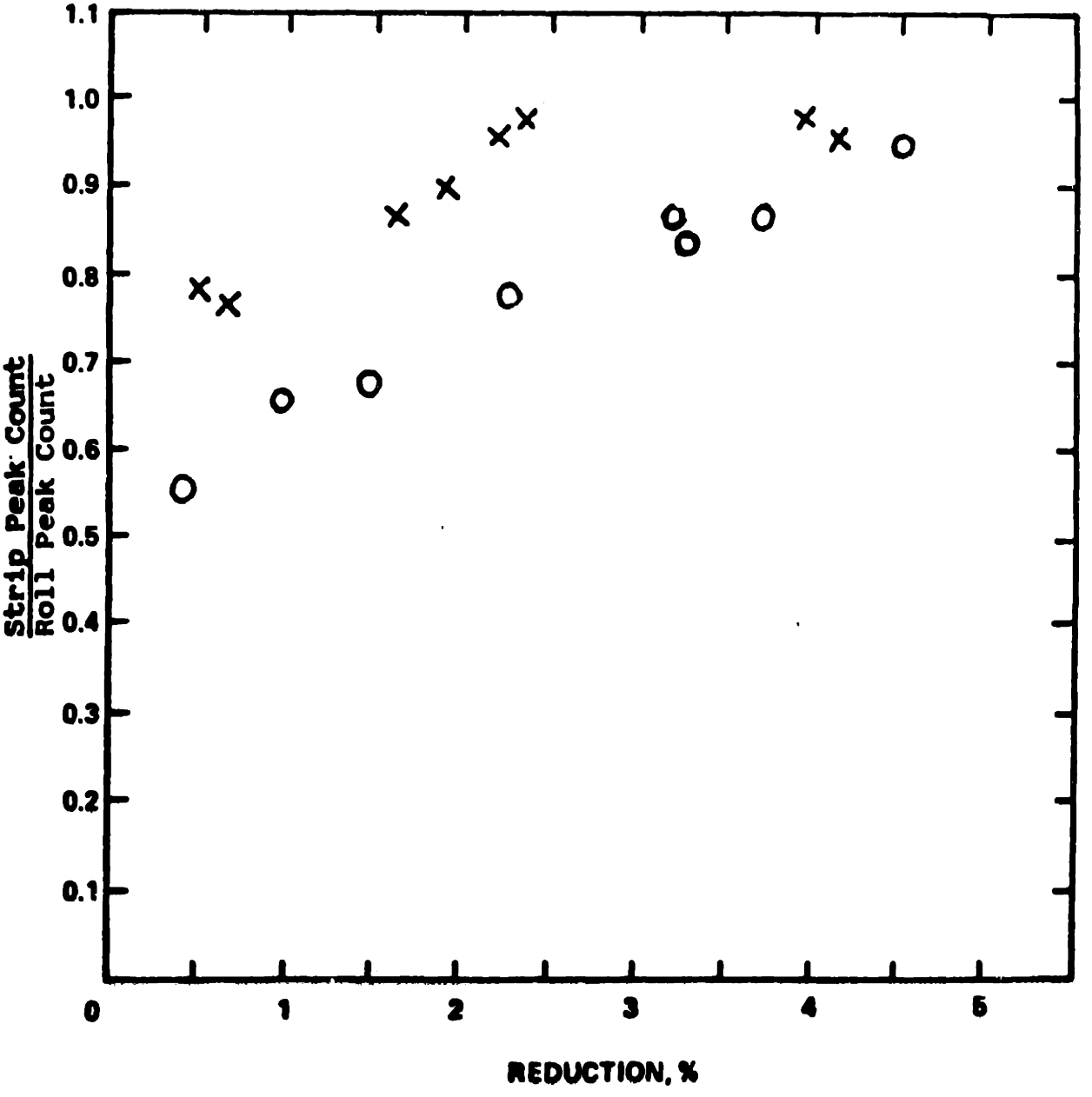

corresponding dry-temper rolling conditions. Qualitatively, entrapment should increase, and transfer efficiency should decrease, with increasing lubricant viscosity and mill speed. These trends are illustrated by Figures 3.12 to 3.15, which present the results of tests performed with lubricants of differing viscosities at two mill speeds. Three lubricants were used; water, a typical temper-rolling lubricant with a viscosity roughly equal to soapy water, and a tallow based tandem tin-mill rolling oil with a static viscosity of 233 S.U.S. units at 104° F. As can be seen, at low speeds significant entrapment occurs only with relatively viscuous lubricants, but, as mill speed increases, noticeable entrapment occurs at low viscosities as well. Since commercial wet-temper mills operate at speeds roughly an order of magnitude greater than those used in these tests, percent transfer levels in commercial wet-temper rolling should be significantly lower than levels in dry-temper rolling under analogous conditions, even with the relatively watery lubricants usually employed. The quantitative effect of lubricant entrapment on transfer efficiency under commercial conditions is difficult to assess at this point, but will be discussed in broad terms in Section III.13.

III.8 Effect of Mill Speed on Transfer

In considering the effect of mill speed on transfer, a distinction must be made between wet- and dry-temper rolling. As was shown in the previous section, increasing mill speed in wet-temper rolling results in increased lubricant entrapment in the roll bite and decreased transfer

Fig. 3.12 Roughness Transfer Vs. Reduction
(LUBRICATION VARIED)
Roll Diameter (inches): 3.197
Roll Roughness: (microinches R_a): ■ 54 ● 54 ♦ 51 ▲ 64.7
Strip: COIL A
initial roughness (microinches R_a): 10
Mill Speed (feet/minute): 50
Strip Tensions (Psi): Entry 10000
Exit 10000

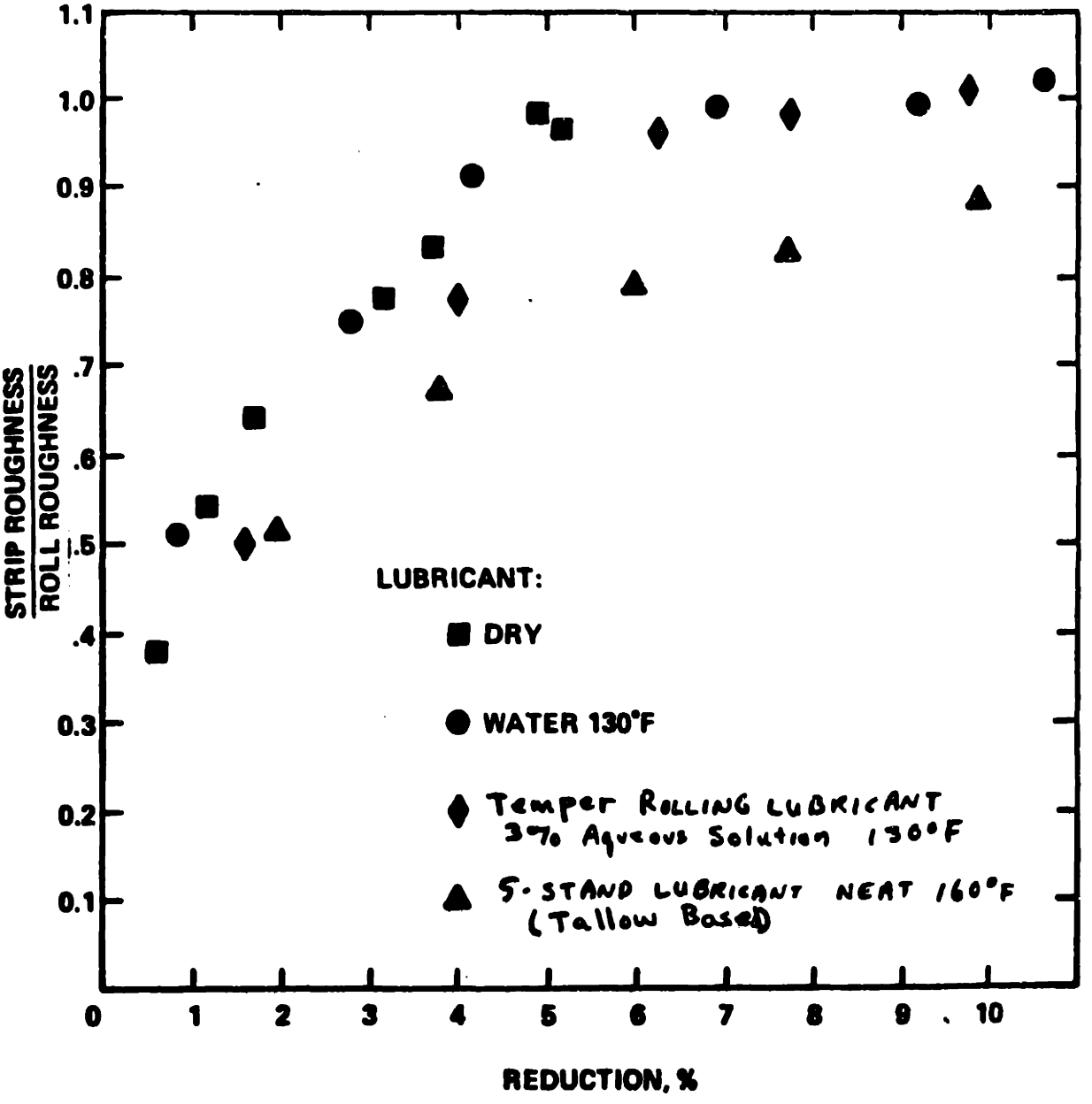

Fig. 3.13 Peak Count Transfer vs. Reduction
(LUBRICATION VARIED)
Roll Diameter (inches): 3.197
Roll Peak Count (ppi_{50}): ■154 ●141 ♦136 ▲146.5
Strip: COIL A
Initial peak count (ppi_{50}): 28
Mill Speed (feet/minute): 50
Strip Tensions (psi): Entry 10000
Exit 10000

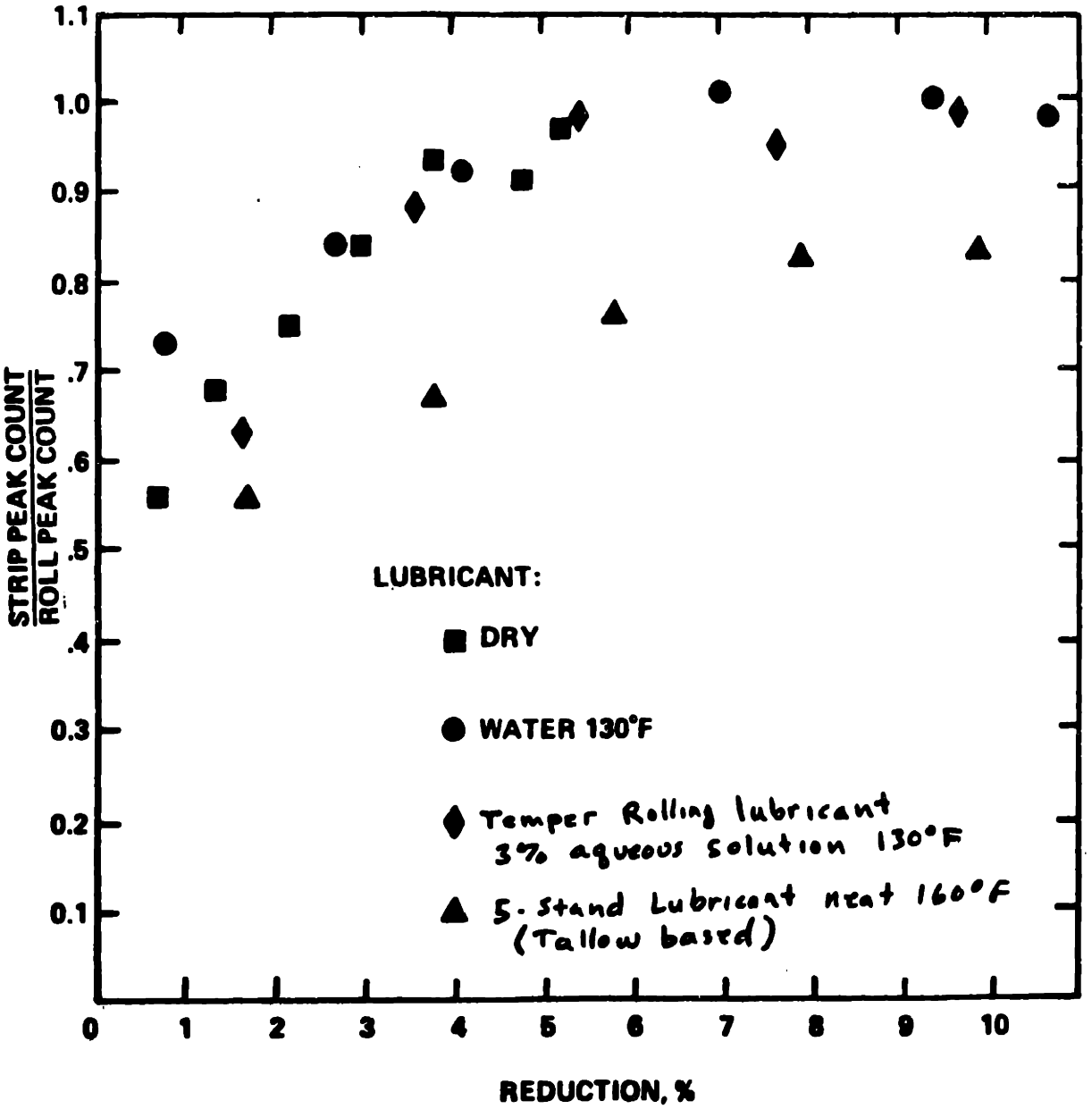

Fig. 3.14 Roughness Transfer vs. Reduction
(Lubrication Varied)
Roll Diameter (inches): 3.197
Roll Roughness: (microinches R_a): ■ 66 ◆62.5 ▲ 63.9
Strip: COIL B
initial roughness (microinches R_a): ■ 21.5 ◆▲ 16.7
Mill Speed (feet/minute): 400
Strip Tensions (Psi): Entry 10000
Exit 10000

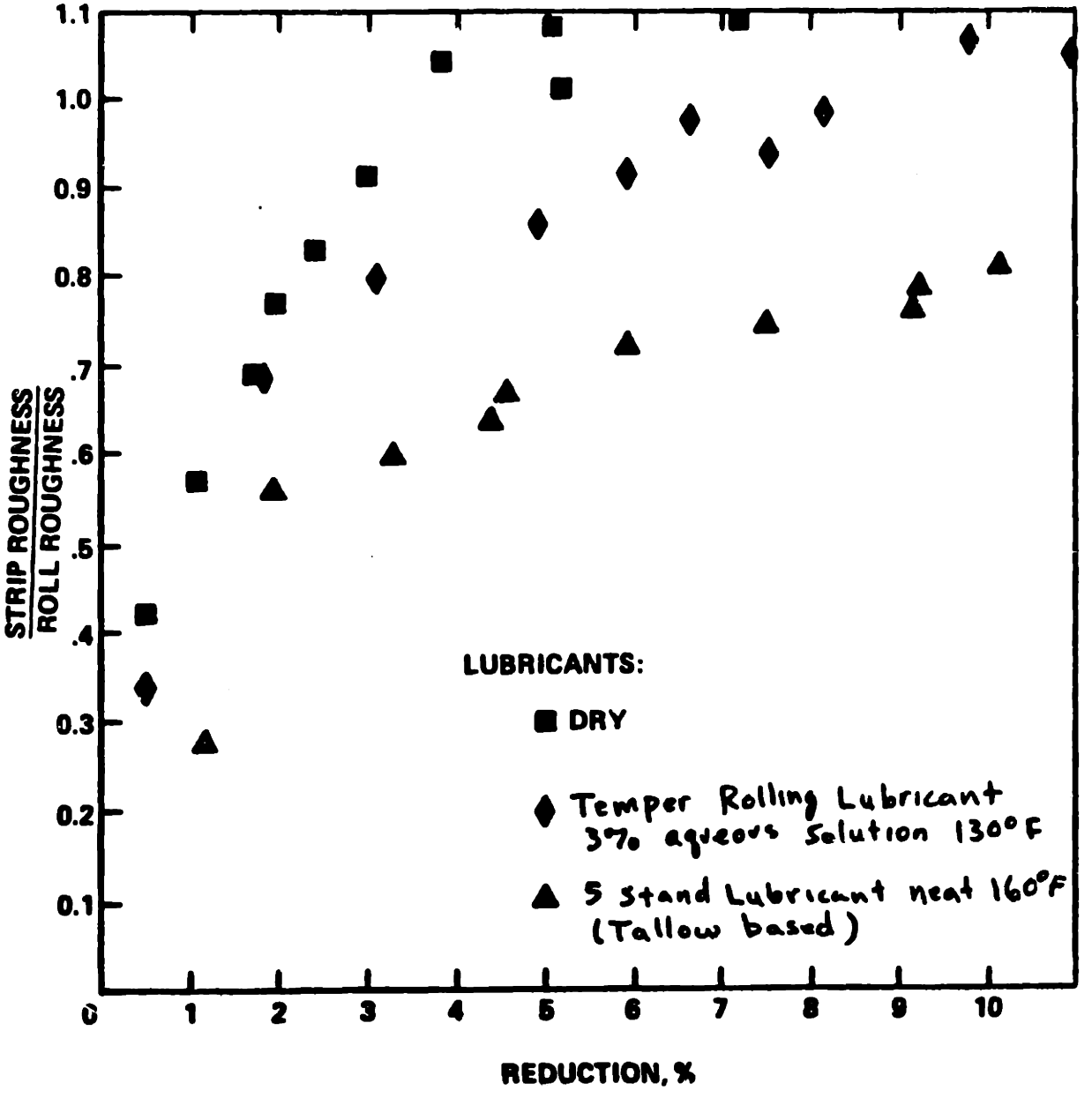

Fig. 3.15 Peak Count Transfer vs. Reduction
(LUBRICATION VARIED)
Roll Diameter (inches): 3.197
Roll Peak Count (ppi_{50}): ■ 131 ♦ 139 ▲ 141.5
Strip: COIL B
Initial peak count(ppi_{50}): ■ 109 ♦ ▲ 87
Mill Speed (feet/minute): 400
Strip Tensions (psi): Entry 10000
Exit 10000

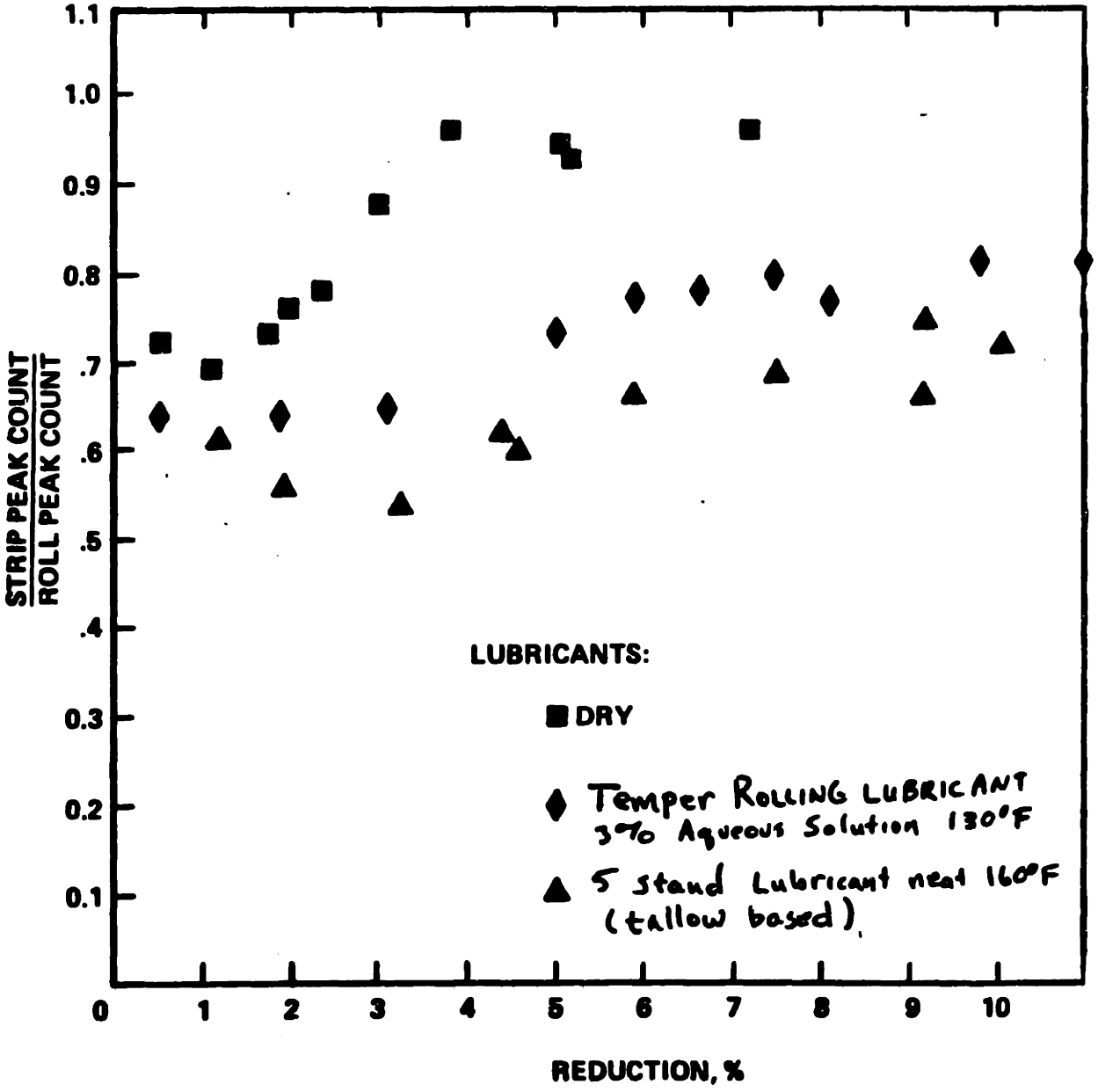

efficiency. Increasing mill speed, however, also increases the compressive yield stress of the strip somewhat, which in turn should increase plastic arc length under otherwise identical conditions. In wet-temper rolling, the effects of this increase are most likely negligible when compared to the effects of increasing lubricant entrapment. In dry-temper rolling, however, an increase in plastic arc length and strip yield stress should lead to increases in both transfer efficiency and rolling force. Figures 3.16 to 3.24 show the results of three sets of dry-temper rolling tests in which the mill speed was varied. As can be seen, transfer does not appear to be noticeably sensitive to changes in mill speed, except in cases when these changes would be expected to cause substantial percentile increases in the compressive yield strength of the strip and, consequently, significant increases in arc length. Thus no noticeable change in transfer is evident when mill speed is increased by a factor of two when rolling annealed strip (Figures 3.19 and 3.20) or a factor of six when rolling heavily work-hardened strip (Figures 3.22 and 3.23). As can be seen from Figures 3.21 and 3.24, the changes in mill speed did not significantly affect rolling force data in these cases, either. For a (roughly) order of magnitude increase in mill speed when rolling annealed strip, however, noticeable increases in both rolling force and transfer efficiency (Figures 3.16, 3.17, and 3.18) are evident. Overall, this data is qualitatively consistent with the theoretical discussion given in Part II, although the influence of mill speed on transfer

Fig. 3.16 Roughness Transfer vs. Reduction
(MILL SPEED VARIED)
Roll Diameter (inches): 3.197
Roll Roughness: (microinches R_a): ■ 66 ○ 61.8
Strip: COIL B
initial roughness (microinches R_a): ■ 21.5 ○ 16.7

Strip Tensions (Psi): Entry 10000
Exit 10000

Lubrication: Dry

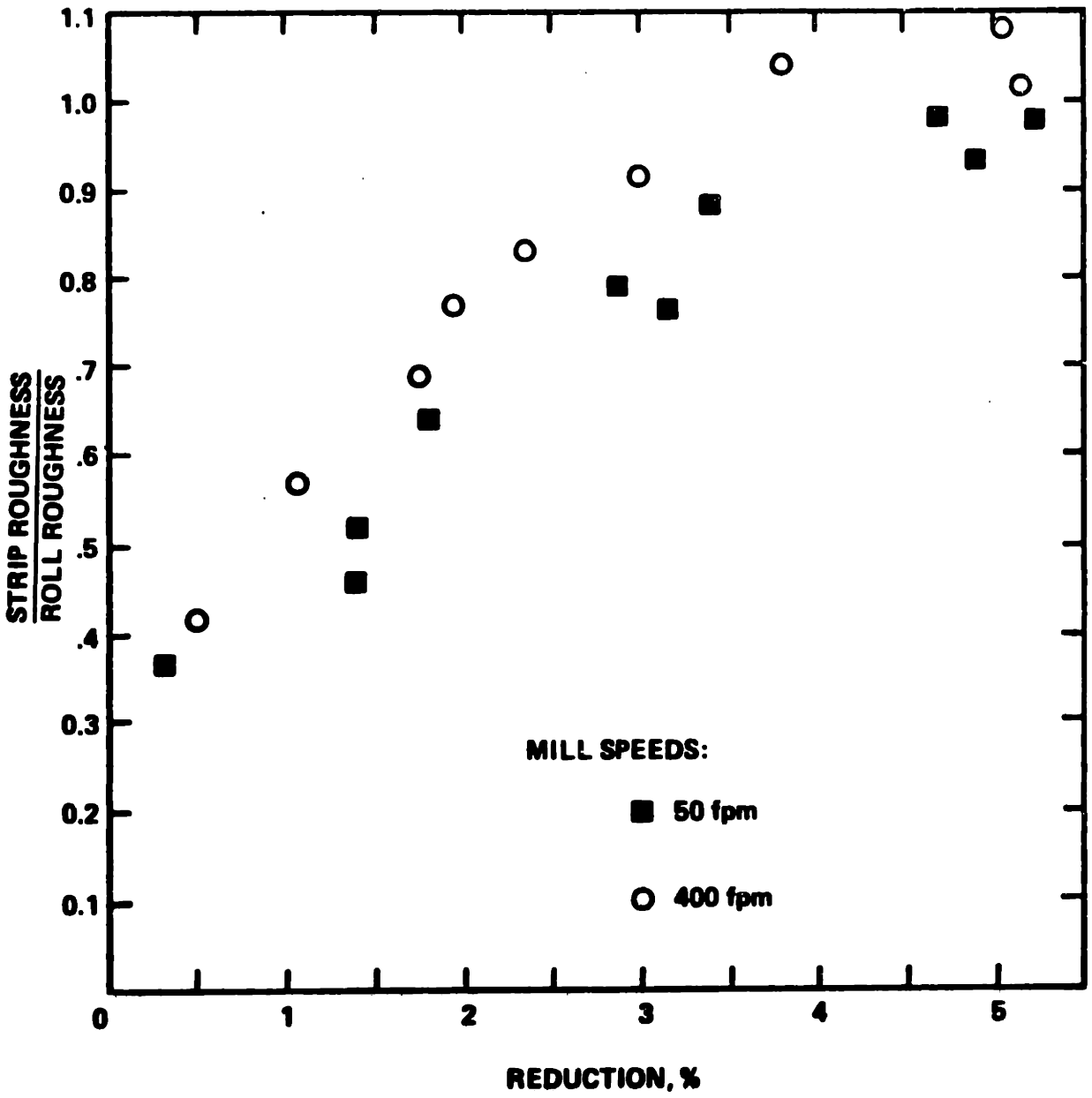

Fig. 3.17 Peak Count Transfer vs. Reduction
(MILL SPEED VARIED)

Roll Diameter (inches): 3.197
Roll Peak Count (ppi_{50}): ■ 131 ○ 136
Strip: COIL B
Initial peak count (ppi_{50}): ■ 109 ○ 87

Strip Tensions (psi): Entry 10000
Exit 10000

Lubrication: DRY

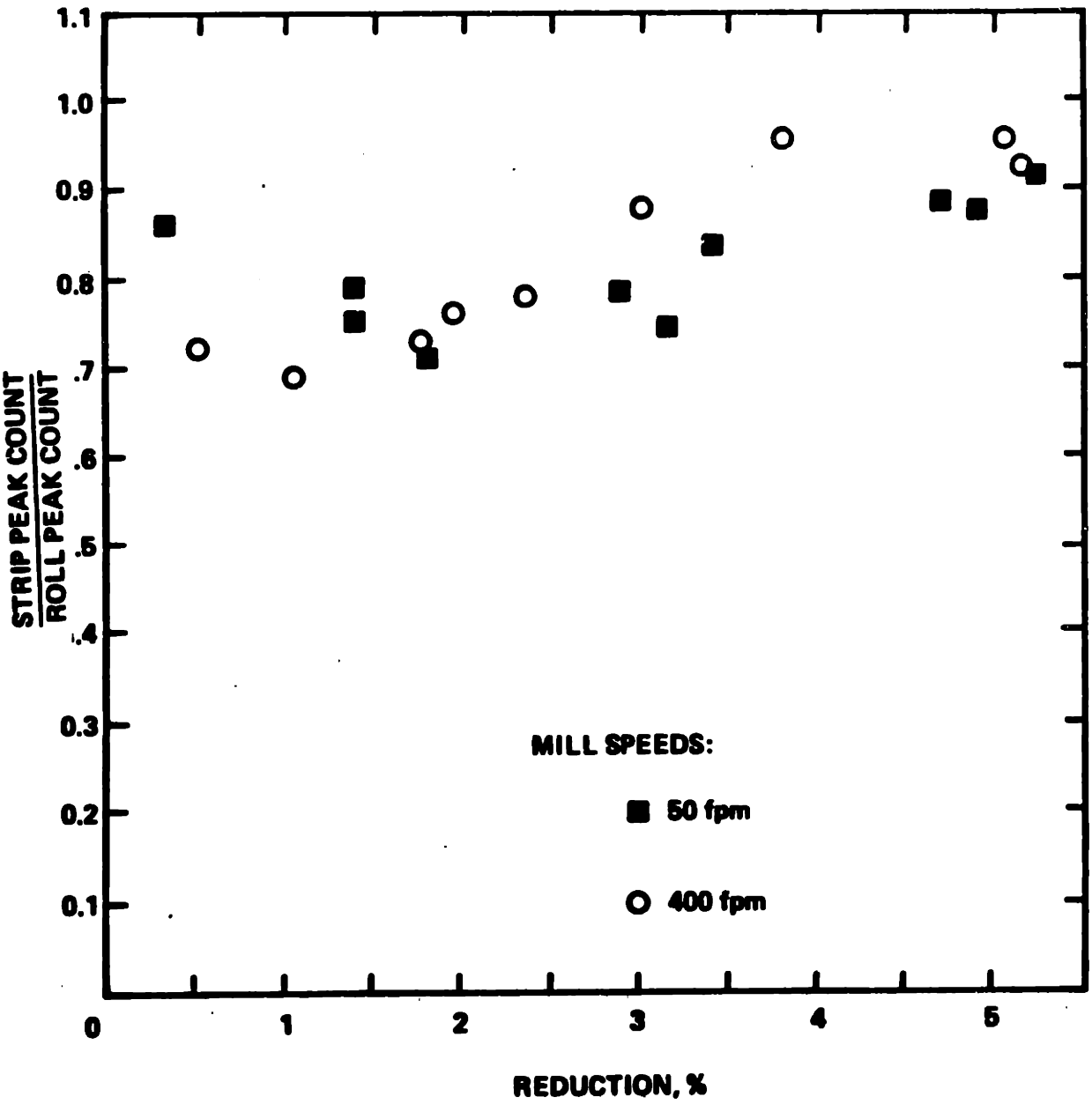

Fig. 3.18 SPECIFIC ROLLING FORCE VS. REDUCTION
(MILL SPEED VARIED)

Roll Diameter (inches): 3.197

Strip: COIL B

Mill Speed (feet/minute): × 50 ○ 400

Strip Tensions (psi): Entry 10000
Exit 10000

Lubrication: DRY

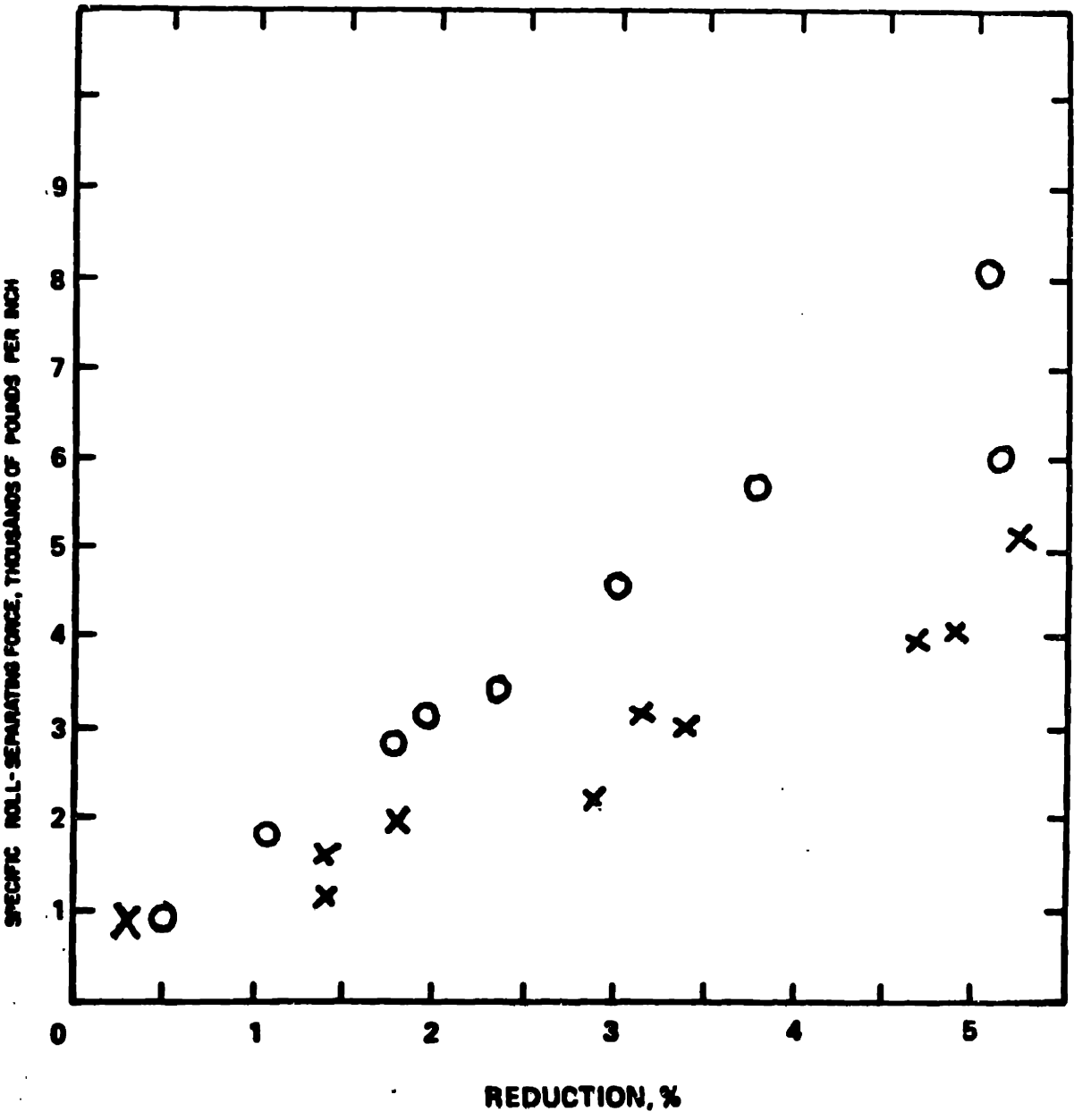

Fig. 3. 19 Roughness Transfer vs. Reduction
(MILL SPEED VARIED)

Roll Diameter (inches): 3.135
Roll Roughness: (microinches R_a): 61.2
Strip: COIL E2
initial roughness (microinches R_a): 19.2
Mill Speed (feet/minute): X 100 O 220
Strip Tensions (Psi): Entry 10000
Exit 10000
Lubrication: Dry

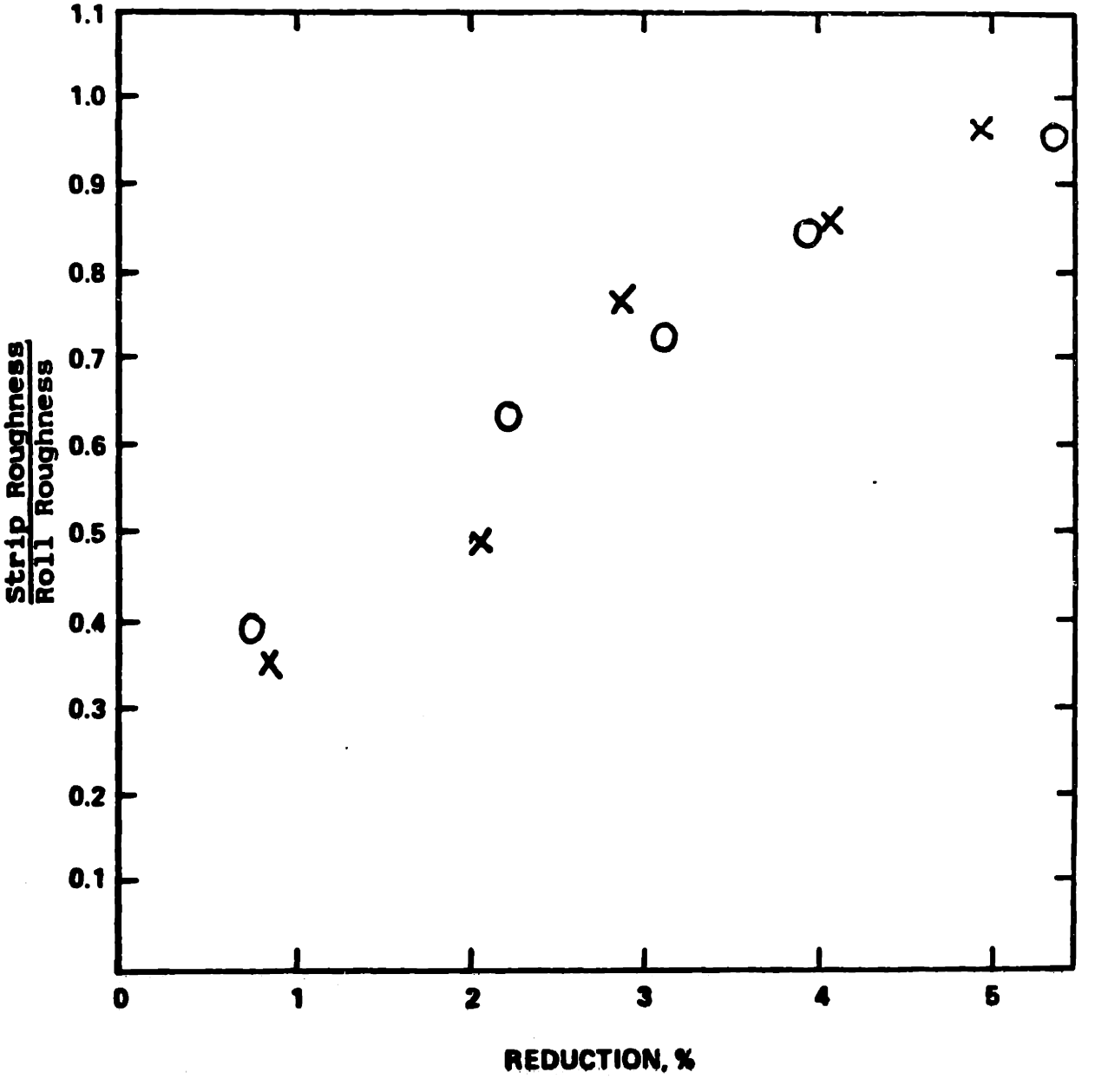

Fig. 3. 20 Peak Count Transfer vs. Reduction
(MILL SPEED VARIED)

Roll Diameter (inches): 3.135
Roll Peak Count (ppi_{50}): 123.5
Strip: COIL E2
Initial peak count (ppi_{50}): 74
Mill Speed (feet/minute): x 100 o 220
Strip Tensions (psi): Entry 10000
Exit 10000

Lubrication: DRY

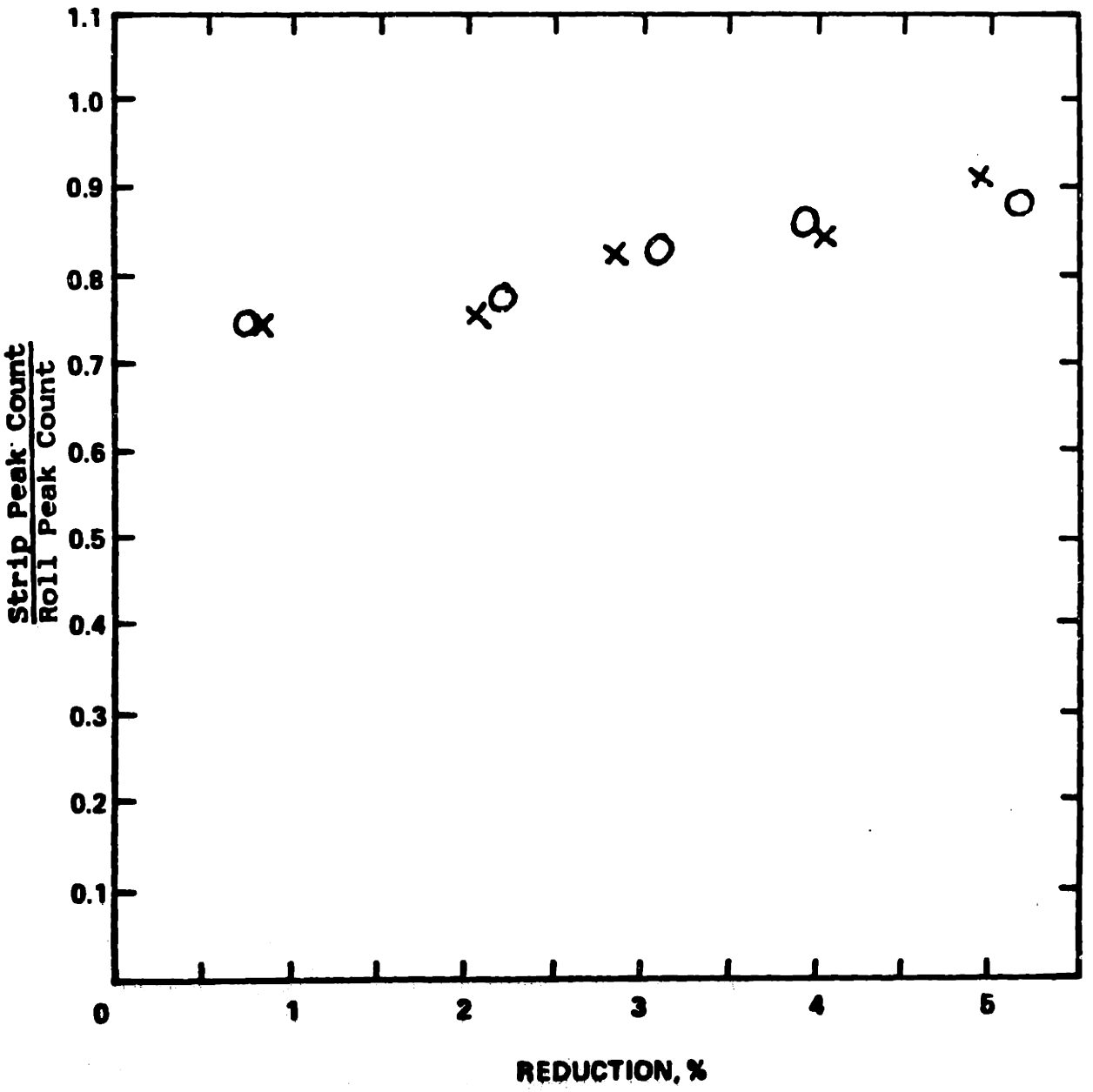

Fig. 3.21 SPECIFIC ROLLING FORCE VS. REDUCTION
(MILL SPEED VARIED)

Roll Diameter (inches): 3.1135

Strip: COIL E2

Mill Speed (feet/minute): X 100 O 220

Strip Tensions (psi): Entry 10000
Exit 10000

Lubrication: DRY

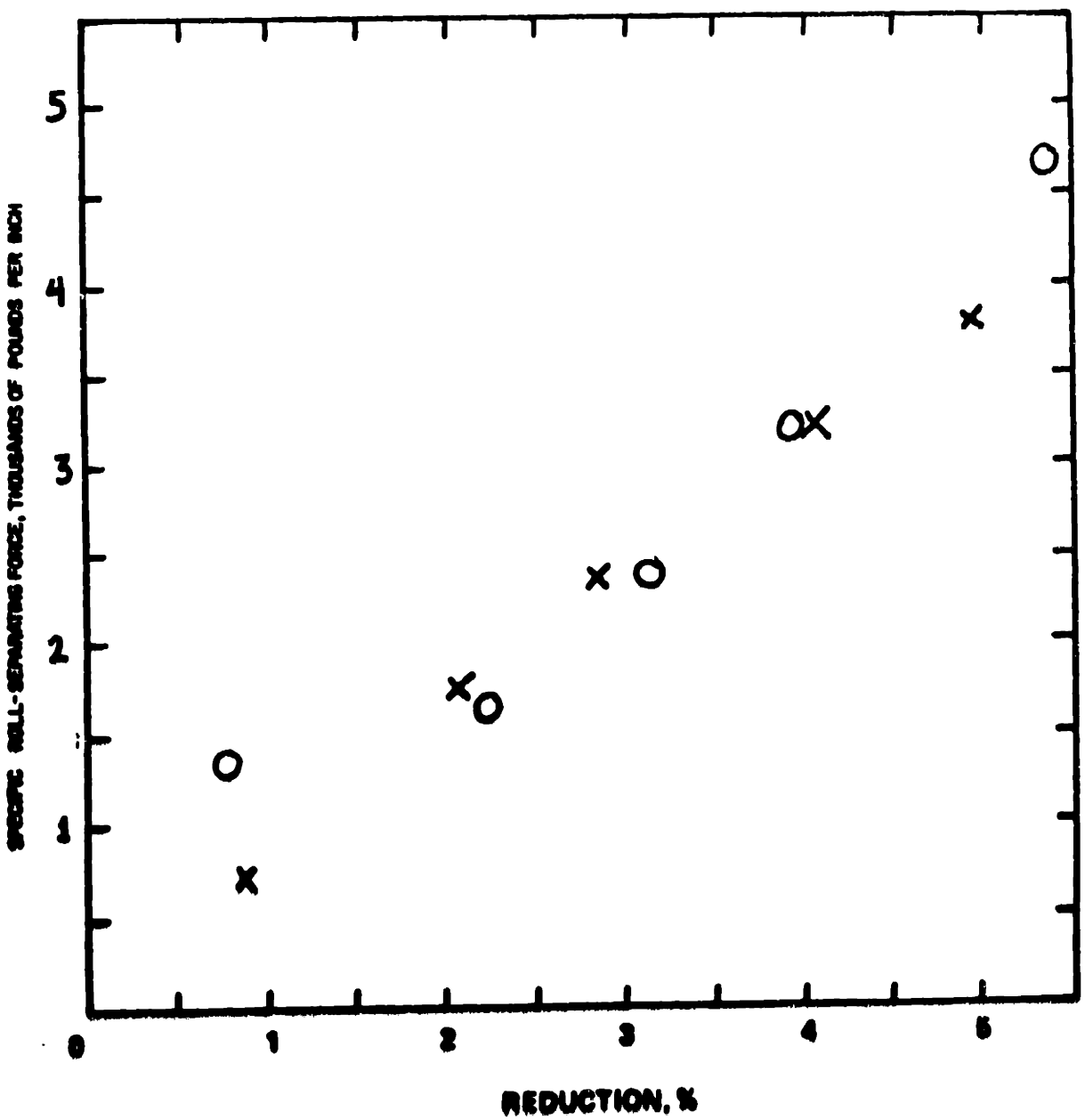

Fig. 3.22 Roughness Transfer vs. Reduction
(MILL SPEED VARIED)

Roll Diameter (inches): 3.197
Roll Roughness: (microinches R_a): × 63.2 ○ 56.3
Strip: COIL C
initial roughness (microinches R_a): × 14.3 ○ 9.6
Mill Speed (feet/minute): × 50 ○ 315
Strip Tensions (Psi): Entry × 11000 ○ 15000
Exit × 11000 ○ 15000
Lubrication: Dry

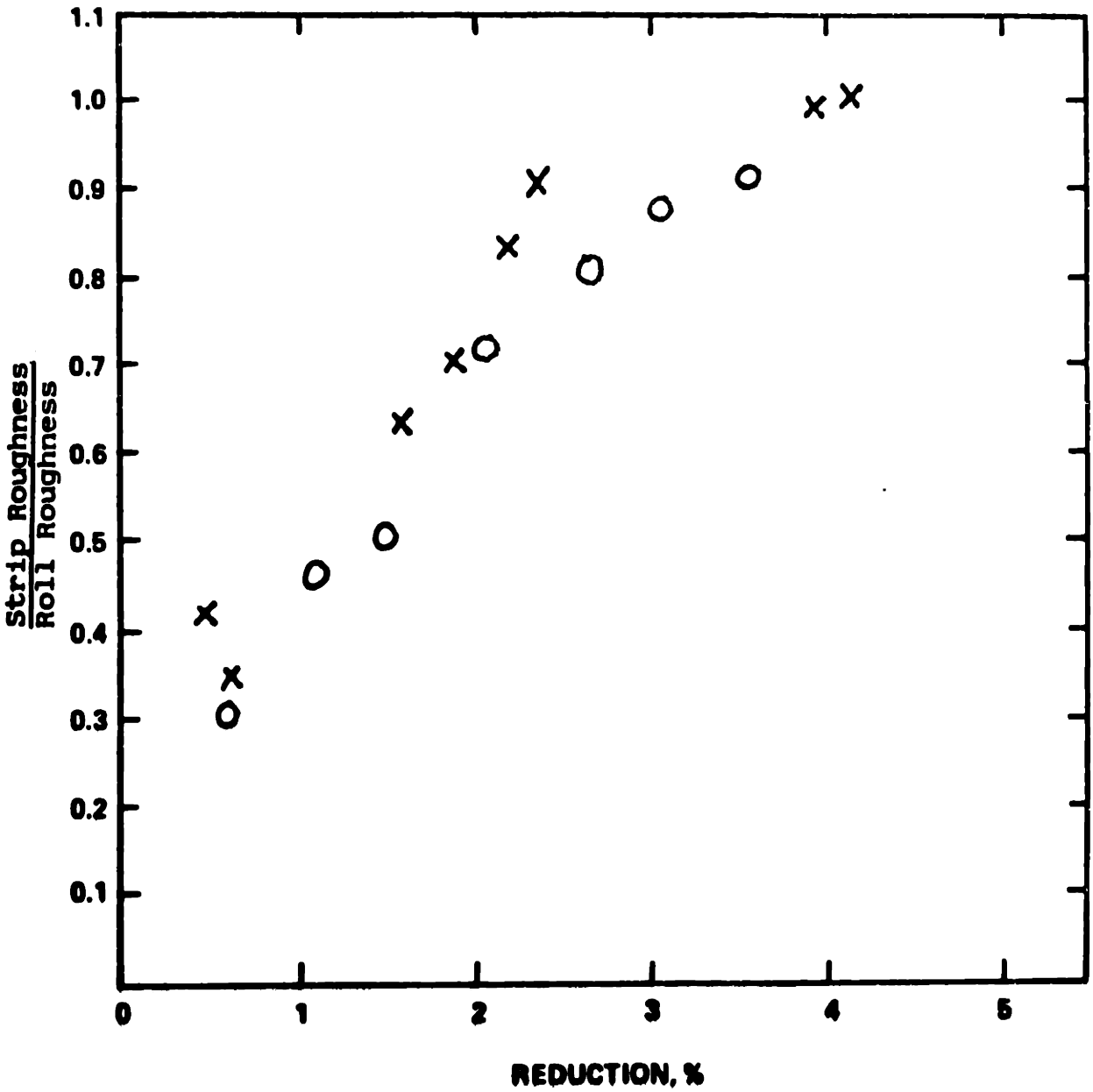

Fig. 3.23 Peak Count Transfer vs. Reduction
(MILL SPEED VARIED)
Roll Diameter (inches): 3.197
Roll Peak Count (ppi_{50}): X 132.5 O 146.5
Strip: COIL C
Initial peak count(ppi_{50}): X 96 O 24
Mill Speed (feet/minute): X 50 O 315
Strip Tensions (psi): Entry X 11000 O 15000
Exit X 11000 O 15000
Lubrication: DRY

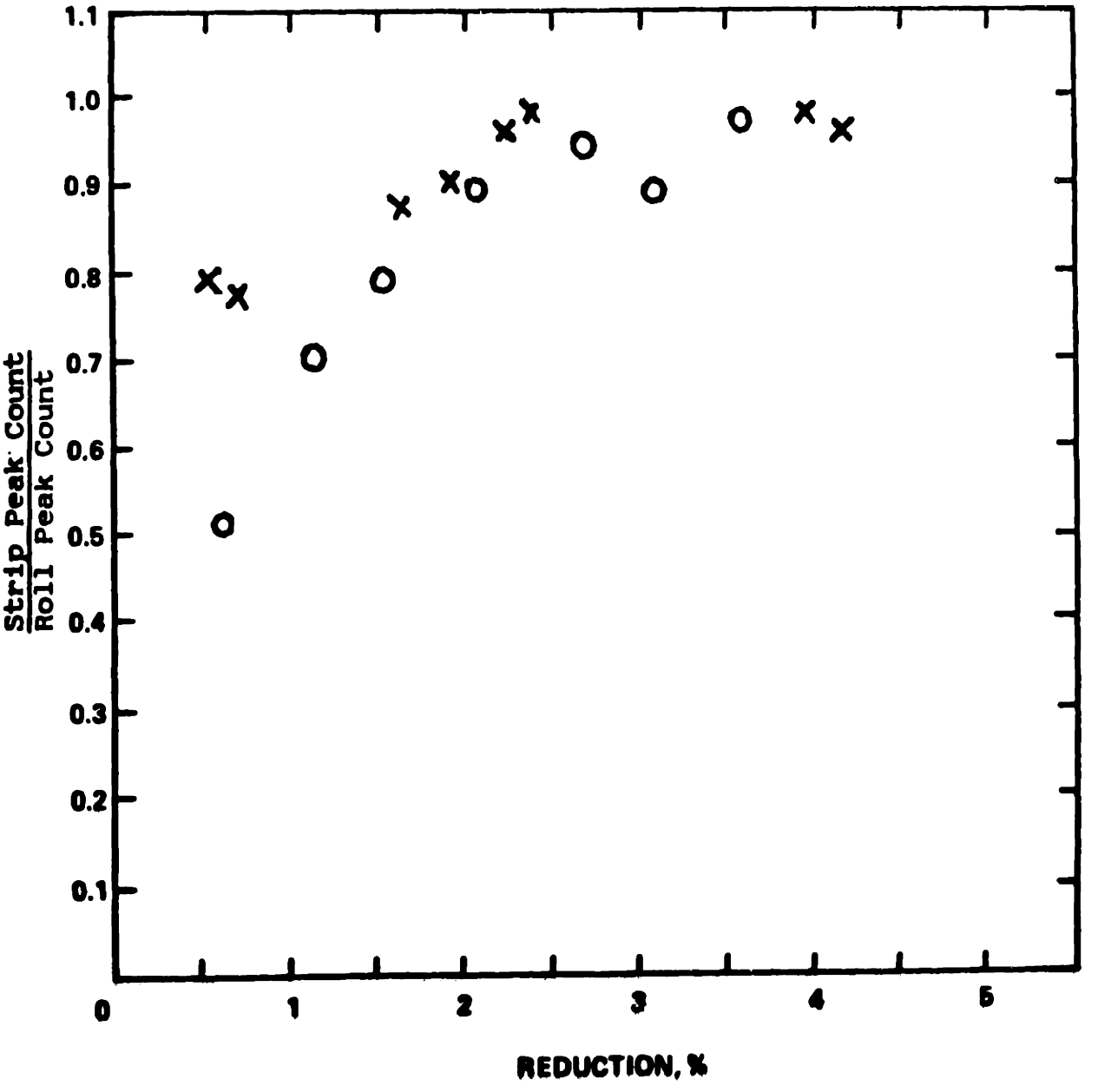

Fig. 3.24 SPECIFIC ROLLING FORCE VS. Reduction

Roll Diameter (inches): 3.197

Strip: COIL C

Mill Speed (feet/minute): x 50 o 315
Strip Tensions (psi): Entry x 10000 o 15000
Exit x 11000 o 15000

Lubrication: DRY

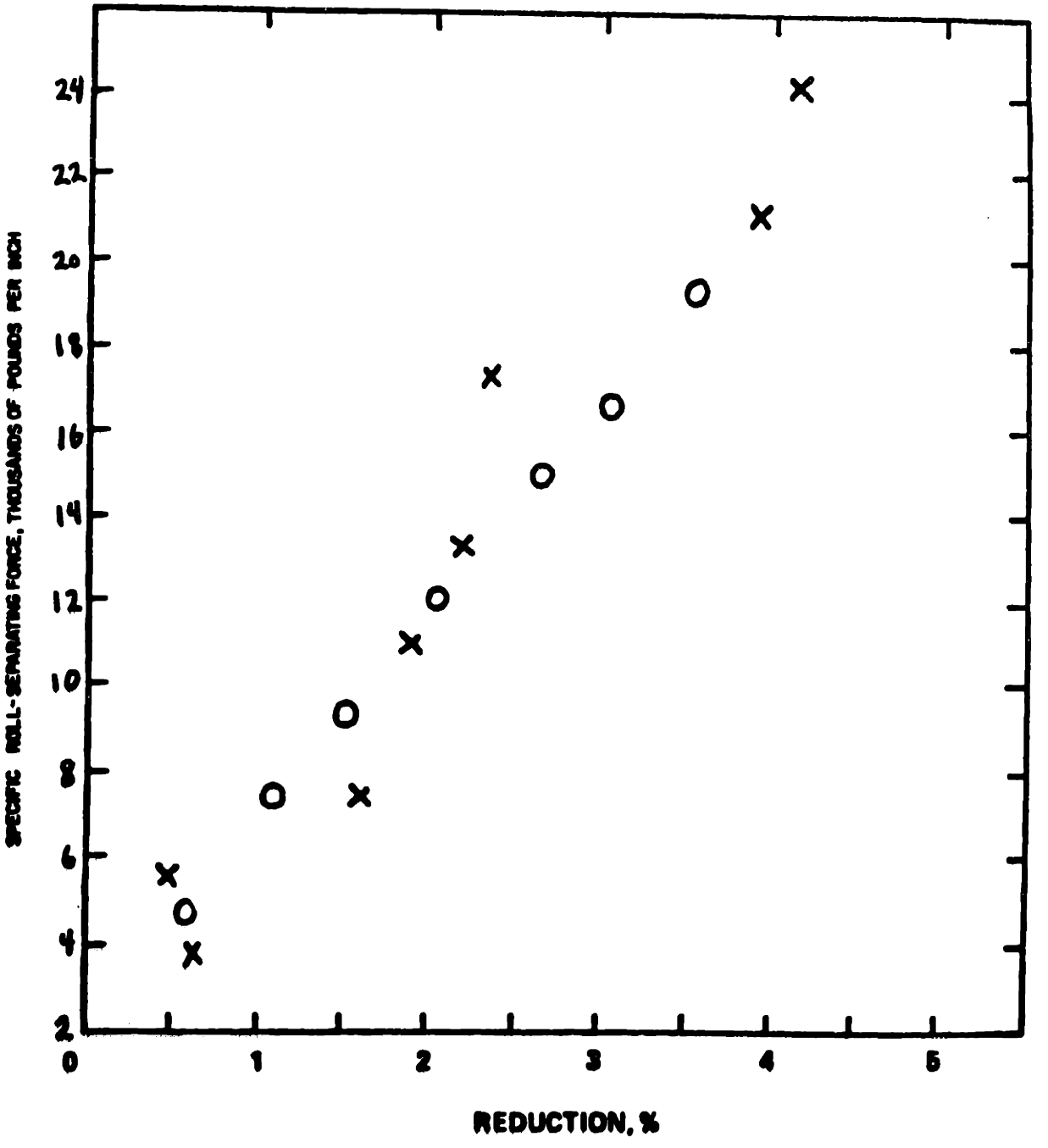

does not appear to be as marked as might have been expected. It indicates that, in commercial dry-temper rolling, both transfer efficiency (at constant extension) and the compressive yield strength of the strip should increase noticably as the mill is accelerated from coil feeding to full production speed. In terms of the actual transfer levels observed, this leads to an interplay of contradictory effects. Increasing mill speed, as noted above, generally increases transfer efficiency at constant extension; however, the accompanying increase in yield strength frequently leads to fluctuations (generally decreases) in extension as full speed is reached. Overall, the influence of extension on transfer is much more marked than that of mill speed, and the portions of coils which receive the heaviest reductions during temper rolling (often the head and tail ends) usually exhibit surface textures closest to that of the rolls used. Data from production mills on the variation of extension and surface transfer with mill speed (obtained by sampling head end, tail end, and interior sections of several coils) is presented in Section III.13 (Figure 3.46) and Appendix II.

III.9 Effect of Strip Gage on Transfer

The most interesting results obtained in this investigation were those from tests on three small coils produced by cold-reducing steel from a single large coil to three different gages. These coils were then annealed to roughly uniform yield stresses, giving essentially the same steel in three thicknesses. From a superficial, qualitative consideration of the arguments given in Part II, and from common sense, one

would expect that increasing the thickness of the strip in temper rolling, with all other factors held constant, would increase both transfer efficiency and rolling force, since it would increase the plastic arc length. The data presented in Figures 3.25 to 3.27, however, indicates that this is not always the case. Although these results appear to contradict the qualitative theoretical reasoning of Part II, they are, in fact, consistent with the corresponding quantitative development; the expression given for the minimum critical reduction required for complete transfer, Equation 2.16, depends on strip gage in a complex manner, but suggests that R should, in general, increase with strip thickness. This is illustrated by Table III.6, which gives values of the critical reduction for complete transfer computed from Equation 2.16 for representative laboratory and production conditions. Further discussion of the influence of strip gage on both transfer efficiency and rolling force is given in Section III.1.

III.10 Effect of Strip Tensions on Transfer

Strip tensions might be expected to influence surface transfer in two ways. First, a large increase in the average tension applied to the strip could significantly decrease its effective compressive yield strength, leading to a decreased plastic arc length and less efficient transfer. Second, a change in the ratio of entry to exit tension could move the position of the neutral point in the roll bite, leading to a

Fig. 3.25 Roughness Transfer vs. Reduction
(Strip Thickness Varied)
Roll Diameter (inches): 3.135
Roll Roughness: (microinches R_a): × 48.7 ○ 61.2 • 58.3
Strip: × Coil #1 ○ Coil #2 • Coil #3
initial roughness (microinches R_a): 20
Mill Speed (feet/minute): 100
Strip Tensions (Psi): Entry × 8000 ○ 10000
Exit × 8000 ○ 10000
Lubrication: Dry

STRIP GAUGE (inches): × .012
○ .0185
• .0295

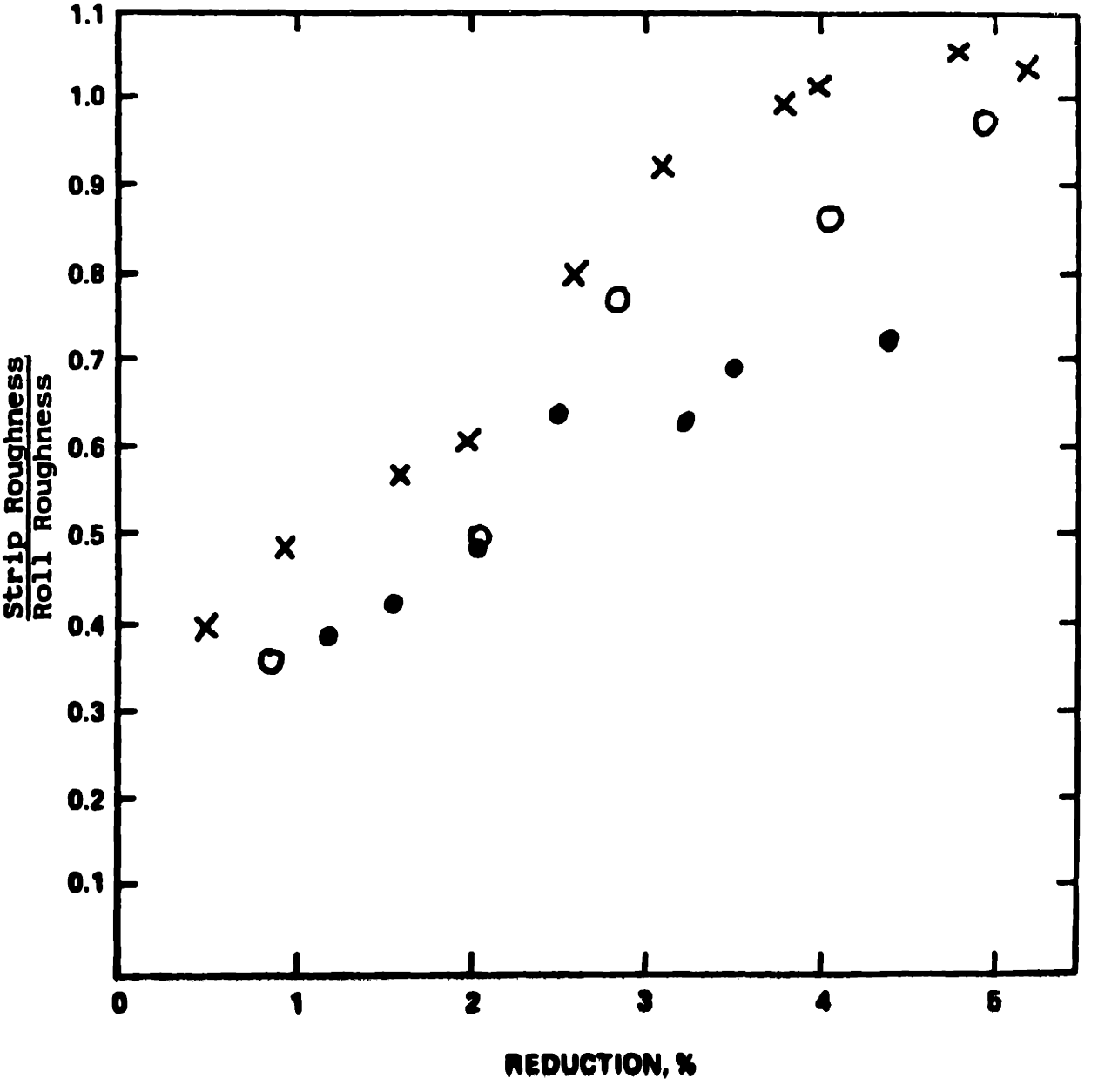

Fig. 3.26 Peak Count Transfer vs. Reduction
(STRIP THICKNESS VARIED)
Roll Diameter (inches): 3.135
Roll Peak Count (ppi_{50}): X 142 O 123.5 • 118
Strip: X COIL E1 O COIL E2 • COIL E3
Initial peak count(ppi_{50}): X 0 74 • 95
Mill Speed (feet/minute): 100
Strip Tensions (psi): Entry X 8000 O • 10000
Exit X 8000 O • 10000
Lubrication: DRY
STRIP GAUGE (inches): X .012
O .0185
• .0295

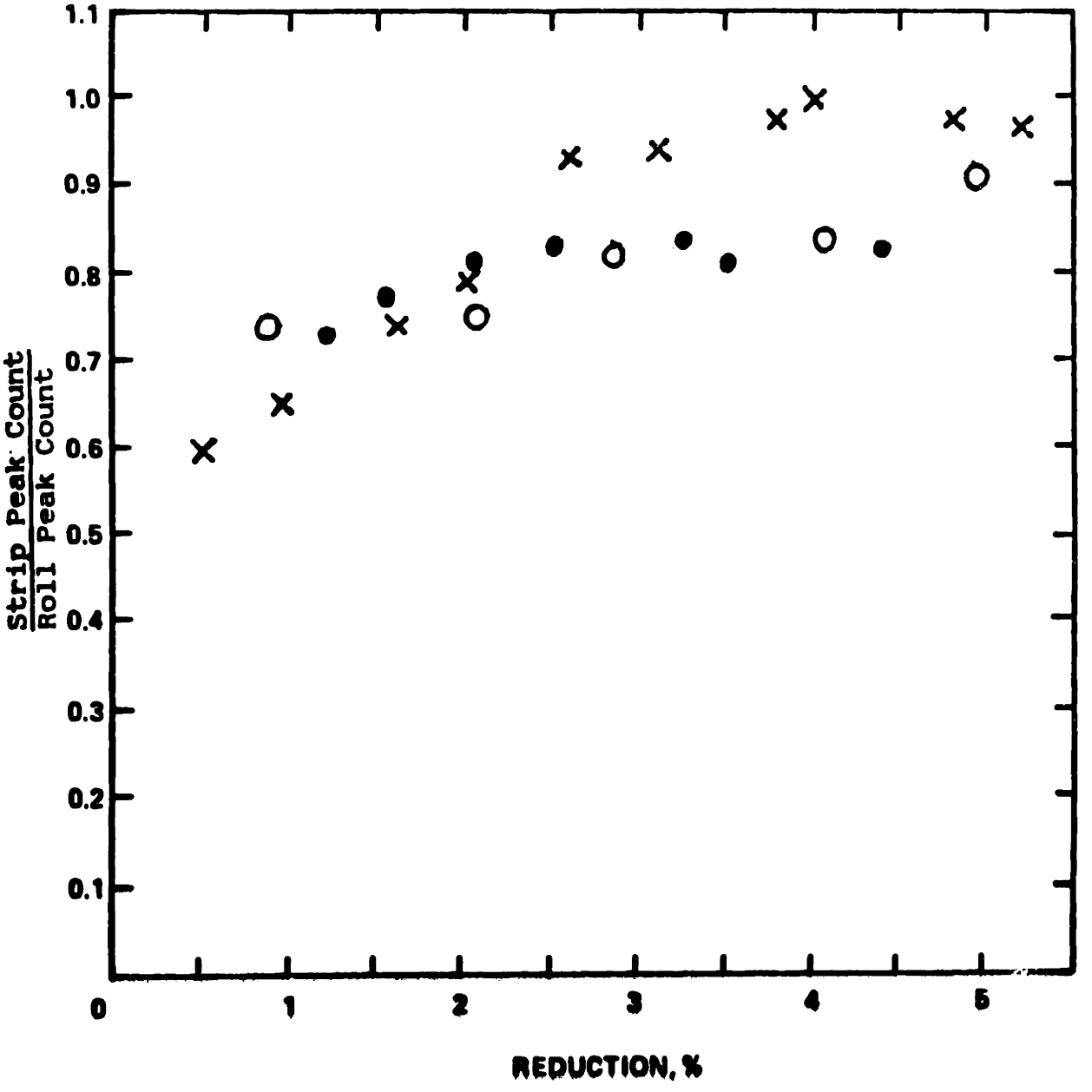

Fig. 3.27 SPECIFIC ROLLING FORCE VS. Reduction
(STRIP THICKNESS VARIED)
Roll Diameter (inches): 3.135

Strip: x COIL E1 o COIL E2 • COIL E3
STRIP THICKNESS (inches): x .012 o .0185 • .0295
Mill Speed (feet/minute): 100
Strip Tensions (psi): Entry x 8000 o• 10000
Exit x 8000 o• 10000
Lubrication: DRY

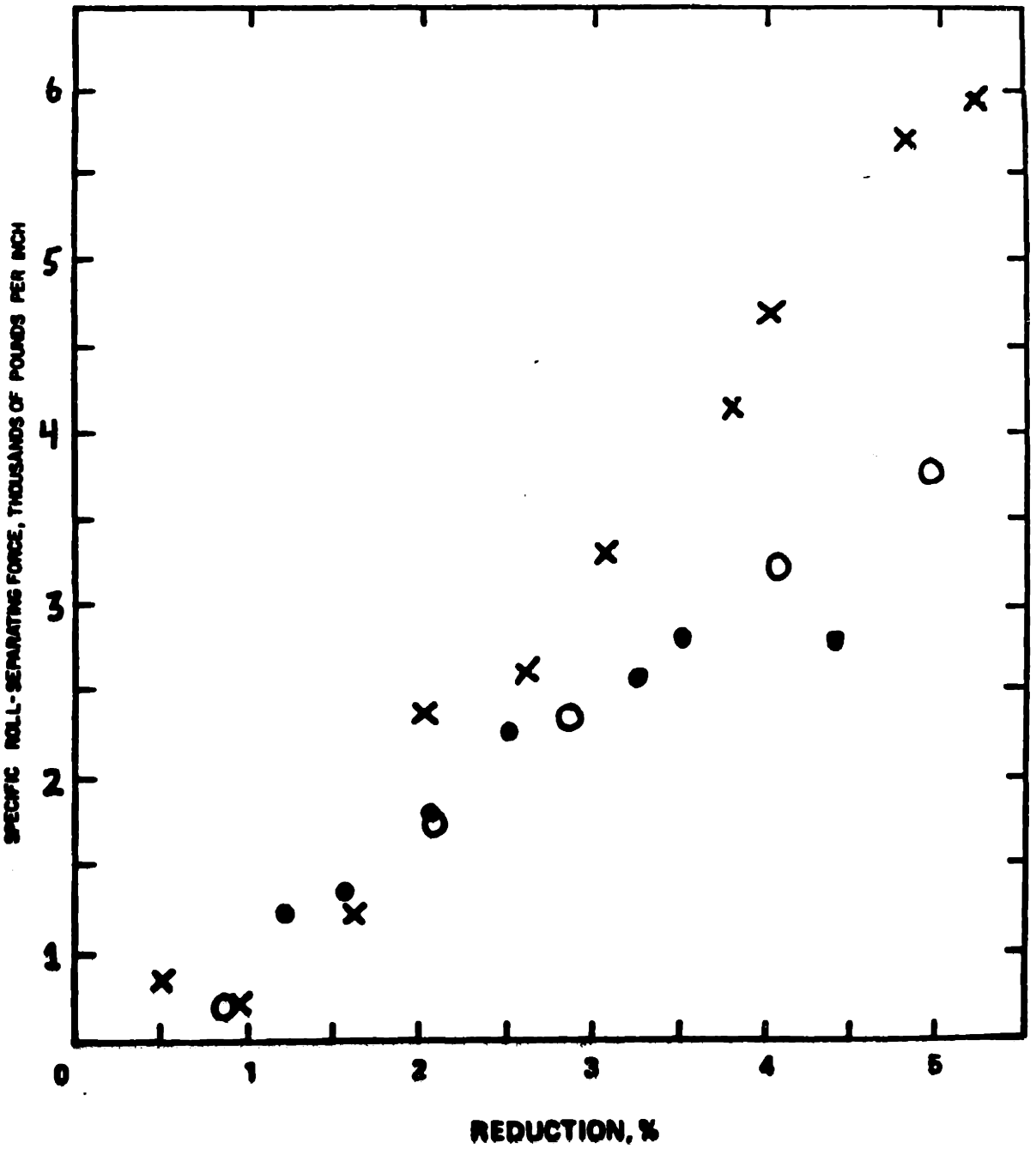

Table III.6

Variation of Calculated Critical Reduction for Complete Transfer (R) With Strip Thickness (t)

R = smallest r satisfying

$$\frac{L_p}{r}\left\{\left[\left(\frac{1}{1-\frac{1}{a}}\right)\left(\frac{1}{2\mu}-\frac{1}{a}\right)\right]^{-\frac{1}{a}} - (1-r)\left[\left(\frac{1}{1+\frac{1}{a}}\right)\left(\frac{1}{2\mu}+\frac{1}{a}\right)\right]^{\frac{1}{a}}\right\} \geq 0$$

where

$$L_p = K\sqrt{\frac{Dtr}{2}} \quad ; \; K = \text{a constant}$$

$$a = \frac{L_{p(2\mu)}}{rt}$$

Roll Diameter, (in.)	K	μ	t, (in.)	R, (%)
3.197	1.25	0.24	0.012	4.3
			0.0185	6.5
			0.0295	10.05
3.197	1.5	0.24	0.012	3.05
			0.0185	4.6
			0.0295	7.2
24	1.0	0.24	0.012	0.93
			0.0185	1.43
			0.0295	2.26

change in the peak pressure achieved along the arc of contact, and thus to a change in the critical reduction necessary for complete transfer.

A number of tests were conducted to evaluate the magnitudes of the influences of average tension and tension ratio on transfer. Early data, such as that presented in Figures 3.2 and 3.3 of Section III.4, indicated that the transfer process was largely independent of the average tension applied to the strip. For this reason, tension levels were not closely monitored in many later tests; tension levels were adjusted (more or less arbitrarily) during each set of tests to give relatively stable rolling forces, to reduce shape defects in the outgoing strip, and occasionally to eliminate high-pitched screeches or whines which sometimes accompanied certain test conditions. This resulted in many sets of data being obtained at slightly different tension levels, and, as can be seen from previous sections, comparisons being made between data sets gathered under nonuniform tension conditions. The author does not feel that the nonuniformity of applied tension significantly confounded the results of these comparisons. On the whole, data taken under most conditions, such as that presented in Figures 3.2, 3.3, and 3.28 to 3.33, showed no marked variation in transfer efficiency with average tension, although considerable scatter is evident in this data, particularly in the small samples obtained at low mill speeds. (As discussed in Section IV.3, temper-rolling reductions become difficult to measure accurately in the laboratory at low speeds.) An appreciation

Fig. 3.28 Roughness Transfer vs. Reduction
(Average Strip Tension Varied)
Roll Diameter (inches): [illegible]
Roll Roughness: (microinches R_a): 51
Strip: Coil A
initial roughness (microinches R_a): 10
Mill Speed (feet/minute): 50
Strip Tensions (Psi): Entry × 10000 ○ 20000
Exit × 10000 ○ 20000
Lubrication: Temper Rolling Lubricant,
3% Aqueous solution, 140°F

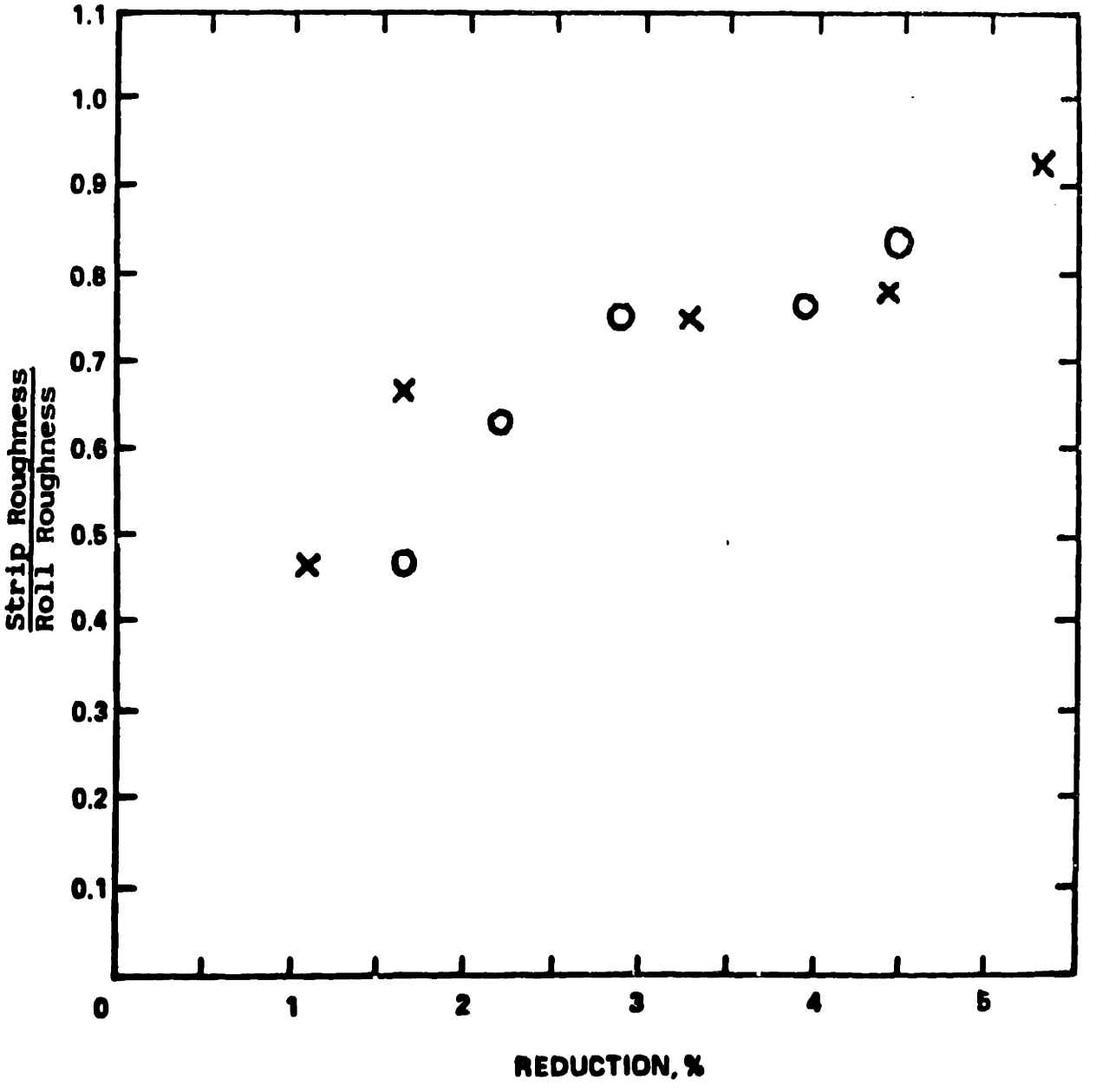

Fig. 3.29 Peak Count Transfer vs. Reduction
(Average Strip Tension Varied)

Roll Diameter (inches): 3.197
Roll Peak Count (ppi_{50}): 136
Strip: Coil A
Initial peak count (ppi_{50}): 28
Mill Speed (feet/minute): 56
Strip Tensions (psi): Entry × 10000 ○ 20000
Exit × 10000 ○ 20000
Lubrication: TEMPER ROLLING LUBRICANT, 3% Aqueous solution, 140°F

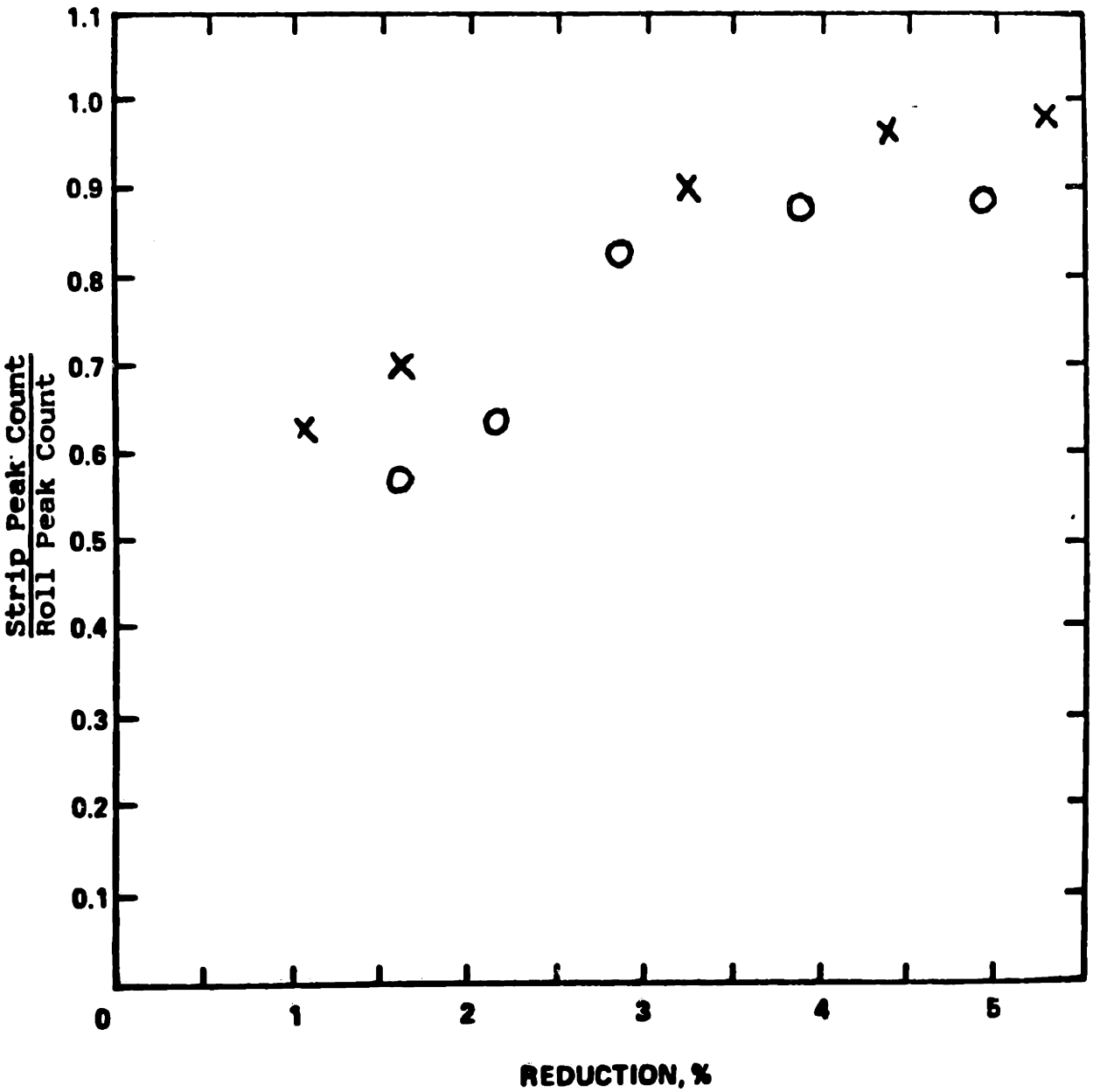

Fig. 3.30 Roughness Transfer vs. Reduction
(Average Strip Tension Varied)
Roll Diameter (inches): 3.197
Roll Roughness: (microinches R_a): 63.2
Strip: COIL C
initial roughness (microinches R_a): 14.3
Mill Speed (feet/minute): 50
Strip Tensions (Psi): Entry × 11000 ○ 20000
Exit × 11000 ○ 20000
Lubrication: DRY

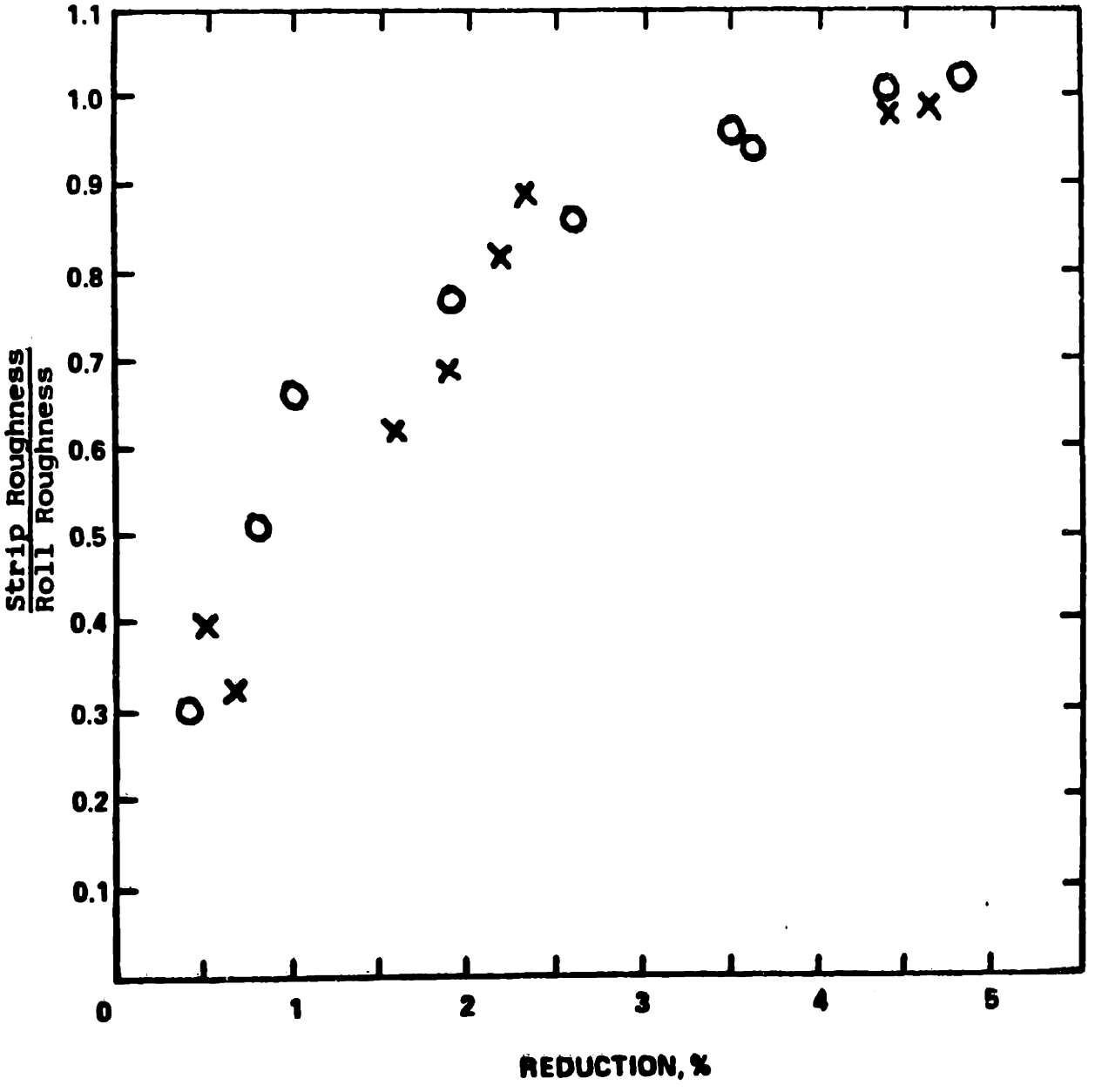

Fig. 3.31 Peak Count Transfer vs. Reduction
(Average Strip Tension Varied)

Roll Diameter (inches): 3.197
Roll Peak Count (ppi_{50}): 132.5
Strip: coil C
Initial peak count (ppi_{50}): 92
Mill Speed (feet/minute): 50
Strip Tensions (psi): Entry x 11000 o 20000
Exit x 11000 o 20000
Lubrication: DRY

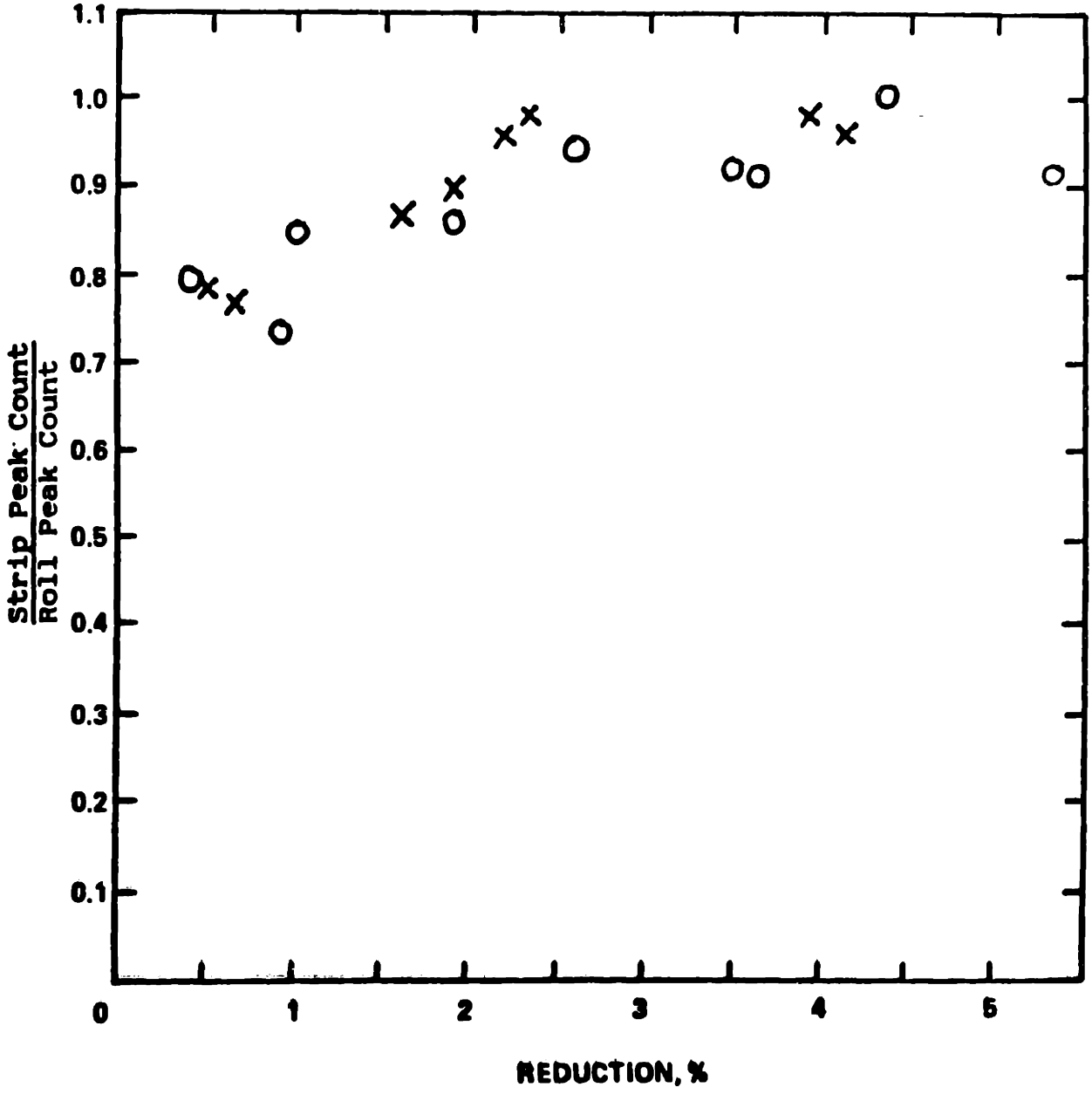

Fig. 3.32 Roughness Transfer vs. Reduction
(Average Strip Tension Varied)
Roll Diameter (inches): 6.343
Roll Roughness: (microinches R_a): 165.9
Strip: Coil B
initial roughness (microinches R_a): 16.7
Mill Speed (feet/minute): 50
Strip Tensions (Psi): Entry x 10000 o 15000
Exit x 10000 o 15000
Lubrication: DRY

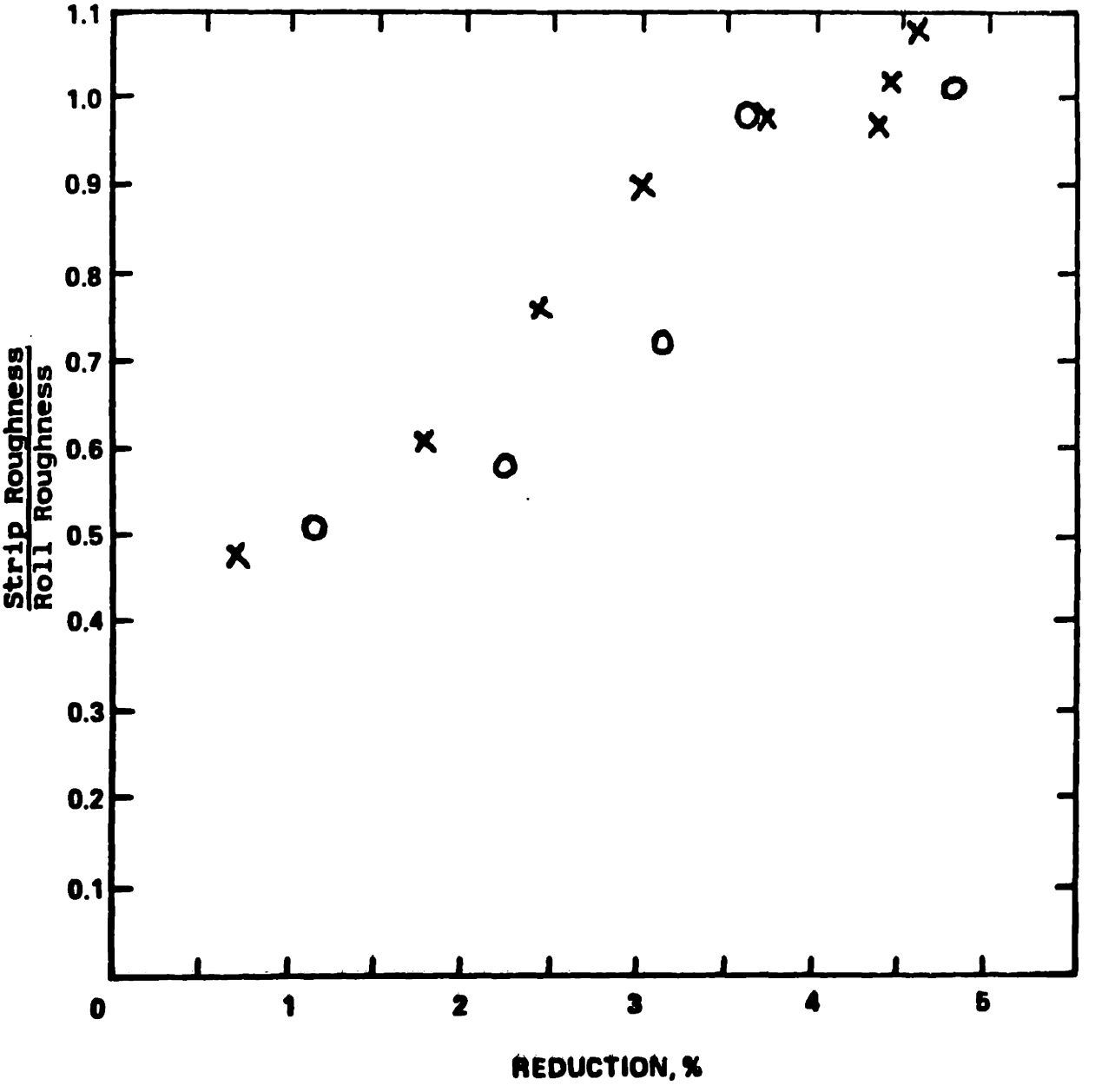

Fig. 3.33 Peak Count Transfer vs. Reduction
(Average Strip Tension Varied)

Roll Diameter (inches): 6.343
Roll Peak Count (ppi_{50}): 100
Strip: coil B
Initial peak count (ppi_{50}): 87
Mill Speed (feet/minute): 50
Strip Tensions (psi): Entry × 10000 ○ 15000
Exit × 10000 ○ 15000

Lubrication: DRY

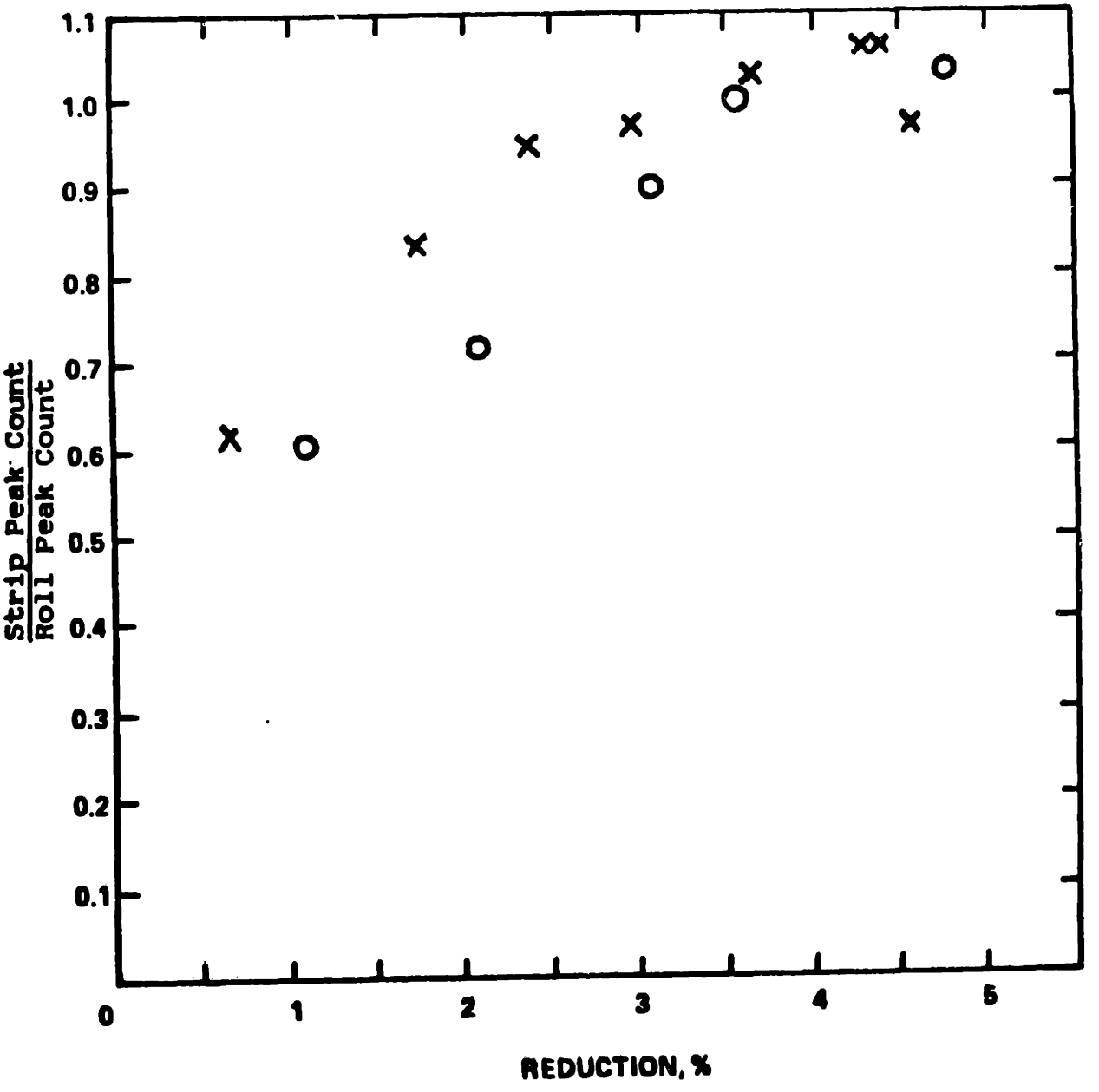

of the magnitude of this scatter in Figures 3.32 and 3.33, for example, can be gained from examining the reported transfer ratios for reductions above 3.5 percent; these points fall (presumably) in the region of complete roll-strip surface transfer, where the transfer ratios should remain constant and equal to unity. Scatter aside, however, this data does indicate that a large increase in average tension can noticeably decrease transfer levels under conditions for which the magnitude of this increase is significant compared to the effective compressive yield stress of the strip; specifically, this trend is most marked in the rolling of annealed strip at low reductions, and of "dead-soft" (e.g., overannealed) strip at all temper-rolling reductions, as illustrated in Figures 3.34 and 3.35. Even in these cases, however, the observed decreases in transfer efficiency are not overwhelming. Overall, this data indicates that, as would be expected from theoretical considerations, a large increase in the average tension applied to the strip can lead to a decrease in transfer efficiency, but that, under most conditions, this decrease is small in magnitude. In particular, changes in average tension of the order of 5000 psi appear to have had little effect in the rolling of coils A, B, and C under laboratory conditions. More importantly, in commercial sheet-temper rolling at high mill speeds (which should give rise to relatively large effective strip yield stresses), where average applied tensions are in general below 15,000 psi (cf Appendix II; note, however, that tensile stress levels would probably be somewhat higher for the

Fig. 3.34 Roughness Transfer vs. Reduction
(Average Strip tension Varied)
Roll Diameter (inches): 3.135
Roll Roughness: (microinches R_a): × 48.7 ○ 50.6
Strip: COIL E1
initial roughness (microinches R_a): 20.9
Mill Speed (feet/minute): 100
Strip Tensions (Psi): Entry × 8000 ○ 16000
Exit × 8000 ○ 16000
Lubrication: DRY

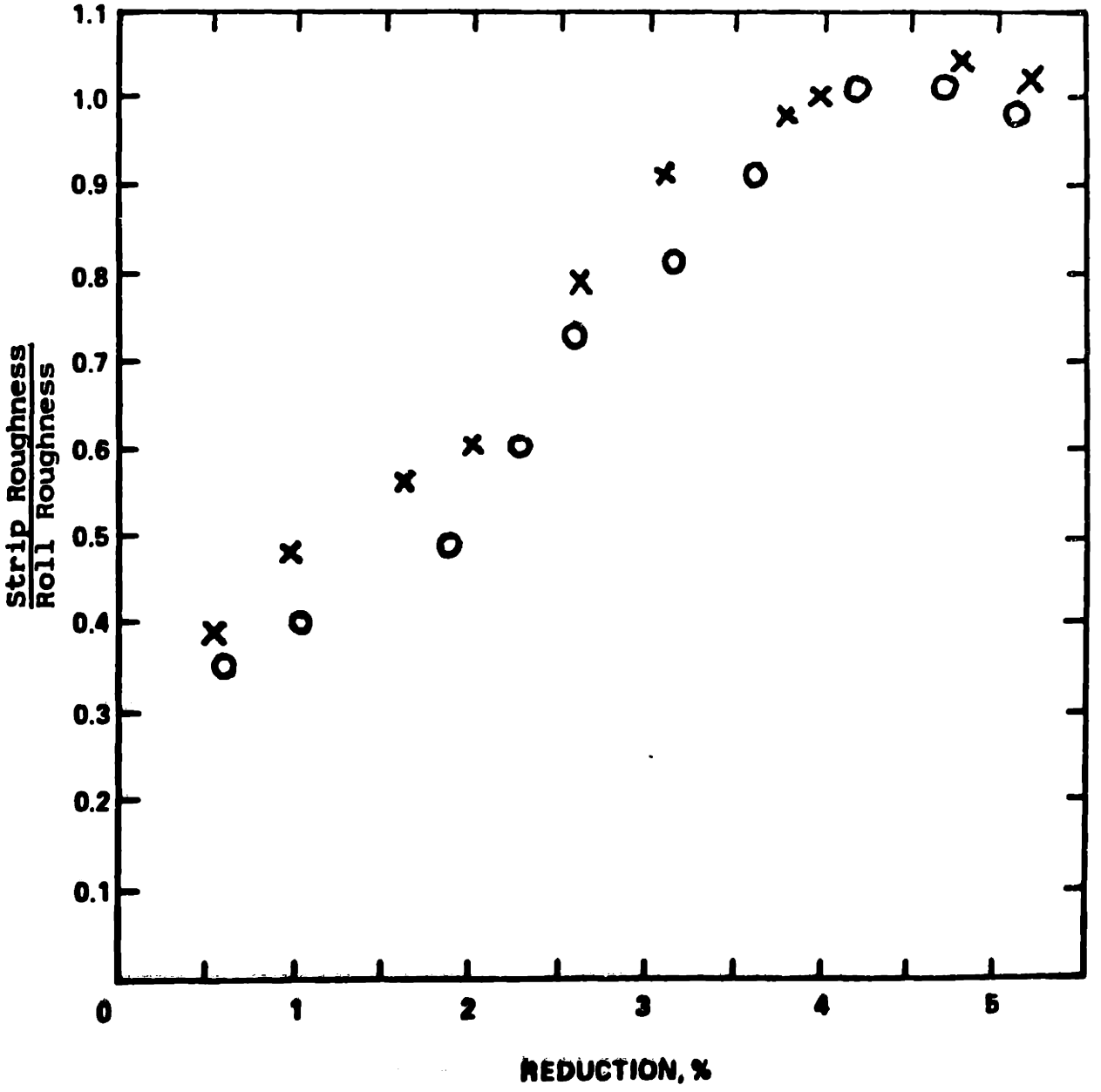

Fig. 3.35 Peak Count Transfer vs. Reduction
(Average Strip Tension Varied)
Roll Diameter (inches): 3.135
Roll Peak Count (ppi_{50}): X 142 O 143
Strip: COIL E1
Initial peak count (ppi_{50}): 74
Mill Speed (feet/minute): 100
Strip Tensions (psi): Entry X 8000 O 16000
Exit X 8000 O 16000
Lubrication: Dry

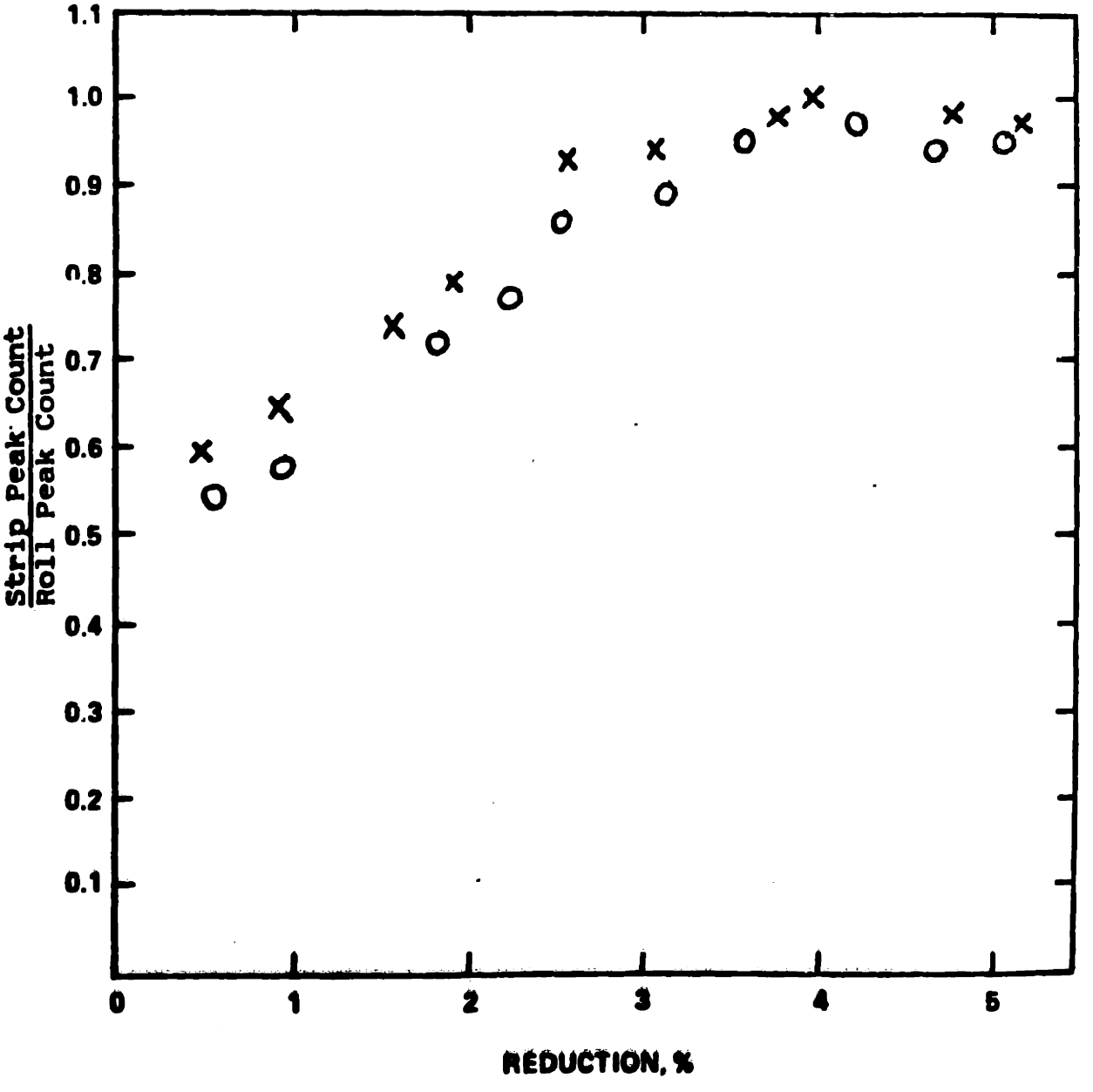

lighter gages typical of tin-temper rolling) the magnitude of the applied strip tension should not significantly influence the transfer levels achieved under given rolling conditions.

A number of tests were also conducted on the influence of the ratio of entry to exit tension on transfer. The results of these tests are shown in Figures 3.36 and 3.37 and in Table III.7; additional results are given in Figure 3.38 in the next section. As can be seen, varying the ratio of entry to exit tension at constant average tension does not appear to have a consistent or marked influence on transfer efficiency, although again there is considerable scatter in some of the data. This is consistent with Roberts' conclusion that, because of the small reduction taken, the average compressive yield stress in the roll bite in temper rolling is influenced much more by the average of the entry and exit strip tensions than by the ratio of these tensions.[30)]

III.11 Quantitative Results; Calculation of Roughness Transfer

The results presented thusfar have been largely qualitative. The theoretical development of Part II does, however, give expressions for the calculation of roughness transfer for arbitrary rolling conditions. While methods for determining values of two parameters necessary to carry out such a calculation——the plastic arc length and effective compressive yield stress of the strip——have not been developed to the point that transfer values can be computed in a practical situation from readily available input data, experimental methods for inferring these quantities are available.

Fig. 3.36 Roughness Transfer Vs. Reduction
(Tension Ratio Varied)
Roll Diameter (inches): 3.135
Roll Roughness: (microinches R_a): x 46.8 o 44.9
Strip: Coil E1
initial roughness (microinches R_a): 20.9
Mill Speed (feet/minute): 110
Strip Tensions (Psi): Entry x 8000 o 20000
Exit x 20000 o 8000
Lubrication: DRY

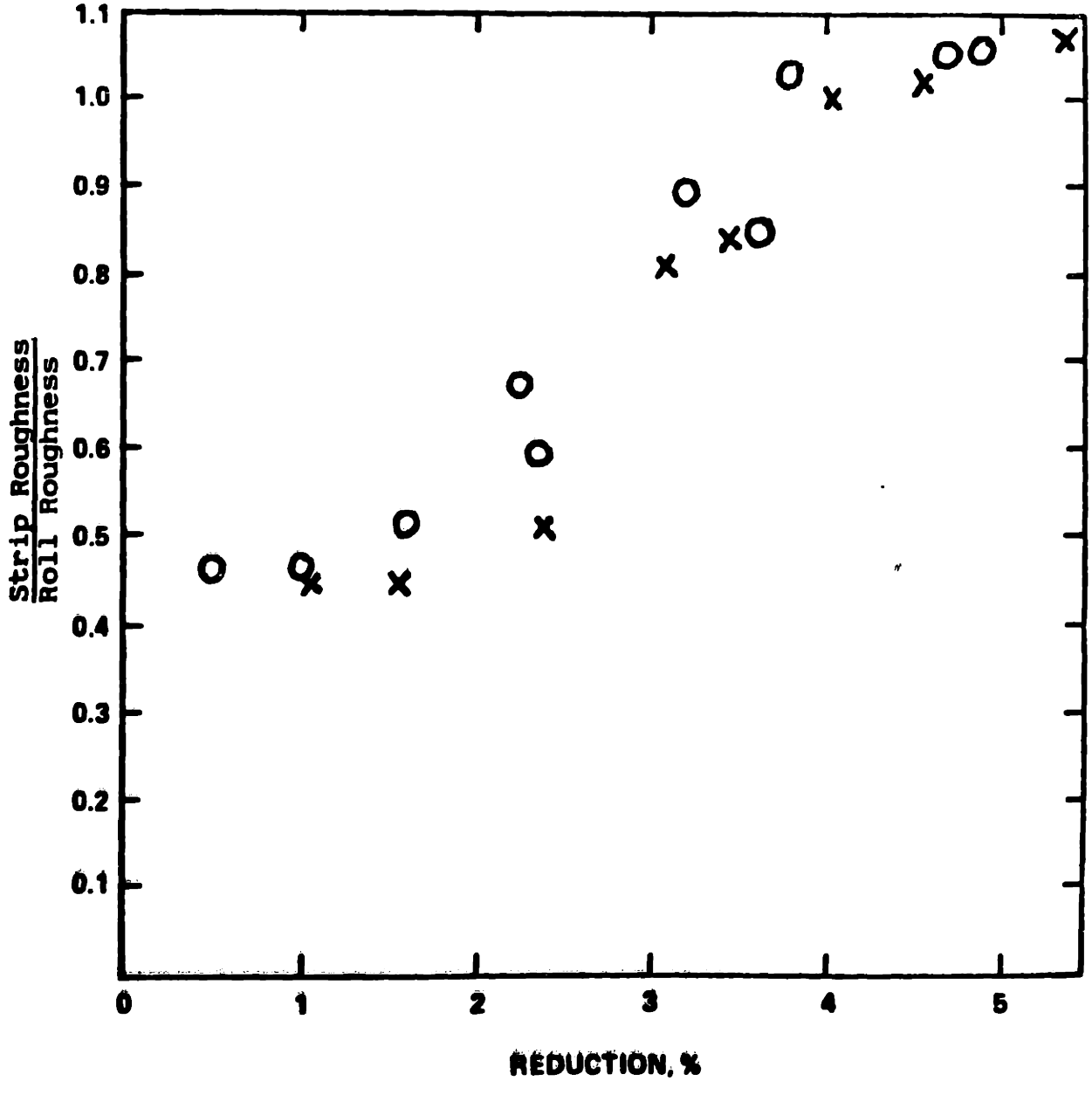

Fig. 3.97 Peak Count Transfer vs. Reduction
(Tension Ratio Varied)
Roll Diameter (inches): 3.135
Roll Peak Count (ppi_{50}): x 135 o 134
Strip: E1
Initial peak count (ppi_{50}): 74
Mill Speed (feet/minute): 110
Strip Tensions (psi): Entry x 8000 o 20000
Exit x 20000 o 8000
Lubrication: DRY

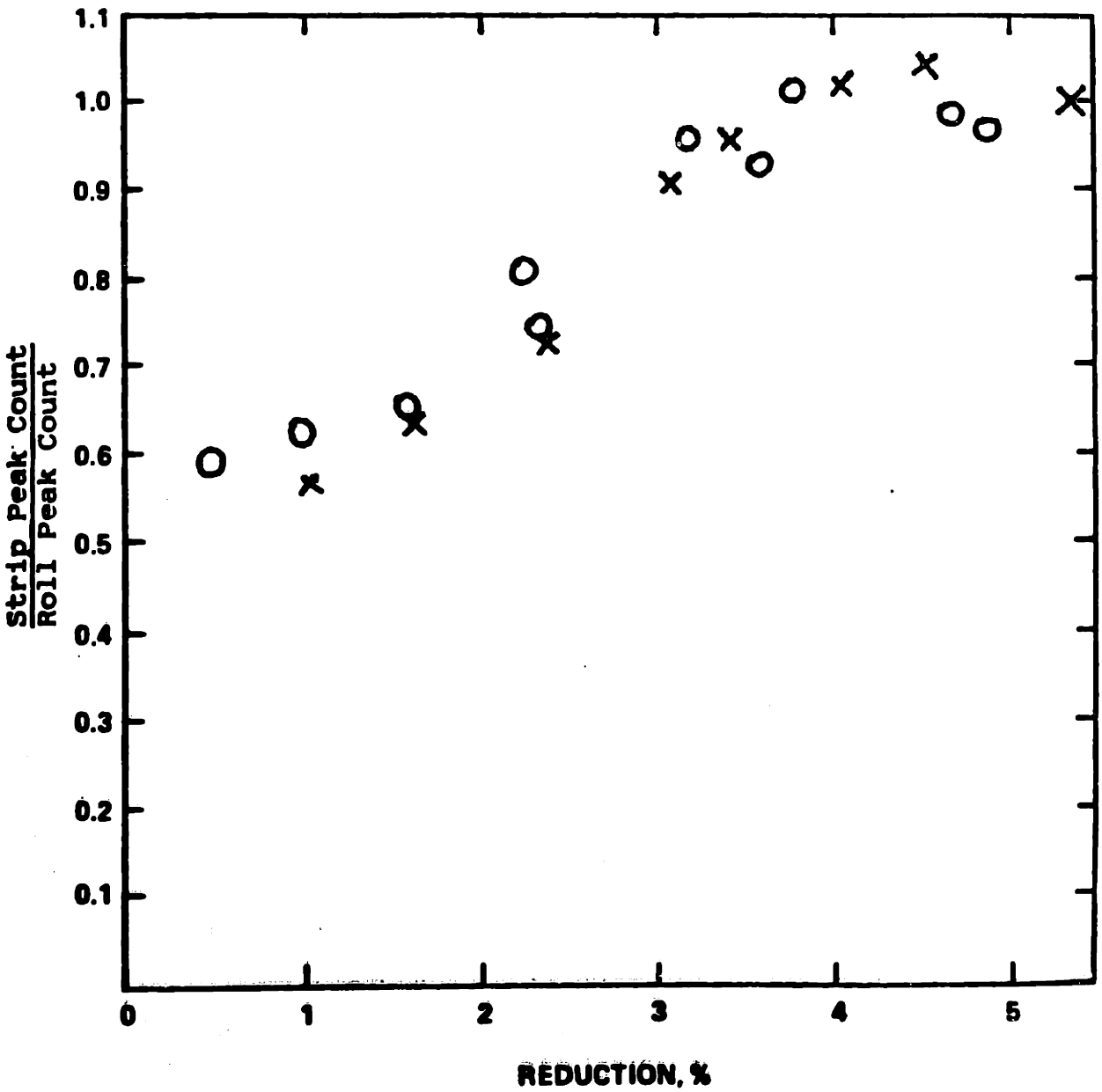

Table III.7

Transfer Values at Various Tension Ratios

Rolls: 6.342-inch diameter
Initial roughness: 102-microinch R_a
Initial peak count: 162 ppi_{50}

Strip: Coil B: Initial roughness: 17-microinch R_a
Initial peak count: 60 ppi

Mill Speed: 100 feet/minute

Lubrication: Dry

Spec	Reduction, %	Tensions, psi Entry	Exit	Average	Strip Roughness / Roll Roughness	Strip Peak Count / Roll Peak Count
1	1.95 ± 0.2	18,928	5,534	12,231	0.47 ± 0.05	0.70 ± 0.05
2	1.85	16,140	15,225	15,683	0.51	0.75
3	1.95	6,420	18,851	12,636	0.52	0.81
4	2.9	19,230	5,379	12,305	0.76	0.86
5	2.85	10,414	18,958	14,686	0.86	0.93
6	2.6	19,448	5,278	12,363	0.865 ± 0.07	0.98 ± 0.07
7	2.5	19,460	5,258	12,359	0.86	0.96
8	2.6	15,306	15,932	15,619	0.97	0.98
9	2.8	19,479	9,798	14,638	0.87	0.97
10	2.9	5,335	19,250	12,292	0.91	1.01

These methods are time consuming and tedious, requiring both roller-die drawing (e.g., pulling the strip through the rolls entirely by tension) and torque-loss measurements in addition to transfer information for each set of trials examined, but can produce a limited amount of data to test the accuracy of the expressions for roughness transfer proposed in Part II. Such data for Bliss mill trials is given in Table III.8 and Figure 3.38; similar data for Nash mill tests is given in Table III.9 and Figure 3.39. Compressive yield stresses and average roll-bite stresses were inferred from roller die drawing data and corrected torque measurements, as described in Subsection II.4.4. Bearing losses were estimated from curves generated by running the mills on face (without strip between the rolls) and measuring the torque thus consumed as a function of the force applied to the rolls. It was assumed that this function would give a valid estimate of bearing losses at corresponding roll forces when rolling with strip. The inferred yield stress and (particularly) average roll-bite pressures, it should be emphasized, are highly approximate; this can be seen from the erratic behavior of the estimates at low reductions, particularly the cases in which the average roll-bite pressure is estimated to be smaller than the effective yield stress of the strip. This scatter is due principally to the necessity of taking a small difference between relatively large entry and exit tension values, which was particularly fraught with error in the case of the Nash mill (cf. Section IV.3), and to the bearing loss corrections, which often accounted for three fourths of the energy

Table III.8

Comparison of Calculated and Empirically Ifferred Mechanical Data for Bliss Mill Trials

$\mu = 0.24$ and $E = 3 \times 10^7$ psi

Rolling conditions given in Figure 3.38

Spec	Reduction, %	Inferred σ_c, psi	Roll Force, lb/in.		Average Roll Bite Stress, psi		Plastic Arc Length incnes	Sticking Zone Length, inches
			meas.	calculated	inferred	calculated		
1	1.2	39,272	1,647	2,180	<0	46,753	0.0266	0
2	1.45	42,086	2,138	2,568	0	51,043	0.0292	0
3	1.75	48,449	2,973	3,352	35,380	59,984	0.0321	0
4	2.65	51,281	4,788	4,782	61,443	70,080	0.0455	0
5	3.05	65,367	7,042	7,049	84,081	91,714	0.0483	0
6	3.65	67,920	8,783	8,781	95,910	102,315	0.0585	0.0029
7	3.9	74,462	10,301	10,379	102,809	114,268	0.0614	0.0059
8	4.45	80,538	12,750	12,769	118,916	128,427	0.0688	0.0134
9	1.3	42,221	1,920	2,484	<0	50,648	0.0277	0
10	1.65	48,446	2,803	3,283	29,604	59,580	0.0312	0
11	1.9	51,956	3,466	3,813	57,845	64,957	0.0335	0
12	2.1	52,266	3,857	3,987	58,151	66,168	0.0352	0
13	3.15	58,673	6,531	6,541	98,857	84,660	0.0526	0
14	3.6	61,217	7,806	7,819	97,242	92,924	0.0597	0.0041
15	4.45	64,480	10,206	10,195	114,800	104,731	0.0732	0.0179
16	4.5	68,950	11,040	11,038	118,952	111,843	0.0729	0.0176
17	1.0	57,727	2,017	3,665	<0	67,624	0.0243	0
18	1.65	52,276	3,023	3,664	12,335	64,290	0.0312	0
19	2.2	62,217	4.814	5,204	56,433	79,247	0.0360	0
20	2.6	58,150	5,328	5,334	62,624	77,605	0.0423	0
21	3.35	60,476	7,167	7,181	80,804	89,284	0.0556	0
22	3.35	64,816	7,681	7,687	87,487	94,738	0.0542	0
23	3.9	71,459	9,886	9,866	101,243	109,812	0.0616	0.0061
24	4.7	73,233	12,261	12,280	122,551	119,884	0.0753	0.0200

Fig. 3.38 Roughness Transfer Vs. Reduction
(TENSION RATIO VARIED; TRANSFER CALCULATED)
Roll Diameter (inches): 6.374
Roll Roughness: (microinches R_a): 65
Strip: COIL E2
initial roughness (microinches R_a): 20.9
Mill Speed (feet/minute): 100
Strip Tensions (Psi): Entry × 10000 ○ 8500 • 16000
Exit × 10000 ○ 15000 • 8000
Lubrication: DRY

– – – – CALCULATED TRANSFER CURVE

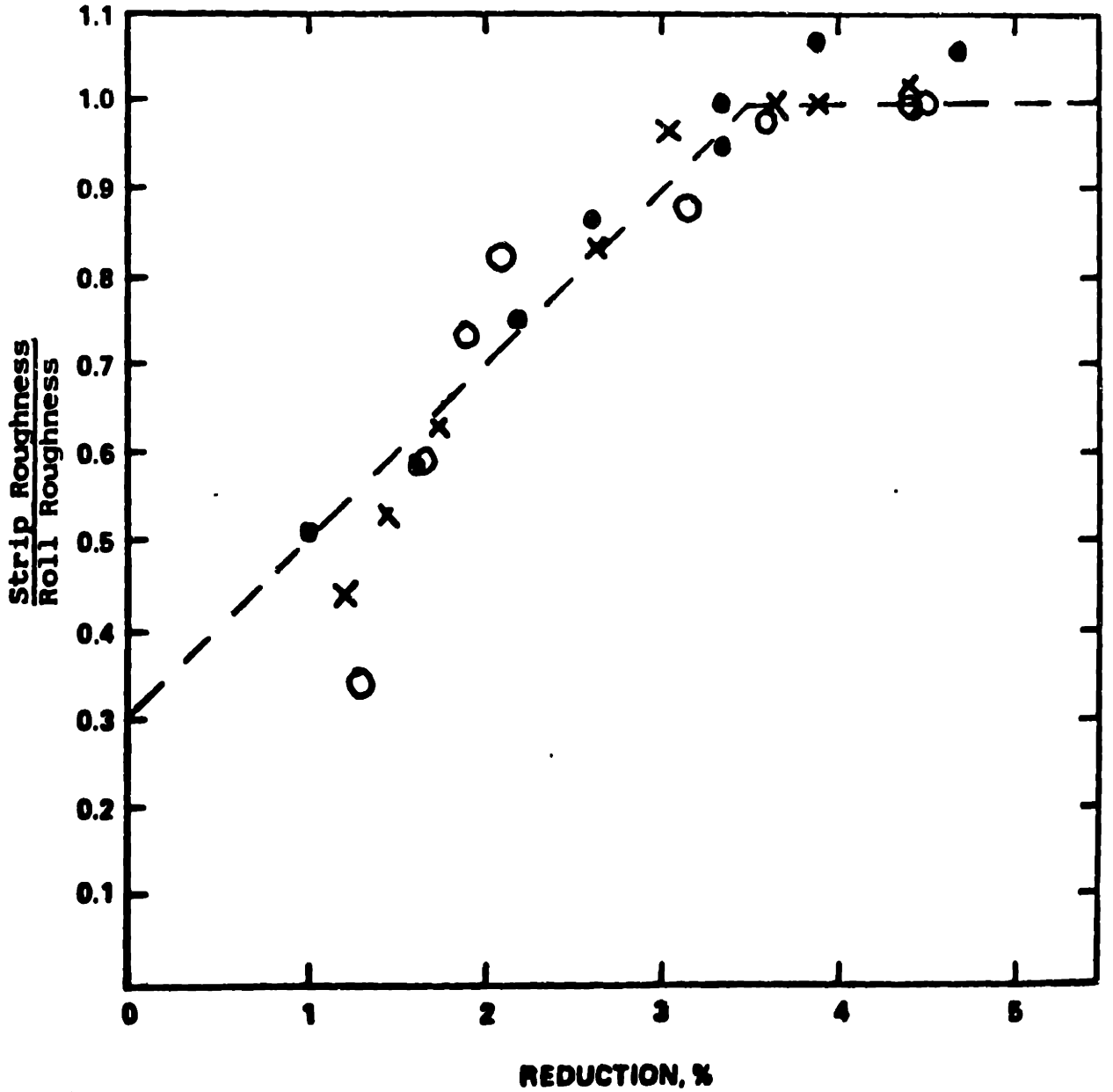

Table III.9

Comparison of Calculated and Inferred Mechanical Data for Nash-Mill Trials

$\mu = 0.24$ and $E = 3 \times 10^7$ psi. Rolling Conditions given in Figure 3.39

Spec	Reduction Percent	Inferred σ_c psi	Roll Force lb/in.		Average Roll Bite Pressure, psi		Plastic Arc Length, inch
			Measured	Calculated	Inferred	Calculated	
1	1.0	<0	660	-	<0	-	-
2	1.65	37,041	1,248	1,544	33,028	41,068	0.0276
3	2.05	41,919	1,424	1,975	36,711	47,094	0.0308
4	2.5	36,715	1,465	1,824	33,217	41,816	0.0340
5	3.05	44,625	2,075	2,533	41,692	51,623	0.0376
6	3.4	43,106	2,447	2,551	44,269	50,337	0.0397
7	4.15	45,027	2,725	2,953	47,524	53,595	0.0438
8	0.9	<0	620	-	<0	-	-
9	1.1	34,099	1,375	1,372	51,902	37,849	0.0271
10	2.0	38,819	1,365	1,774	44,116	43,542	0.0304
11	2.95	38,209	1,612	2,064	40,466	44,080	0.0369
12	3.15	39,220	2,284	2,279	48,606	45,843	0.0397
13	3.7	37,346	2,386	2,390	46,992	44,595	0.0443
14	4.3	41,049	2,655	2,690	53,712	49,041	0.0446
15	4.65	32,400	2,469	2,469	41,856	40,426	0.0533
16	5.0	45,048	2,996	3,237	56,054	54,725	0.0481

Fig. 3.39 Roughness Transfer vs. Reduction
(Lubrication Varied; transfer calculated)
Roll Diameter (inches): 3.135
Roll Roughness: (microinches R_a): 66.8
Strip: COIL E3
initial roughness (microinches R_a): 20.7
Mill Speed (feet/minute): 100
Strip Tensions (Psi): Entry 10000
Exit 10000
Lubrication: x DRY
O Temper Rolling Lubricant
3% Aqueous solution 140°F
— — — CALCULATED TRANSFER CURVES
(arc lengths extrapolated using Equation 2.22)

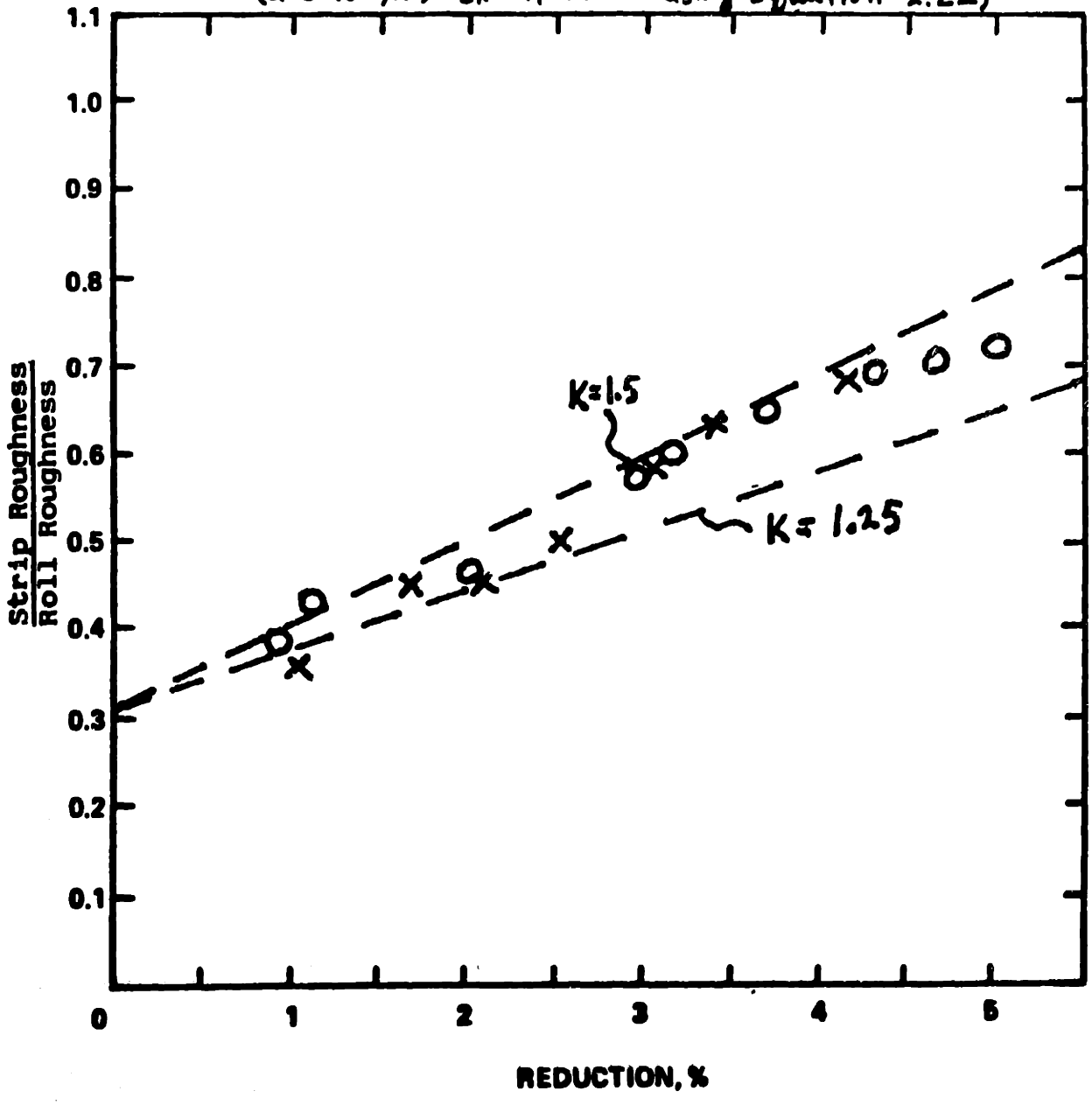

input to the mill at low reductions. Bearing these comments in mind, the author feels that the estimates are nonetheless reasonably accurate for extensions greater than three percent, particularly in the case of the Bliss mill. Tables III.8 and III.9 were constructed by using the inferred yield stress values to estimate the plastic arc length for each test; the arc lengths reported are those which, when used in the rolling force equations of Section II.4 with the inferred yield stresses, gave calculated rolling force values roughly equal to the corresponding measured values. In no case, however, was an arc length smaller than the rigid roll arc length used. As a check, an average roll-bite pressures were calculated from Equation 2.29 and compared with empirically inferred values. As can be seen from the Tables, the assumed arc lengths give calculated average stresses that agree, in all but one case, within twenty percent of inferred values for reductions above three percent.

The transfer curves shown in Figures 3.38 and 3.39 were calculated from Equation 2.4, with R set equal to the smallest reduction for which the calculated sticking zone length was greater than zero. For the Bliss mill trials, this condition was reached at 3.5 percent. This condition was not reached, however, in the Nash mill trials; values of R of 10.05 and 7.2 percent were calculated by assuming, as in Table III.6, that at this reduction the plastic arc length was (respectively) 25 and 50 percent greater than the applicable rigid roll estimate. From the Bliss mill data, it seems likely that the actual arc length in this case was

somewhere between these two values. It should be mentioned that the friction coefficient assumed has a marked influence on the c·itical reduction calculated, but a relatively slight effect on the calculated rolling force for a fixed arc length. A value of 0.24 was used in these cases because it was deemed reasonable based on previously published data (cf Subsection II.4.2 ..nd Reference 42). It is encouraging to note that the same coefficient gives reasonable results for both sets of data, since the steels rolled in these sets were chemically identical. The same coefficient was used for both wet- and dry-temper rolling data in the case of the Nash mill trials; the low test speed produced apparently negligible lubricant entrapment, and rolling force and transfer data both indicated that the presence of a lubricant had little effect on process mechanics in this case.

On the whole, the limited data presented in this section agrees rather well with the theoretical expressions proposed in Part II. In closing, some comment on the legitimacy of the inferred effective strip yield stresses and (doubly) inferred arc lengths used to construct this data are in order. Although no expressions for these parameters were given in the theoretical development, expected qualitative trends in their behavior as other parameters are varied were discussed. Theoretical considerations indicated that the effective compressive yield strength should increase with increasing reduction; the yield stress values reported in Tables III.8 and III.9 are consistent with this trend. It was also concluded that the ratio of the plastic-arc length

to the rigid roll arc length should be roughly equal to unity at low reductions, and should increase with both reduction and yield strength at constant reduction. Figure 3.40 shows a plot of this ratio versus reduction for the data of Tables III.8 and III.9; as can be seen, the inferred arc lengths are consistent with these trends as well, although considerable scatter is evident in the Nash mill data. Finally, the more stable Bliss mill arc lengths are plotted in Figure 3.41 against well-known arc length formulas (the rigid roll arc length and equations proposed by Hitchcock[50] and Roberts[30]) to show that their magnitudes are reasonable from the point of view of traditional rolling theory.

III.12 Comparison With Previous Work

A large number of papers describing indentation experiments have been published in recent years (cf Section II.2 for a brief survey); among these, a few have given numerical results for the case of a hard, rough flat indenting a smooth, soft workpiece. Though these experiments generally involve "saw tooth" surfaces (see Figure 3.42) and purely normal loading, the overall geometry of the tests, as well as the aspects of the process generally studied, are comparable to those of temper-rolling transfer experiments. The results of these tests should thus be reconcilable with the results reported above. In this section, this is shown to be the case for the data of Bay and Wanheim[22] and Demkin and Izmailov[23].

Fig. 3.40 Variation of ratio of inferred arc lengths to rigid roll arc lengths with reduction

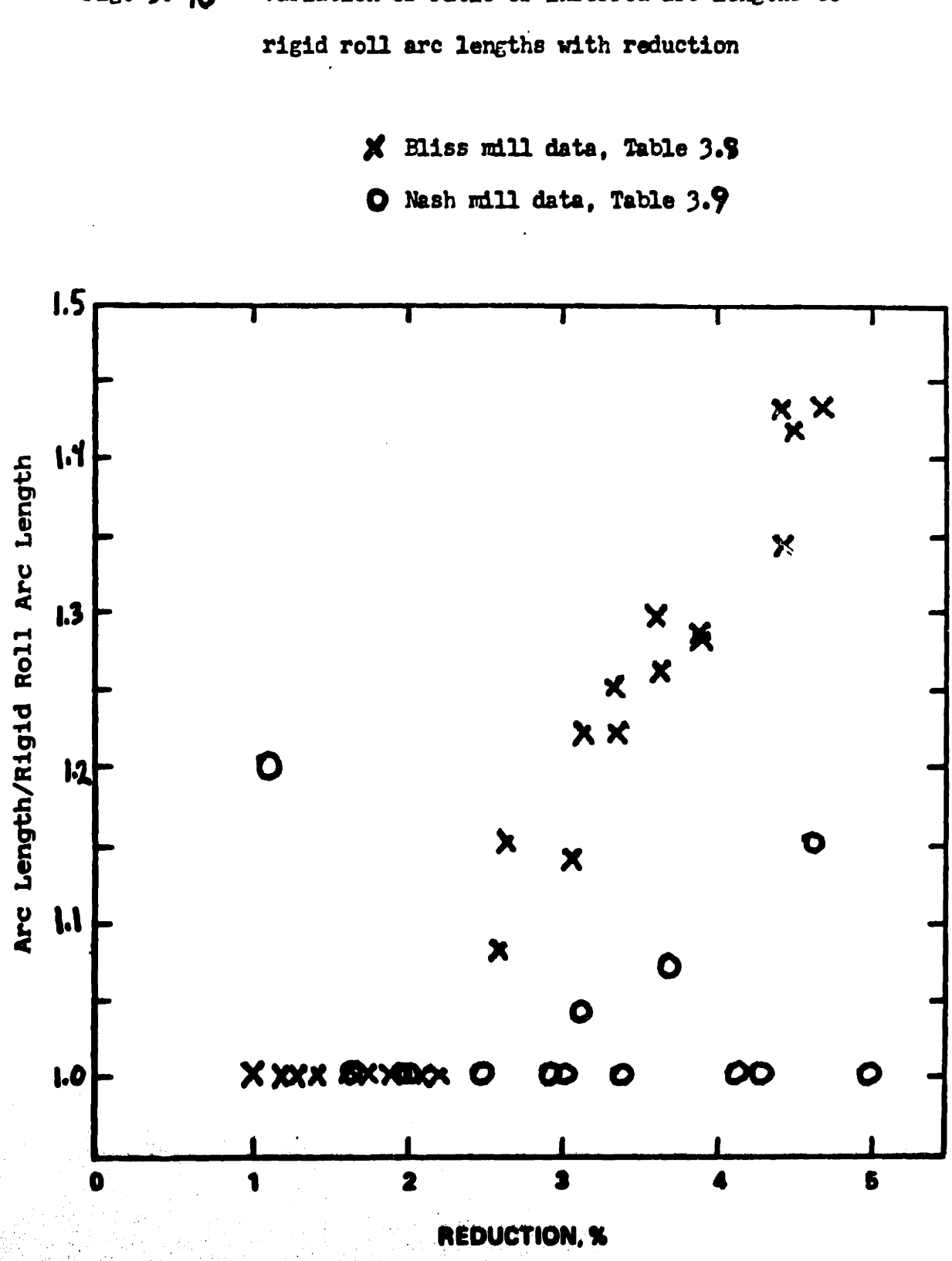

Fig. 3.41 Comparison of inferred Bliss mill arc lengths (✱) with arc lengths calculated by three well-known methods

— Rigid Roll theory $L_p = \sqrt{\frac{Dtr}{2}}$

– – – Roberts' theory $L_p = \frac{1}{2}\left[\frac{Dr\mu}{2} + \sqrt{\left(\frac{Dr\mu}{2}\right)^2 + 2Dtr}\right]$

o Hitchcock's theory $L_p = \sqrt{\frac{D'tr}{2}}$; $D' = D\left(1 + \frac{4.63f}{\bar{e}tr}\right)$

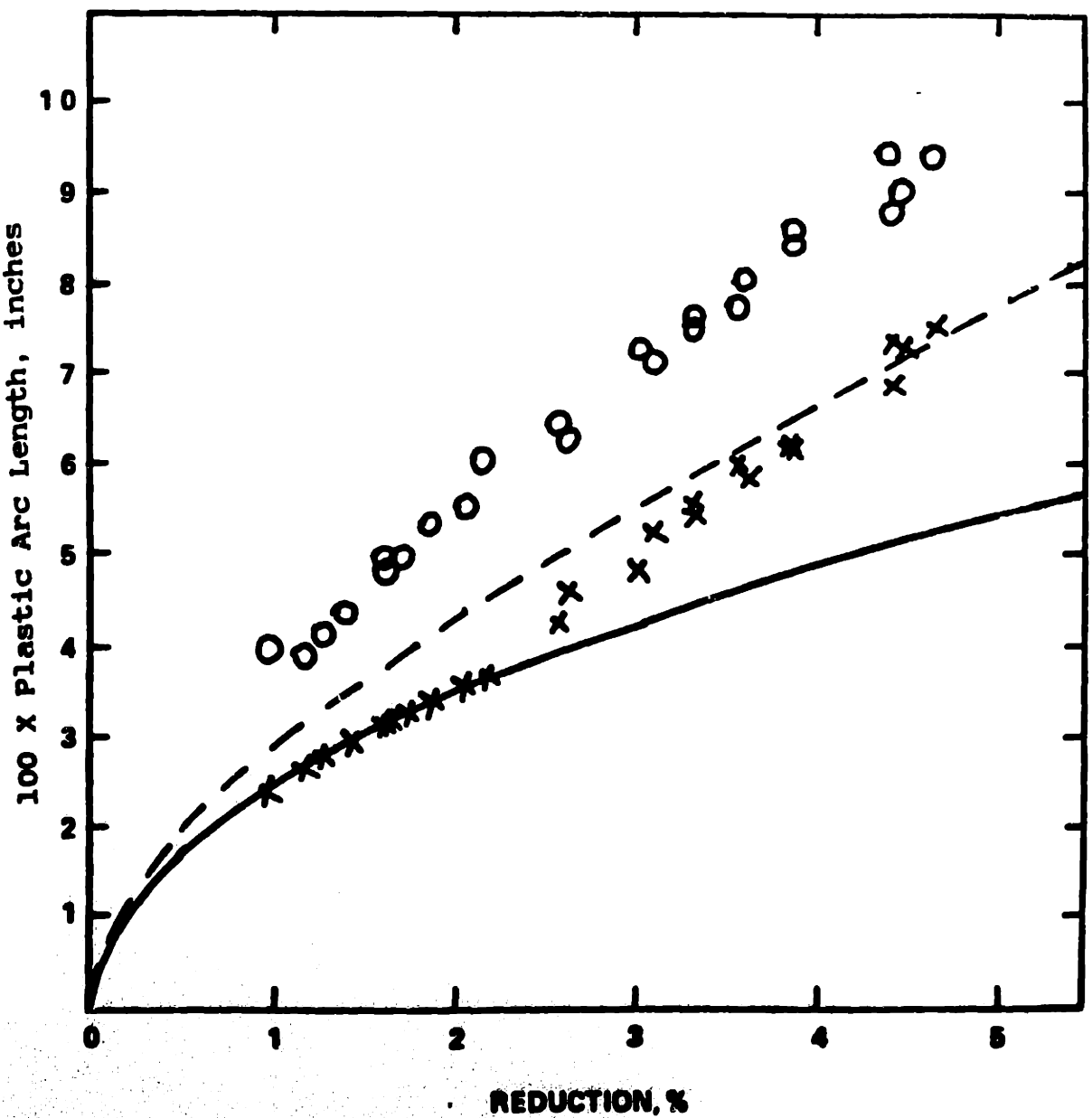

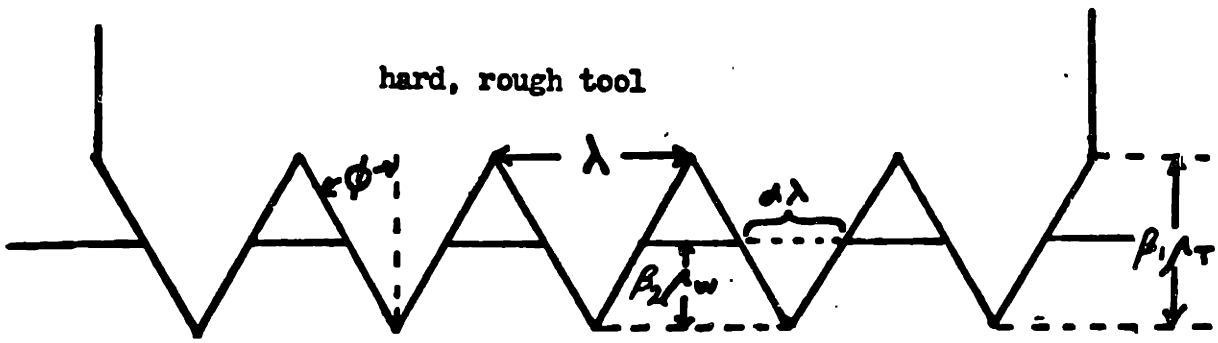

$4 < \beta_1 \approx \beta_2 < 6$

$\beta_2 \to \beta_1$ as $t \to 1$

Fig. 3.42 Indentation of soft, infinitely smooth workpiece by hard tool with rough "saw-tooth" surface.

Note that for this case, the ratio of real to apparent area of contact (α) is identical to the ratio of workpiece to tool roughness (Λ_w/Λ_t), since, from geometry (defining t as the ratio of workpeice to tool roughness and noting that $\Lambda_w = t\Lambda_t$)

$$\alpha\lambda = 2\beta_2 t \Lambda_t \tan\phi$$

and $$\lambda = 2\beta_1 \Lambda_t \tan\phi$$

which yields $\alpha \cong t$

As stated above, indentation experiments are usually carried out using specimens with simple, carefully prepared surface profiles. The geometry applicable to the situtation under consideration is shown in Figure 3.42. These tests differ from temper-rolling trials in two other important ways: The loading applied is generally purely normal, and the results are reported as ratios of the real to apparent areas of contact, rather than ratios of workpiece to tool roughness. In this comparison, the average roll-bite pressure will be assumed to correspond to the normal pressure applied to the indentor. Also, the ratios of real to apparent area of contact and workpiece to tool roughness will be assumed to be equal. As seen from the simple geometrical argument given in Figure 3.42, these ratios are approximately equal for a rigid tool indenting a rigid-perfectly plastic flat, and thus should be roughly equal in indentation tests at high pressures.

Qualitatively, since some elastic flattening should occurs at the tool-workpiece interface prior to actual surface penetration, the ratio of real to apparent area of contact should rise steadily with pressure at pressures below the compressive yield stress of the workpiece, while the roughness transfer ratio should remain constant at its initial value. Once the compressive yield strength is reached, however, the temper-rolling transfer ratio should

rise rapidly in comparison with the indentation area ratio (due to the combined shear and normal loading in temper rolling, as opposed to purely normal indentation loading; cf Section II.3), and should reach unity at a substantially lower pressure.

Figure 3.43 shows the ratio of strip to roll roughness as a function of the ratio of (calculated) average roll-bite pressure to (inferred) effective compressive yield strength of the strip for the data given in Tables III.8 and III.9. As can be seen, this data falls on a relatively tight curve. To avoid cluttering and confusion, only sample points are plotted against the indentation results for comparison. The comparison of the transfer data with the results of Bay and Wanheim is given in Figure 3.44; the comparison with the results of Demkin and Izmailov is given in Figure 3.45. As can be seen, the general qualitative trends described above are clearly evident in both cases.

III.13 Comments on Production Data

A table of mechanical and transfer data from a commercial dry-temper mill is given in Appendix II. At present, quantitative methods for calculating roll forces and surface transfer have not been developed sufficiently to examine this data in detail. Some important qualitative comments, however, concerning the differences between laboratory and production conditions, and the effects of these differences on observed results, are in order at this point.

The main difference between temper rolling on a laboratory versus a production mill is a large difference in

Fig. 3.43 Variation of roughness transfer with ratio of average roll bite pressure to effective compressive yield stress of strip for temper rolling data given in Tables 3.8 and 3.9

O Nash mill data (Table 3.9)

× Bliss mill data (Table 3.8)

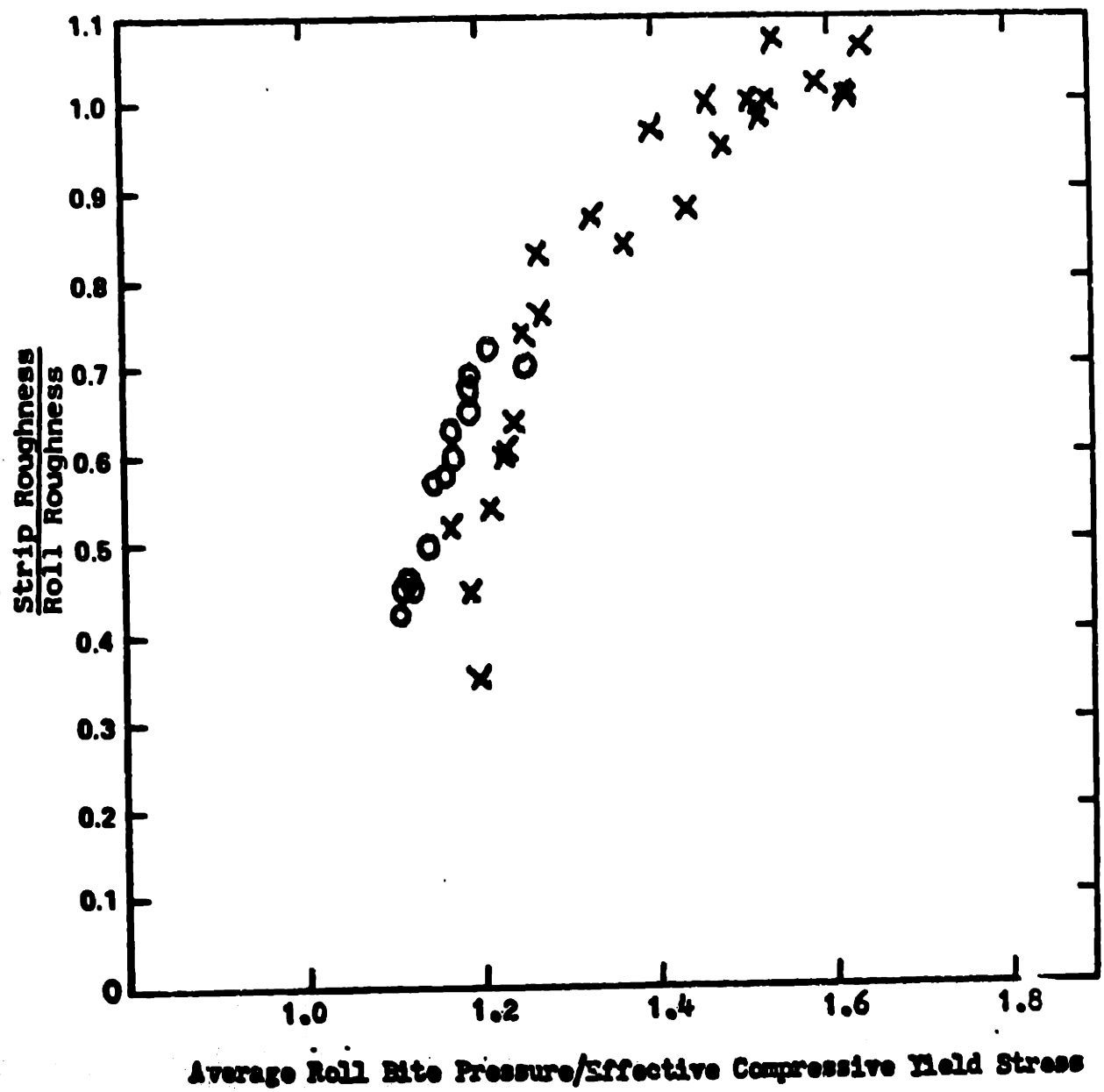

$$\frac{\text{real area of contact}}{\text{apparent area of contact}}$$

or

$$\frac{\text{strip roughness}}{\text{roll roughness}}$$

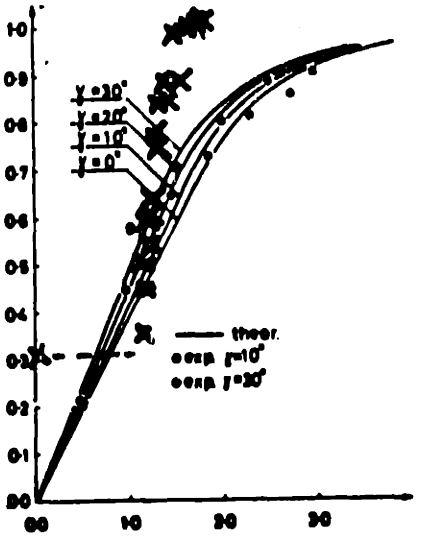

$$\frac{\text{average normal pressure}}{\text{compressive yield stress}}$$

---✱ data from temper-rolling tests, specimens 1-13 and 17-20, Table 3.8

Fig. 3.44 Comparison of temper rolling transfer data with surface contact data given in Fig. 7 of paper by Bay and Wanheim (ref. 22)

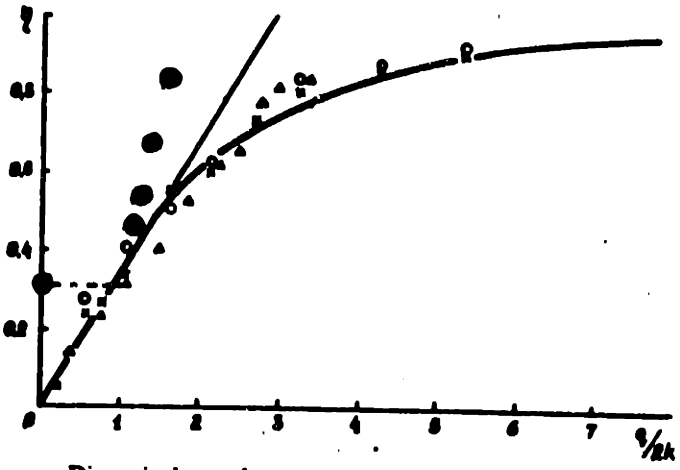

Dimensionless real contact area *vs.* dimensionless pressure.
Experimental results: ×, indentation; O, compression; ▲, indentation of array of wedges with $2\theta = 90°$.
- - -● temper rolling (specimens 1-4, Table 3.8)

Fig. 3.45 Comparison of surface transfer data (Table 3.8) with surface contact data given in Fig. 4 of paper by Demkin and Izmailov (ref.23)

horizontal axis: ratio of normal pressure to compressive yield stress

vertical axis: ratio of real area of contact to apparent area of contact (equivalent to ratio of strip to roll roughness)

scale. Production mills operate at much higher speeds, and employ much larger work rolls, than the mills used to generate the data presented above. The difference in work-roll diameter (a factor of four or five increase over the Bliss mill) is particularly critical; it leads to a corresponding large increase in plastic arc length, and thus to a substantial decrease in the critical reduction for complete transfer. In the dry-temper rolling of 0.030-inch-thick mild-annealed stock this critical reduction is roughly nine percent for Nash-mill conditions (see Figure 3.39), but approximately one percent for production conditions (3,000 feet/minute mill speed, 24-inch-diameter work rolls). This has made it necessary to take comparatively large reductions to produce data over a reasonable range of transfer levels in laboratory tests. Production-mill operators should realize that low reduction (<1 percent) transfer levels should be much higher under commercial conditions than under laboratory conditions; comparison of the data in Table A.4 with that presented above illustrates this point rather clearly.

A second difference arrises in wet-temper rolling tests. At the high mill speeds employed in commercial wet-temper rolling, significant lubricant entrapment occurs even with the relatively inviscid wet-temper lubricants currently in common use. This can significantly alter the mechanics of the process (as compared to dry-temper rolling), leading to less efficient and generally less consistent transfer (see Figure 3.46 below). In the author's experience, roughness transfer levels observed in commercial wet-temper rolling are

roughly 30 percent less than those observed in dry-temper rolling under identical conditions; the corresponding critical reduction in the lubricated case is about 50 percent larger than the dry-temper rolling value. Because of limitations in mill power and in the footage (and cost) of laboratory coils, it is difficult to operate a laboratory mill at speeds within even a factor of three of the production conditions; consequently, it is difficult to generate wet-temper rolling data in the laboratory in which lubricant entrapment occurs to a significant extent. This greatly limits the utility of any such data, particularly with regard to quantitative modeling.

Aside from scale, it should be realized that the laboratory data was taken under constant and well-monitored conditions. In commercial rolling, mill conditions are continually changing; the operator is constantly altering tensions, rolling forces, and mill speed to ensure proper shape, surface texture, and mechanical properties in the final product. In general, for example, the mill is operating at low speeds at the head and tail end of each coil and at full speed in the middle. An increase in mill speed increases the compressive yield strength of the strip and leads to a (generally) slightly lower extension in the center of the coil (see Appendix II). Due to the overwhelming influence of extension on transfer, this results in the head and tail ends of a coil having a different texture than the center of the coil. This point is illustrated for 0.036-inch-thick electrogalvanizing line stock in Figure 3.46. As can be

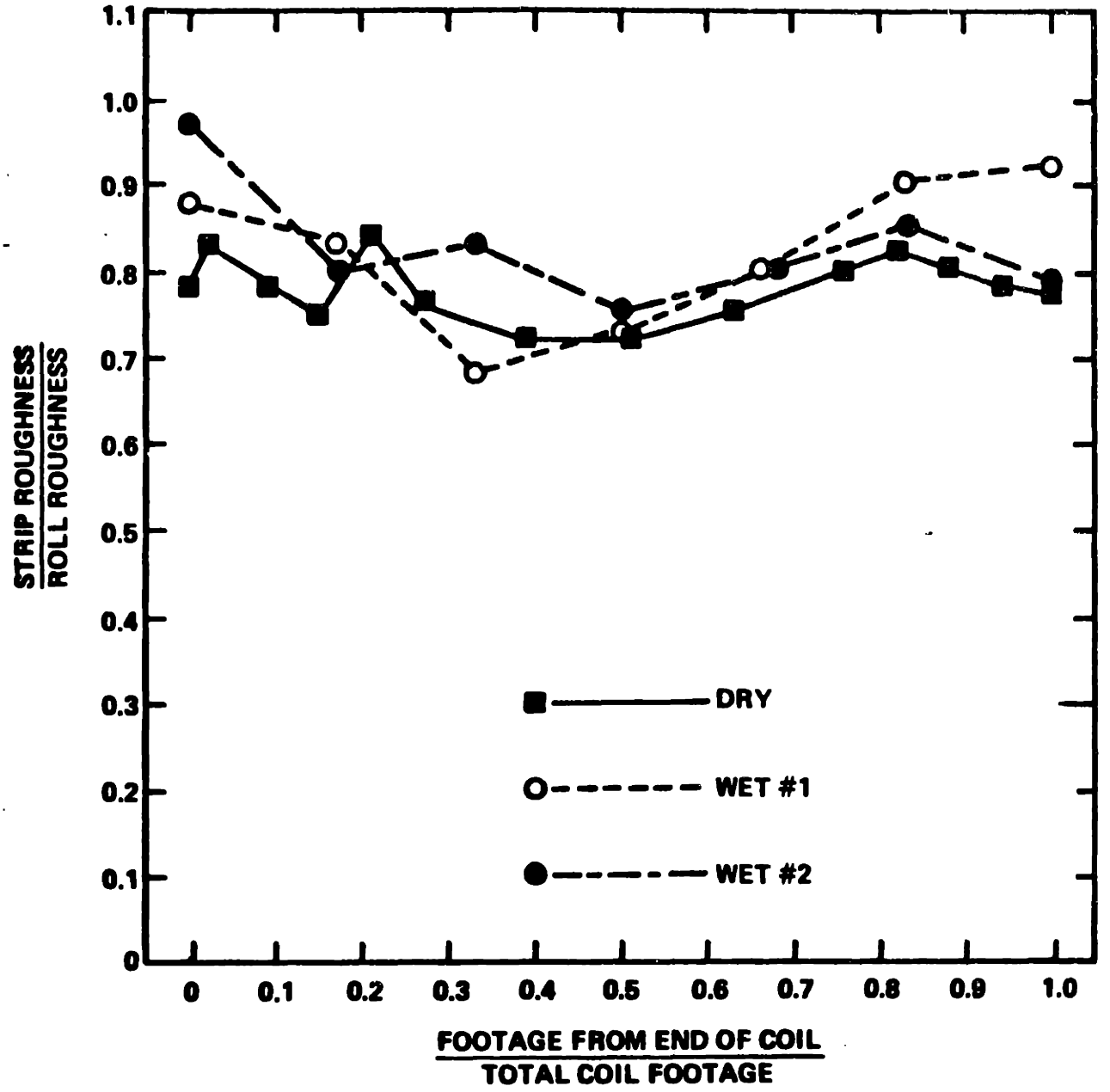

Figure 3.46

ROUGHNESS TRANSFER AT VARIOUS COIL FOOTAGES ON THE 84" TEMPER MILL, NORTH SHEET MILL, U. S. STEEL GARY WORKS. ROLLS: 24" DIAMETER CHROME PLATED, 61 μin. AA (DRY) AND 41 μin. AA (WET) ROUGHNESS; STRIP: EGL PRODUCT, REDUCED 0.5-0.75% (DRY) AND 1% (WET)

seen, the wet-temper rolled coils show more scatter in roughness through their length; forces and extensions are more difficult to control in wet-temper rolling. Although all of the readings in Figure 3.46 fall within the roughness range specified for the strip (25 to 50 microinches), this, of course, need not always be the case; sheet consumers should realize that some variation in surface texture through the body of a coil will inevitably occur, and that head or tail end profile readings thus provide only an approximate indication of a coil's surface properties.

The above discussion makes it clear that the value of the laboratory data presented in Sections III.4 to III.11 lies not at present in its quantitative predictive power, but rather in the qualitative indications it gives as to how specific rolling variables influence surface transfer. The implications of the data in this regard to commercial temper rolling are given in Section IV.5.

DISCUSSION

IV.1 Strip Gage Effects

As mentioned in Sections II.5 and III.9, the most interesting trends encountered in this investigation were the observed decreases in both rolling force and transfer efficiency with increasing strip thickness. Neither of these trends is markedly inconsistent with theory; the observed influence of strip gage on transfer is predicted by the quantitative analysis of Part II (cf Equation 2.35 and Table III.6), and a decrease in rolling force with increasing strip thickness is commonly observed in mill practice (tin mills, which roll lighter gages than sheet mills, are invariably designed to deliver higher rolling loads) and predicted by Roberts' temper-rolling model.[30] Nonetheless, these results came as a surprise to the author, and are somewhat contrary to both common sense and the qualitative reasoning of Part II. A brief discussion of the mechanisms which seem to account for these trends is thus probably in order.

The observed influence of strip gage on surface transfer is best rationalized by considering the likely effect of variations in strip thickness on roll-bite geometry and mechanics, as illustrated in Figure 4.1. As can be inferred from Equations 2.22 and 2.35, increasing the strip thickness at constant reduction lengthens the arc of contact somewhat, but sharply reduces the slope of the roll bite pressure function. The maximum roll bite pressure achieved in the rolling of thin strip, Figure 4.1a, is thus likely to be larger than that achieved with thicker strip, Figure 4.1b.

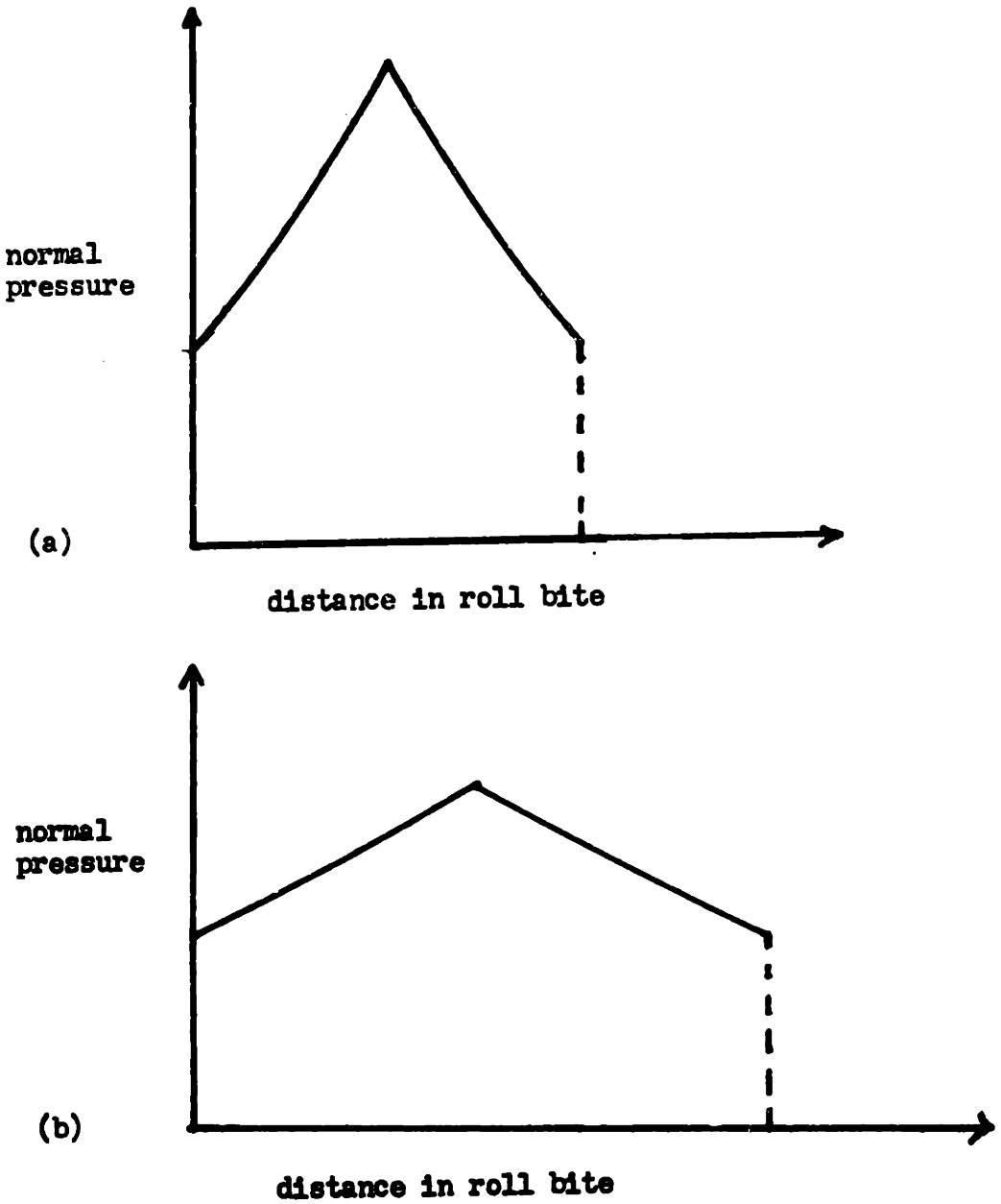

Fig. 4.1 Effect of strip thickness on normal pressure distribution in roll bite. (a) Thin strip; shorter arc length, larger pressure distribution slope. (b) Thicker strip; longer arc length, smaller pressure distribution slope.

Since the magnitude of this stress determines the maximum shear stress developed at the roll-strip interface, a decrease in strip thickness should lead to a decrease in the critical reduction required for complete transfer, and thus to an increase in transfer efficiency.

The mechanisms which account for the observed decrease in rolling force with increasing gage are not as clear, but are probably related to variations in strip yield stress with strip thickness, and to elastic effects. An increase in strip thickness leads to a decrease in the average strain rate, and thus, by Equation 2.24, probably leads to a decrease in the effective strip yield stress. As mentioned in Subsection II.4.4, this yield stress may additionally decrease with the ratio of roll diameter to strip thickness, although the reasons for this possible trend are not presently clear. An increae in strip yield stress directly influences the plastic roll force (although in this case the corresponding decrease in plastic arc length probably more than balances this effect), and more importantly significantly increases the elastic rolling force (cf Equation 2.31). As strip thickness is decreased, therefore, elastic effects probably begin to dominate, and the mill load necessary to obtain a significant reduction probably rises substantially. Experience in the rolling of thin foils indicates that, for a given mill, there probably exists a minimum thickness (formulas for which have been proposed by Stone, Roberts, and several others[61,62,63]) beyond which the strip

cannot be reduced. For the Nash mill, under applicable conditions, this thickness is probably roughly 0.04 inch; as can be seen from Figure 3.27, the most marked rise in rolling force with decreasing gage occurs in going from thicker strip to a gage reasonably close to this value.

Finally, it should be mentioned that only one set of data on gage effects has been obtained to date, and that, since the materials for these tests required two months of intermittent effort (for reduction, heat-treatment trials, annealing, etc.,) to produce, it is unlikely that substantial additional data will be obtained in the near future. The trends discussed above are, however, consistent with the quantitative theory of Part II, which has generally been reliable in predicting qualitative trends, and with mill experience. Moreover, limited conversations with production personnel indicate that, in commercial temper rolling, it is often difficult to attain desired levels of extension and surface transfer when rolling very thin strip, since the rolling forces required to do so are apparently near or beyond the capacity of the mill.[64])

IV.2 Role of Rolling Force in the Transfer Process

Many readers may be surprised to find no section in Part III on the effect of rolling force on transfer, and very little mention of this parameter in Part II; rolling force is often cited as a factor which might influence sheet surface quality,[11,12] and it seems reasonable to expect that the degree to which the roll surface is coined into the strip

would depend on the force used in pressing them together. The results of this investigation, however, indicate that the relationship between rolling force and transfer efficiency is an indirect one. An increase in rolling force will generally lead to an increase in surface transfer; this is not due to any strong causal link, however, but rather to the fact that increasing the rolling force generally increases other quantities——such as plastic arc length, reduction, and maximum roll-bite shear stress—which do exert a fundamental and direct influence on the transfer process. In some cases, such as (for example) in the rolling of very thin strip, a large increase in rolling force produces little or no increase in reduction, and consequently no significant increase in transfer efficiency. On the other hand, a large increase in reduction invariably produces significantly increased roll-strip surface matching, regardless of rolling conditions, provided this matching is not already complete. It therefore seemed more natural to the author to discuss the transfer process in terms of stress and deformation rather than overall force, and to formulate the quantitative analysis of the process in terms of a strain, reduction. This analysis was qualitatively extremely simple, although somewhat involved mathematically. A formulation based on rolling force would probably be considerably more complicated, since it would lack this underlying qualitative simplicity.

IV.3 Accuracy of Experimental Results

The principal errors in the experimental results presented in Part III and Appendix II probably stemmed from practical constraints; it is impractical, on the one hand, to construct a fully instrumented laboratory mill specifically designed for temper-rolling research, or on the other hand to carefully instrument a commercial-temper mill and roll under specified conditions, regardless of the quantity and quality of the resulting product. As a consequence, all laboratory data was obtained on mills designed for more general cold-rolling research; instruments often recorded readings less than five percent of full scale, and mechanical aberations which have little effect on higher-reduction rolling tests, such as slight strip gage variations and changes in strip tensions, caused wide variations in the parameters under study. Production data, on the other hand, was obtained under conditions more akin to an observational study than a controlled experiment; rolling was carried out under normal, constantly changing conditions as the mill operator adjusted various parameters to ensure acceptable product quality, and the prevailing conditions were recorded at more or less random intervals. In addition, production mills are not instrumented as accurately as laboratory mills (nor, in all fairness, do they need to be, as long as the operator is familiar with the gage readings typical of the most desirable rolling conditions); the author did not have the opportunity to check the accuracy of the instrumentation of the production mills used in this investigation, and though any sudden

failure of a gage would probably be detected and corrected, the possibility exists that some of the instruments monitored may have drifted gradually but significantly out of calibration. The difficulties involved in obtaining accurate temper-rolling data may well account for the dearth of published empirical studies of the process (in spite of its economic importance); in turn, this lack of a substantial temper-rolling literature, particularly concerning experimental methods, contributed somewhat to the inaccuracy of early test data, since techniques had to be refined mainly by trial and error.

In more precise terms, the accuracy of the laboratory data reported in Part III depended most strongly on the magnitude of the parameters monitored. Any variation in conditions which tended to increase rolling force, torque, etc., and thus lead to numerically larger measurements, tended also to increase the accuracy of the data obtained under these conditions. Data obtained at low speeds, low reductions, or on extremely soft strip was thus generally erratic and difficult to reproduce, whereas data obtained at higher speeds and reductions on harder strip was on the whole more stable and reliable. Data obtained on the Bliss mill was also generally less erratic than that obtained on the Nash mill, particularly with regard to strip tensions, since a slight eccentricity in the Nash mill entry tension brake drum caused variations in strip tension that could alter reduction by up to one or two percent—an insignificant factor in the experiments the mill was designed for (and is

primarily used for), but a serious problem in temper-rolling tests. In the balance, the author feels that little confidence should be placed on individual transfer or rolling-force measurements taken at speeds below 100 fpm and reductions less than two percent, but that averaged results from several tests conducted under these conditions, and those obtained at higher reductions and speeds, are as reliable as most published rolling data.

The accuracy of the production results presented in Appendix II is dependent primarily on that of the mill instrumentation itself, since the conditions used were those for which the mill and instrumentation were designed. Specifically, five measurement systems were employed: Those to determine surface texture, rolling force, mill speed, extension, and strip tension. Production surface texture measurments were not as accurate as those made in the laboratory, since rolls were profiled at only one circumferential position and fewer profilometer traces were taken on strip samples; these measurements, however still probably estimated the desired parameters accurately enough for the purposes of comparison between various experimental conditions. Reduction and mill speed were both determined from mill bridle-roll rpm measurements; since reduction strongly influences strip stretcher strain sensitivity and ductility, this measurement system is almost certainly well maintained, and reported extensions and mill speeds are thus probably quite accurate. The accuracy of roll-force measurements is difficult to assess; there is (to the author's knowledge) no

published data with which they can be compared, and an experienced operator familiar with the mill in question can product acceptable strip even if the rolling load cells are damaged or out of calibration. On the whole, however, the reported values are not unreasonable, and it is likely that any serious, sudden load cell failure would be repaired; it therefore seems likely that the reported values are accurate to within (very roughly) 15 percent. The tension measurements are probably the least accurate; they were obtained by multiplying tension motor current measurements from a single motor by the number of motors on the relevent side of the mill (two on entry, three on exit) and then converting amperes to pounds by a calculated conversion factor. This process involves an assumed motor efficiency and the assumption that all motors on a given side of the mill are operating at the same current level. Considering the low tension levels characteristic of this data, however, it is unlikely that tension measurement errors will seriously affect comparisons with calculated roll forces or transfer levels, if methods to make such calculations are developed in the future.

As mentioned in the preceding paragraph, the assessment of experimental errors in the present data is complicated by the nearly complete lack of previous data for comparison. To the author's knowledge, no production rolling force data has appeared previously in the open literature. Limited laboratory roll force data published by Roberts[30] is consistent with that reported in this thesis, but was

obtained on the same laboratory mills. Roughness transfer levels measured by Barney and Robb on a commercial tin-temper mill[11] are roughly equal to those reported in Appendix II, but are apparently uncorrected for roll wear, and in any event are of limited use for comparison, since corresponding rolling conditions (particularly extensions) are not reported.

IV.4 Accuracy of Theoretical Analysis; Statistical Nature of Subject

It is difficult to evaluate the accuracy of the theoretical analysis presented in Part II, because this analysis has not been fully developed at this point and has been tested with only a limited amount of approximate data. Some clear goals for further development are evident, however, and these point to areas where extension or improvement of the existing treatment seems necessary or desirable. From the point of view of surface transfer, it seems most worthwhile to concentrate future efforts on developing an expression for plastic arc length in terms of input process variables; such an expression, when used with Equations 2.4 and 2.16, would provide a method of calculating percent transfer levels with reasonable effort from readily available input information. As discussed in Subsection II.4.4, however, the development of such an expression will probably require an analysis of the stresses in the elastic zones, as well as the development of an expression for the effective strip yield stress. A priori, there is no reason to expect the elastic analysis to be significantly more involved or difficult than the plastic analysis already carried out, although very little prior work

in this area is available (cf Part VI). The production of an expression for the effective yield stress, on the other hand, presents more of a problem. Since this is a material property, any such expression will probably be based (at least partly) on empirical correlation, and will thus be only as accurate an widely applicable as the data used to produce it. Moreover, it is not, strictly speaking, physically real quantity that can be measured directly, at least not easily; additional inaccuracies will arise in correlating highly approximate inferred values like those reported in Tables III.8 and III.9. These additional inaccuracies could be avoided by abandoning the assumption of a constant roll bite yield stress and assuming that, at point X, the yield stress is given by some function $\sigma_c(X)$. Revision of this assumption would, however, involve essentially redoing the entire analysis, starting from the differential equation

$$\frac{p(X)}{2}\frac{dh(X)}{dX} - \sigma_s(X) = \frac{d\left[\frac{h(X)}{2}\left[p(X) - \sigma_c(X)\right]\right]}{dX} \qquad (4.1)$$

which, depending on the form of $\sigma_c(X)$, could be very difficult to solve. The available data, although limited, indicates no need for so drastic a revision; the present treatment appears promising, and may, with moderate revisions, be accurate enough to predict actual transfer levels to within inherent statistical scatter in many rolling situations.

The last sentence of the preceeding paragraph introduced a very important consideration which has been ignored to this point: That surface properties (and, to a lesser

extent, rolling force, spindle torque, and all other measured quantities) are random variables, possessing an inherent dispersion or uncertainty, an accuracy beyond which it is pointless to attempt to measure or calculate them. In one set of 17 strip specimens (some of which were used in Figures 3.10 and 3.11), for example, the sample variances were on average greater than 5 percent of mean for roughness measurements, and nearly 13 percent of mean for peak count measurements. This was under laboratory conditions, with eight traces being taken per sample; in production situations, where one trace per sample is more typical, much larger variances (from "true" values; the sample variance from mean of a sample of one is, by definition, zero percent) would be expected. This is not merely an academic distinction, brought up purely to excuse the author from further modifying and improving his analysis (in fact, it suggests that the deterministic approach to the problem taken in this thesis is inappropriate, and that a probabilistic treatment based on assumed distributions would be more in keeping with the physical reality of the process), but rather an important aspect of the nature of surface texture which is frequently overlooked by sheet producers, consumers, and researchers. The deterministic approach to the calculation of roughness transfer taken in this thesis is probably not overly naive, in view of the typical roughness dispersion quoted above; any expression for peak count transfer arrived at in the future, however, should, based on this consideration, predict both a probable transfer value and a probable error. This consideration

should also be borne in mind by anyone reading the three-digit numbers typically output by a commercial profile meter; it is unlikely that more than one of these digits is significant, particularly when less than four traces are taken.

IV.5 Implications to Mill Practice

The theoretical discussion of Part II, as outlined in Sections II.5 and III.4 to III.10, indicates that the easily controlled rolling variables that influence (percent) surface transfer most strongly are extension, roll diameter, the initial mechanical, geometric, and surface properties of the strip, and lubricant viscosity. With the exception of lubricant viscosity, the values of these variables are all essentially fixed in a given rolling situation by the design of the mill, the product to be rolled, and the formability and ductility requirements of the processed sheet. In most rolling situations, therefore, the percent transfer level attainable is, for all intents and purposes, determined by input variables; as will come as no surprise to mill operators, the surface properties of the finished sheet can best be changed in most cases by changing the texture of the work rolls used. Equations 2.4 and 2.16 can in principle be used to estimate the percent roughness transfer levels typical of given rolling conditions, and thus the roll texture necessary to produce sheet with specified surface properties; however, further work, specifically the development of a plastic arc length formula, is necessary to make such estimates possible without an impractical amount of materials testing. Further work may also lead to the development of a complimentary

method of calculating percent peak count transfer. Until this work is completed, a rough idea of the transfer levels typical of dry-temper rolling of 0.030-inch strip can be gained from Appendix II; similar data on dry- and wet-temper rolling of 0.036- inch strip is given in Figure 3.46. It should be emphasized, however, that these levels are strongly dependent on extension and strip gage (transfer levels increase with increasing extension at constant gage, but decrease with increasing gage at constant extension).

This thesis has more immediate implications to other aspects of mill operation, such as mill design and the likely effect of day-to-day changes in mill practice (e.g., switching from dry- to wet-temper rolling) on transfer levels. Regarding mill design, this work indicates that transfer levels closer to unity (the ideal value, since in this case the final sheet surface texture would be that of the work rolls used) can be insured by designing mills with work rolls as large as practical (from rolling-force considerations) and (for dry-temper mills at least) with the maximum possible operating speed. Regarding day-to-day changes in mill practice, the results indicate that rolling variables sometimes manipulated to reduce rolling loads and increase roll life can noticeably influence percent-transfer levels. Large increases in average strip tension, for instance, which can reduce rolling forces, also lead to slight decreases in transfer efficiency. And the use of wet-temper rolling lubricants, which improves roll life, strip quality, and general mill cleanliness, can reduce transfer levels

significantly (roughly 20 to 40 percent) over corresponding dry-temper rolling conditions, although the difference is frequently made up by the increased extensions typically used in wet-temper mills. As to lubricant selection, transfer levels closer to unity are achieved by minimizing the viscosity of the lubricant chosen. Water appears to be the best wet-temper lubricant from the point of view of surface transfer, although its value in keeping the mill free of dust is uncertain and its use obviously leads to difficulties in strip rust prevention. This work also indicates that the mill operator can alter transfer levels somewhat even in cases when most rolling variables are fixed. Increased or decreased transfer can be achieved, for example, by rolling as near as possible to the upper or lower bounds (respectively) of specified extension ranges.

Finally, it should be emphasized that percent transfer levels discussed in this thesis are based on the acutal, in situ texture of the mill work rolls employed. Roll cleaning practices, such as flushing with pressurized fluids or "facing" (e.g., rolling below face at extremely high loads and speeds) can significantly damage work-roll texture; roll texture obviously also wears off, the amount of wear apparently depending on the linear footage rolled, the loads used in rolling, and the state of lubrication (roll texture tends to deteriorate more rapidly in wet- than in dry-temper mills, although overall roll life increases due to the virtual elimination of roll marking resulting from increased mill cleanliness). While a more detailed discussion of roll-blast

wear is beyond the scope of this thesis, some method of correcting for this wear (from previous experience or formal study) will be necessary if the present transfer equations, in a more developed form, are to be used for on-line quality control.

V. CONCLUSIONS

1) The surface transfer process in temper rolling can be modeled as an indentation process in which the roughness peaks of the rolls are pressed into the strip surface. Complete roll-strip surface matching requires that the strip surface flow plastically and mold itself around the asperities of the roll surface. Due to material constraint considerations akin to those encountered in the analysis of hardness indentations, the strip surface layer can transmit surprisingly high normal stresses to the substrate without deforming markedly itself. the strip surface deformation necessary for roll-strip surface matching thus probably results more easily from shear stresses, rather than normal stresses, at the roll-strip interface.

2) The transfer level (the degree of roll-strip surface matching) achieved under otherwise constant rolling conditions increases with increasing extension, increasing roll diameter, decreasing strip thickness, decreasing average tension, and increasing strip yield stress. In dry-temper rolling, transfer levels additionally increase with increasing mill speed and remain constant with variations in work roll (and presumably initial strip) roughness, at least within the range of roughnesses commonly encountered. In wet-temper rolling, transfer levels decrease with increasing mill speed and lubricant viscosity due to increased lubricant entrapment. The above

trends were all predicted from theoretical considerations and verified by fairly extensive laboratory temper-rolling experiments. The theory developed in Part II makes no clear prediction concerning the influence of roll roughness on the transfer process in wet-temper rolling, and no meaningful data on this point is currently available.

3) On a more basic level, any variation in rolling conditions which leads to an increase in plastic arc length, maximum roll bite pressure, the slope of the roll bite pressure function, or the effective coefficient of friction along the arc of contact should also increase surface transfer levels. Since increases in these quantities generally lead to an increase in rolling force, transfer efficiency should increase with rolling force in most cases. A method of calculating the ratio of final strip to work-roll roughness by examining the maximum value of a theoretical roll bite pressure function was partially developed and tested against a limited amount of empirical data. Theoretical and measured transfer levels agreed rather well in this comparison, indicating that this method is worthy of further development.

VI FUTURE WORK

As has been stressed at several points in this thesis, particularly in Section IV.4, future theoretical work on this subject should concentrate on a more accurate analysis of stresses and overall forces in the elastic entry and exit zones of the roll bite and on the development of expressions for the plastic arc length and effective compressive yield strength of the strip. Previous elastic analyses by Ford, Bland, and Ellis,[65] Jortner,[52] and Cosse and Economopoulos[33] should be helpful in determining the basic equations to be solved in the calculation of elastic stresses. In turn, an accurate determination of the elastic stresses (and the relative lengths of the entry and exit zones), as discussed in Subsection II.4.4, should be useful in producing a plastic arc length formula, or at least an iterative computational scheme for estimating this parameter. Any expression for the effective strip yield stress, however, will probably rely substantially on empirical correlation, since this is a material property.

The experimental data presented in Part III is, in the author's opinion, fairly comprehensive and consistent; nonetheless, further worthwhile experimental work could be carried out in several areas. Tests in which the strip roughness is varied, and tests in which the strip roughness is greater than the roll roughness, would be particularly interesting. Data to supplement existing information on gage effects (Section III.9) and estimated arc lengths and yield stresses (Section III.11) would also be of value. Most

importantly, further production mill data, particularly from wet-temper mills, would be of great benefit, since there seems to be an almost total lack of such data in the open literature.

Finally, work on the factors influencing (and methods of correcting for) the wear of work-roll surface finish would also be of value, since the transfer equations developed in this thesis assume that the in situ texture of the roll is known, and this texture cannot be monitored continuously or measured frequently in commercial situations.

References

1. T. G. Nilan, Detailed Surface Roughness Characterization of Cold-Rolled Steel Sheet," Iron and Steelmaker, Vol 3, 1976, pp. 21-28.

2. R. D. Butler and R. J. Pope, "Surface Roughness and Lubrication in Press Working of Autobody Sheet Steel," Sheet Metal Industries, Vol. 44, 1967, pp. 579-592 and 597.

3. M. Kotyk and J. W. Stewart, "The Influence of Surfaces and Shapes on Formability of Carbon Steel Sheet and Strip," paper presented at Material Forming Seminar, ASTME, January 20, 1969.

4. W. L. Roberts, Cold Rolling of Steel, Marcel Dekker, New York, 1978, pp. 775-6.

5. T. G. Nilan, unpublished work (1981).

6. W. L. Roberts, Cold Rolling of Steel, Marcel Dekker, New York, pp. 249-251.

7. I. Imai, T. Kikuma, N. Tsuzuki, T. Tushimitsu, H. Matsumoto, and Y. Euhori, "Study on a Jumping Phenomenon in Wet-Temper Rolling of Annealed Tin Plates with Light Reduction." Proc. of Int. Conf. on Steel Rolling, Vol. II. ISIJ, Tokyo, 1980, pp. 1203-1214.

8. J. R. McPhee, unpublished work (1966).

9. E. Rabinowicz, Friction and Wear of Materials, New York, Wiley, 1965, Section 3.4.

10. D. C. Litz, "Cold Rolling of Light-Gage Strip on a Laboratory Mill," Blast Furnace and Steel Plant, Vol. 55, 1967, pp. 1027-1035.

11. D. V. Barney and G. C. Robb, "An Analysis of the Characteristics and Preparation of Tin-Temper Mill Blast Rolls," Iron and Steel Engineer Year Book, 1969, pp. 520-525.

12. W. L. Roberts, "Influence of Rolling Lubricant on Sheet and Strip Quality," in Tribology in Iron and Steel Works, ISI publication 125, ISI, London, 1970, pp. 320-326.

13. E. Rabinowicz, Friction and Wear of Materials, New York, Wiley, 1965, Section 3.1.

14. P. K. Gupta and N. H. Cook, "Statistical Analysis of Mechanical Interaction of Rough Surfaces," ASME Journal Of Lubrication Technology, Vol. 94, 1972, pp. 19-26.

15. E. Rabinowicz, Friction and Wear of Materials, New York, Wiley, 1965, p. 21.

16. A. J. W. Moore, "Deformation of Metals in Static and in Sliding Contact," Proc. of the Royal Society of London, Vol. 195A, 1948, pp. 231-244.

17. J. B. P. Williamson, "Topology of Solid Surfaces," in Interdisciplinary Approach to Friction and Wear, Proceedings of NASA symposium, San Antonio, Texas, 1967, pp. 85-143.

18. J. A. Greenwood and G. W. Rowe, "Deformation of Surface Asperities During Bulk Plastic Flow," Journal of Applied Physics, Vol. 36, 1965, pp. 667-668.

19. J. Pullen and J. P. B. Williamson, "On the Plastic Contact of Rough Surfaces," Proceedings of the Royal Society of London, Series A, Vol. 327, 1972, pp. 159-173.

20. T. H. C. Childs, "The Persistence of Asperities in Indentation Experiments," Wear, Vol. 25, 1973, pp. 3-16.

21. D. Tabor, The Hardness of Metals, Oxford University Press, Oxford, 1951.

22. N. Bay and T. Wanheim, "Real Area of Contact Between a Rough Tool and a Smooth Workpiece at High Normal Pressures," Wear, Vol. 38, 1976, pp. 225-234.

23. N. B. Demkin and V. V. Izmailov, "Plastic Contact Under High Normal Pressure," Wear, Vol. 31, 1975, pp. 391-402.

24. R. Hill, The Mathematical Theory of Plasticity, Clarendon Press, Oxford, 1950, p. 295, eqn. 22.

25. D. R. Milner and G. W. Rowe, "Fundamentals of Solid Phase Welding," Metallurgical Reviews, Vol. 7, 1962, pp. 443-480.

26. E. Holmes, "Influence of Relative Interfacial Movement and Frictional Constraint In Cold-Pressure Welding," British Welding Journal, Vol. 6, 1959, pp. 29-37.

27. N. Bay and T. Wanheim, "Real Area of Contact and Friction Stress at High Pressure Sliding Contact," Wear, Vol. 38, 1976, pp. 201-209.

28. W. L. Roberts, Cold Rolling of Steel, Marcel Dekker, New York, chapters 9 and 10.

29. W. L. Roberts, Cold Rolling of Steel, Marcel Dekker, New York, Sections 9-15 and 9-19.

30. W. L. Roberts, "An Approximate Theory of Temper Rolling," Iron and Steel Engineer, Vol. 49, 1972, pp. 56-68.

31. E. M. Tret'yakov, Investigation of the Plastic Flow of Metals (in Russian), Nauka, Moscow, 1970, pp. 16-32.

32. N. N. Solomoichenko, "Analytical Determination of Metal Pressure on the Rolls in Temper Rolling." Communication 1. Ivz VUZ Chern. Met., 1978 (6), pp. 70-73 (BISI Translation 17836). Communication 2. Izv. VUZ. Chern. Met., 1978 (8), pp. 61-64 (BISI Translaton 17990).

33. P. Cosse and M. Economopoulos, "Mathematical Study of Cold Rolling," C. N. R. M., No. 17, December, 1968, pp. 15-32.

34. B. B. Hundy, "Inhomogeneous Deformation During the Temper Rolling of Annealed Mild Steel," Journal of the Iron and Steel Institute, Vol 181, 1955, pp. 313-315.

35. J. F. Butler, "Inhomogeneous Deformation and its Relationship to Strain Markings on Annealed and Temper-Rolled Sheets," in Flat Rolled Products, III, Met. Society of AIME Conf., Vol. 16, New York, Interscience, 1962, pp. 65-84.

36. D. R. Bland and R. H. Ford, "The Calculation of Roll Force and Torque in Cold-Strip Rolling With Tension," Proc. Institution of Mechanical Engineers, Vol. 159, 1948, pp. 144- 153.

37. J. D. Keller, "Cold-Rolling Strip Part II," Steel, Vol. 128, 1951, pp. 92-96.

38. M. C. Shaw, A. Ber, and P. A. Mamin, "Friction Characteristics of Sliding Surfaces Undergoing Subsurface Plastic Flow," ASME Journal of Basic Engineering, Volume 82D, 1960, pp. 342-346.

39. T. Wanheim, "Friction at High Normal Pressures," Wear, Vol. 25, 1973, pp. 225-244.

40. T. Wanheim, N. Bay, and A. S. Peterson, "A Theoretically Determined Model for Friction in Metal Working Processes," Wear, Vol. 28, 1974, pp. 251-258.

41. E. Orowan, "The Calculation of Roll Pressure in Hot and Cold Flat Rolling," Proc. Inst. of Mechanical Engineers, Vol. 150, 1943, pp. 140-167.

42. S. J. Dokos, "Sliding Friction Under Extreme Pressures 1," Journal of Applied Mechanics, Vol. 13, 1946, pp. A148-A156.

43. T. Von Karman, "Beitrag Zur Theorie des Walzverganges," Zeitschrift für Angewandte Mathematik und Mechanik, Vol 5, 1925, p. 139.

44. W. L. Roberts, Cold Rolling of Steel, Marcel Dekker, New York, Section 9-9.

45. G. F. Simmons, Differential Equations With Applications and Historical Notes, McGraw-Hill, New York, 1972, pp. 47-48.

46. E. Siebel and W. Leug, "Investigations into the Distribution of Pressure at the Surface of the Material in Contact with the Rolls," Mitt.K.W. Inst. Eisenf., Vol. 15, 1933, pp. 1-14.

47. G. T. Van Rooyen and W. A. Backofen, "Friction in Cold Rolling," Journal of the Iron and Steel Institute, Vol. 186, 1957, pp. 235-244.

48. D. Kobasa and R. A. Schultz, "Experimental Determination of the Length of the Arc of Contact in Cold Rolling," Iron and Steel Engineer Year Book, 1968, pp. 283-288.

49. J. W. Kannel and T. A. Dow, "The Evolution of Surface Pressure and Temperature Measurement Techniques for Use in the Study of Lubrication in Metal Rolling, ASME Journal of Lubrication Technology, Vol 96F, 1974, pp. 611-616.

50. J. H. Hitchcock, "Elastic Deformation of Rolls During Cold Rolling," ASME Report of Special Research Committee on Roll Neck Bearings, June, 1935, pp. 33-41.

51. W. L. Roberts, "The Frictional Characteristics of Rolling Lubricants," Proc. of the 11th Mechanical Working and Steel Processing Conference, AIME, New York, 1969, pp. 299-314.

52. D. Jortner, "An Analysis of the Mechanics of Cold-Strip Rolling," Doctoral Dissertation, College of Engineering and Science, Carnegie Institute of Technology, March 1958.

53. W. L. Roberts, Cold Rolling of Steel, Marcel Dekker, New York, Section 8-29.

54. W. L. Roberts, Cold Rolling of Steel, Marcel Dekker, New York, Section 8-35.

55. H. Hertz, Gesammelte Werke, Band I, Leipzig, 1895, p. 155.

56. W. L. Roberts, Cold Rolling of Steel, Marcel Dekker, New York, Section 9-5.

57. E. Rabinowicz, Friction and Wear of Materials, New York, Wiley, 1965, pp. 61-62.

58. R. J. Bentz and R. A. Dickinson, "Instrumented Rolling Mill for Cold-Rolling Research,: Blast Furnace and Steel Plant, Vol. 55 (1967), pp. 319-324.

59. "Surface Texture Measurement of Cold-Rolled Streel Sheet —SAE J911," SAE Handbook, Part I, 1981, pp. 10.1-10.2.

60. E. Rabinowicz, Friction and Wear of Materials, New York, Wiley, 1965, pp. 60-61.

61. W. L. Roberts, Cold Rolling of Steel, Marcel Dekker, New York, Sections 9-17, 9-24, and 9-25.

62. M. D. Stone, "Rolling of Thin Strip," Iron and Steel Engineer Year Book, 1953, pp. 115-128.

63. W. L. Roberts, "A Simplified Cold-Rolling Model," Iron and Steel Engineer Year Book, 1965, pp. 925-937.

64. L. E. Chopp (Senior Process Engineer, Sheet Production, Technical Implementation Program, U. S. Steel Irvin Plant), private communication.

65. R. H. Ford, F. Ellis, and D. R. Bland, "Cold Rolling with Strip Tension, Part III," Journal of the Iron and Steel Institute," Vol. 171, 1952, pp. 245-249.

APPENDIX I: DERIVATIONS

A.1 Equation 2.8 (Von Karman's Equation)

A derivation of a form of this equation valid for a circular arc of contact and assumed slipping friction is given by Roberts.[44] The argument given below is valid for the Amonton, Shaw, or Orowan friction models. This derivation nominally assumes a planar arc of contact and a constant strip yield stress; however, since dh/dX and $d\sigma_c/dX$ are not assumed constant or zero in any step of the arugment, the final result is actually valid for any arc shape and any reasonable roll-bite yield stress function $\sigma_c(X)$.

Figure A.1 shows the stresses acting on a differential element of strip material in the entry region of the roll bite. Equilibrium of horizontal forces (neglecting second order differentials) gives

$$2p(x)\tan\alpha dx - 2\sigma_s(x)\cos\alpha dx = (h(x) + dh)(\sigma + d\sigma) - h(x)\sigma \simeq d(h(x)\sigma) \qquad (A.1)$$

Since α is very small in temper rolling, $\cos\alpha \simeq 1$.

Notice also that

$$\tan\alpha \simeq \frac{1}{2}\frac{dh(x)}{dx}$$

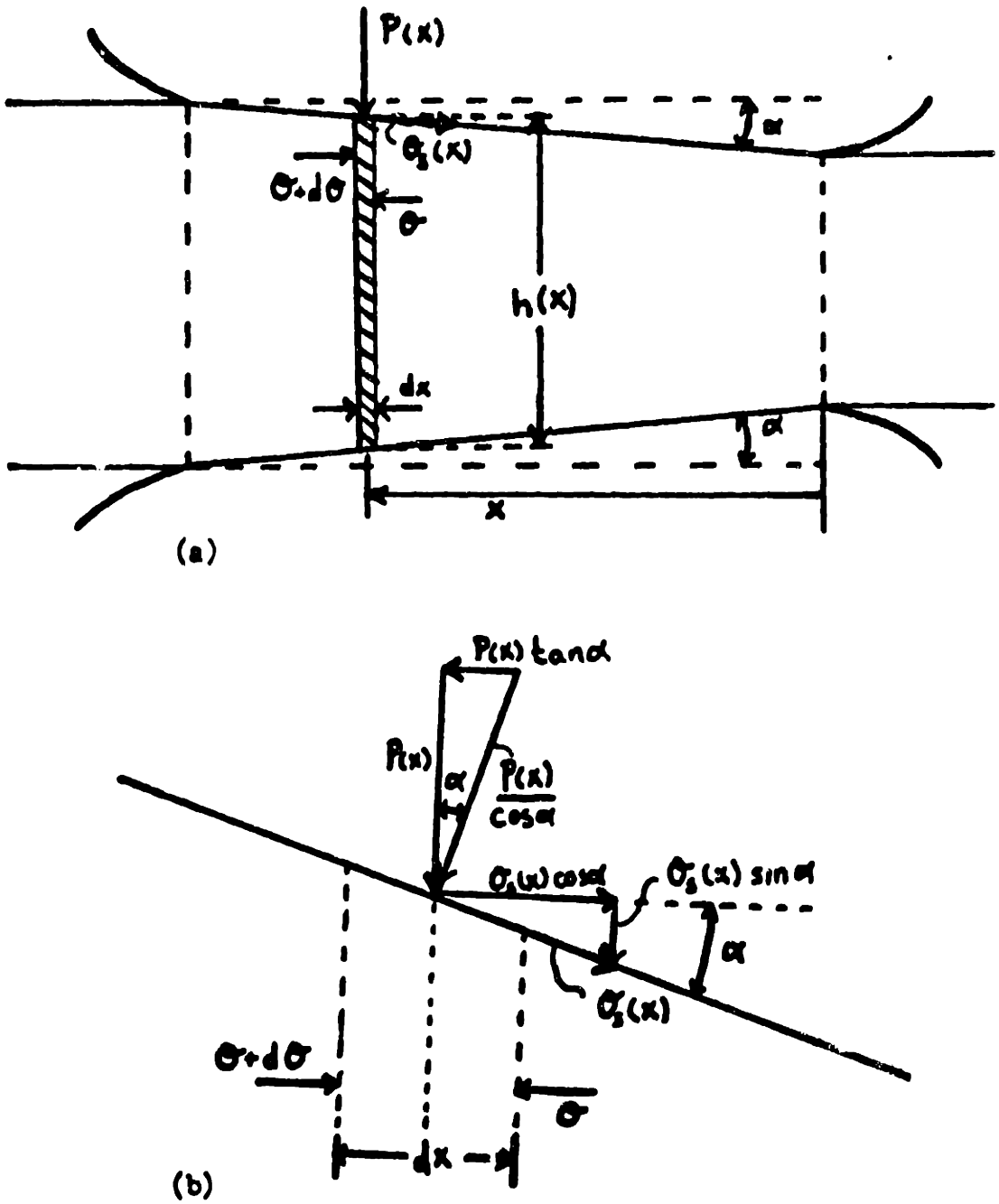

Fig. A.1 (a) Modification of Fig. 2.5 showing stresses on differential element of strip material in entry region of roll bite. (b) Decomposition of stresses on element at the roll-strip interface.

Substitution into Equation A.1 and rearrangement gives

$$\frac{p(x)}{2}\frac{dh(x)}{dx} - \sigma_s(x) = \frac{1}{2}\frac{d(h(x)\sigma)}{dx} \qquad (A.2)$$

The total vertical stress on the element is $p(X) + \sigma_s(X)\sin\alpha$; by Tresca's yield criterion, therefore

$$p(X) + \sigma_s(X)\sin\alpha = \sigma_c + \sigma \qquad (A.3)$$

For the Orowan, Shaw, and Amonton friction models (cf Subsection II.4.2),

$$0 \leq \sigma_s(X) \leq p(X)\mu$$

where μ is a friction coefficient generally less than 0.3. Thus

$$1 \leq \frac{p(x) + \sigma_s(x)\sin\alpha}{p(x)} \leq 1 + \mu\sin\alpha \qquad (A.4)$$

since $\sin\alpha$ is small,

$$1 + \mu\sin\alpha \approx 1$$

and Expression A.4 gives

$$p(X) + \sigma_s(X)\sin \approx p(X) \qquad (A.5)$$

Substitution of Equations A.3 and A.5 into Equation A.4 and rearrangement gives

$$\frac{p(X)}{2}\frac{dh(X)}{dx} - \sigma_s(X) = \frac{d\left[\frac{h(X)}{2}(p(X)-\sigma_c)\right]}{dX}$$

which is the desired version of Equation 2.8 for the entry region. Reversing the sign on the shear-stress term gives the form for the exit region by essentially the same argument.

Note that, strickly speaking, the assumed geometry gives Amonton's law in the form

$$\sigma_s(X) = \frac{\mu p(X)}{\cos\alpha}$$

however, since cos $\alpha \approx$ 1 as noted above,

$$\sigma_s(X) \simeq \mu p(X)$$

(alternatively, the above statement can be interpreted as defining a new Amonton friction coefficient, $\mu' = \mu \cos\alpha$, which differs inperceptibly from μ).

A.2 Pressure Distribution Equations (Equations 2.12, 2.14, and 2.17)

Equation 2.12 (planar arc, slipping friction)

substituting

$$h(X) = t\left(1 - 4 + \frac{X}{L_p}r\right)$$

and $\sigma_s(X) = \mu p(X)$

into Equation 2.8 gives the relevant differential equation, Equation 2.11:

$$\frac{dp(X)}{dX} \pm \frac{2\mu}{h(X)}\, p(X) = \frac{\sigma_c rt}{L_p h(X)}$$

where the plus and minus signs apply respectively to the exit and entry regions. This is a first-order differential equation of the general form

$$\frac{dy}{dx} + q(x)y = s(x) \qquad \text{(A.6)}$$

The general solution of which is[45]

$$y = \frac{1}{f(x)}\left(\int f(x)s(x)dx + C\right)$$

where (A.7)

$$f(x) = \exp\left\{\int q(x)dx\right\}$$

Applying Equation A.7 to Equation 2.11 gives, for the entry side,

$$f_1(x) = \exp\left(2\mu\int h(x)^{-1}dx\right)$$

$$= \exp\left(\frac{2\mu L_p}{rt}\ \ln h(x)\right)$$

$$= (h(x))^a \quad ; \quad a = \frac{2\mu L_p}{rt} \qquad \text{(A.8)}$$

by a virtually identical argument, for the exit side

$$f_o(x) = (h(x))^{-a} \tag{A.9}$$

further application of Equation A.7 gives

(entry side)

$$\int f_i(x)s_i(x)dx = \frac{\sigma_c rt}{L_p} \int (h(x))^{a-1}dx \tag{A.10}$$

$$= \frac{\sigma_c}{a} h(x)^a$$

(exit side)

$$\int f_o(x)s_o(x)dx = \frac{\sigma_c rt}{L_p} \int (h(x))^{-a-1}dx \tag{A.11}$$

$$= -\frac{\sigma_c}{a} h(x)^{-a}$$

combining Equations A.8 through A.11 with Equation A.7 gives

$$p_i(x) = \frac{\sigma_c}{a} + C_i h(x)^{-a} \tag{A.12}$$

$$p_o(x) = C_o h(x)^a - \frac{\sigma_c}{a}$$

Evaluation of the constant C_i and C_o using the boundary conditions $P_i(L_p) = P.(0) = \sigma_c$ gives the desired pressure function, Equation 2.12.

Equation 2.14 (nonplanar arc, slipping friction)

substituting

$$h(X) = t\left[1 - r + \left(\frac{X}{L_p}\right)^n r\right]$$

and

$$\sigma_s(X) = \mu p(X)$$

into Equation 2.8 gives the relevant differential equation:

$$\frac{dp(x)}{dx} \pm \frac{2\mu p(x)}{h(x)} = \frac{\sigma_c n t r}{L_p h(x)} \left(\frac{x}{L_p}\right)^{n-1}$$

where the plus and minus signs apply to the entry and exit regions respectively. Again applying Equation A.7, the integrating factors are given by

(entry region)

$$f_1(x) = \exp\left\{\frac{2\mu}{t}\int \frac{dx}{1 + r\left(\frac{x}{L_p}\right)^n r}\right\}$$

since $r \ll 1$ and $\frac{X}{L_p} < 1$

$$\left(1 - r + \left(\frac{x}{L_p}\right)^n r\right)^{-1} \simeq 1 + r - \left(\frac{x}{L_p}\right)^n r \qquad \text{(A.13)}$$

and

$$f_1(x) \simeq \exp\left\{\frac{2\mu}{t}\int\left[1 + r - \left(\frac{x}{L_p}\right)^n r\right] dx\right\}$$

$$= \exp\left\{\frac{2\mu}{t}\left[(1 + r)x - \frac{L_p r}{n+1}\left(\frac{x}{L_p}\right)^{n+1}\right]\right\}$$

since $r << 1$, $n \geq 1$, and $\frac{x}{L_p} \leq 1$,

$$(1 + r)x \gg \frac{L_p r}{n + 1}\left(\frac{x}{L_p}\right)^{n+1}$$

therefore

$$f_1(x) \simeq e^{bx} \tag{A.14}$$

where

$$b = \frac{2\mu}{t}(1 + r)$$

similarly for the exit region

$$f_o(x) = \exp\left\{\int \frac{-2\mu}{h(x)}\, dx\right\} \simeq e^{-bx} \tag{A.15}$$

(by virtually identical arguments)

Continuing with the standard method for the entry region,

$$\int f_1(x)s_1(x)dx = \int \frac{\sigma_c n t r}{h(x)L_p}\left(\frac{x}{L_p}\right)^{n-1} e^{bx} dx$$

again using approximation A.13 and noting

$r << 1$, $\left(\frac{x}{L_p}\right) \leq 1$, and $n \geq 1$

$$\frac{\sigma_c ntr}{h(x)L_p}\left(\frac{x}{L_p}\right)^{n-1} \simeq \frac{\sigma_c nr}{L_p}\left[(1+r)\left(\frac{x}{L_p}\right)^{n-1} + r\left(\frac{x}{L_p}\right)^{2n+1}\right]$$

$$\simeq \frac{\sigma_c nr(1+r)}{L_p}\left(\frac{x}{L_p}\right)^{n-1}$$

Using the series expansion for e^{bX} thus gives

$$\int f_1(x)s_1(x)dx \simeq \frac{\sigma_c nr(1+r)}{L_p}\int \sum_{k=0}^{\infty}\frac{(bx)^k}{k!}\left(\frac{x}{L_p}\right)^{n-1}dx$$

$$= \sigma_c nr(1+r)\left(\frac{x}{L_p}\right)^{n} S_1(bx) \qquad (A.16)$$

where

$$S_1(bX) = \sum_{k=0}^{\infty}\frac{(bX)^k}{k!(n+k)}$$

Note that the term-by-term integration was permissible, since the series integrated is a power series with infinite radius of convergence, and that $S_1(X)$ converges for all real X and all $n \geq 1$ by the comparison test with the series expansion of e^{bX}.

Similarly for the exit region

$$\int f_0(x)s_0(x)dx = \frac{\sigma_c ntr}{L_p}\int \frac{1}{h(x)}e^{-bx}dx$$

$$\simeq \frac{\sigma_c nr(1+r)}{L_p^{\,n}} \int \sum_{k=0}^{\infty} \frac{(-bx)^k}{k!} x^{n+k-1} dx$$

$$= \sigma_c nr(1+r) \left(\frac{x}{L_p}\right)^n S_2(bx) \qquad (A.17)$$

where

$$S_2(bX) = \sum_{k=0}^{\infty} \frac{(-bX)^k}{k!(n+k)}$$

where the same integration argument applies, and the convergence of $S_2(bX)$ is assured by comparison with the series expansion of e^{-bX}.

Substitution of Equations A.14 through A.17 into Equation A.7 and application of the boundary conditions $P_i(L_p) = P_o(0) = \sigma_c$ gives the deisred pressure function, Equation 2.14.

Equation 2.17 (planar arc, sticking friction)

in this case

$$h(X) = t\left[1 - r + \left(\frac{X}{L_p}\right) r\right]$$

and

$$\sigma_s(X) = \sigma_c/2$$

Von Karman's equation reduces to

$$\frac{dp}{dX} = \frac{\sigma_c}{h(X)} \left[\frac{tr}{L_p} + 1\right]$$

where the plus and minus signs apply (respectively) to the exit and entry regions. These equations can be integrated directly to find p(X). For the entry region

$$p_i(x) = \left[\frac{tr}{L_p} - 1\right] \frac{\sigma_c}{t} \int \left(\frac{t}{h(x)}\right) dx$$

$$= \left[\frac{tr}{L_p} - 1\right] \frac{\sigma_c}{t} \left(\frac{L_p}{r} \ln\left(\frac{h(x)}{t}\right) + C_i \right) \qquad \text{(A.18)}$$

For the exit region

$$p_o(x) = \left[\frac{tr}{L_p} + 1\right] \frac{\sigma_c}{t} \int \left(\frac{t}{h(x)}\right) dx$$

$$= \left[\frac{tr}{L_p} + 1\right] \frac{\sigma_c}{t} \left(\frac{L_p}{r} \ln\left(\frac{h(x)}{t}\right) + C_o \right)$$

Application of the boundary conditions

$p_i(L_p) = P_o(o) = \sigma_t$ determines the values of the constants C_i and C_o and yields Equation 2.17.

A.3 Plastic Roll Force Equations (Equation 2.18)

Plastic roll force is given by

$$f_p = \int_{x_n}^{L_p} p_i(x)dx + \int_0^{x_n} p_o(x)\,dx \qquad (A.20)$$

two cases must be distinguished: slipping friction only (Case I), and combined slipping and sticking friction (Case II).

For Case I, the pressure function is completely determined by Equation 2.12. The middle bound on the integrals in Equation A.20 is determined by the condition

$$p_i(x_n) = p_o(x_n)$$

or

$$\frac{1}{a} + (1 - \frac{1}{a})\left(\frac{t}{h(x_n)}\right)^a = (1 + \frac{1}{a})\left(\frac{h(x_n)}{t(1-r)}\right)^a - \frac{1}{a}$$

in general $a \ll 1$ and $1/a \approx 0$ for temper rolling, giving

$$\left(\frac{t}{h(x_n)}\right)^a \simeq \left(\frac{h(x_n)}{t(1-r)}\right)^a$$

or

$$\left(h(x_n)\right)^2 \simeq t^2(1 - r)$$

which yields $$\left(1 - r + \left(\frac{x_n}{L_p}\right)r\right)^2 \simeq (1 - r)$$

or

$$\frac{x_n}{L_p} r \simeq \sqrt{1 - r} - 1 + r$$

since $r << 1$, $\sqrt{1 - r} \simeq 1 - r/2$ giving

$$x_n \simeq \frac{L_p}{2} \tag{A.21}$$

Equation A.20 thus yields

$$f_p = \sigma_c \left\{ \int_0^{L_p/2} (1 + 1/a) \left(\frac{h(x)}{t(1-r)} \right)^a dx + \int_{L_p/2}^{L_p} (1 - 1/a) t^a \left(h(x)\right)^{-a} dx \right\} \tag{A.22}$$

evaluating integrals,

$$\int_{L_p/2}^{L_p} \left(h(x)\right)^{-a} dx = \left[\frac{-L_p}{tr(a-1)} h(x)^{-(a-1)} \right]_{L_p/2}^{L_p}$$

$$= \frac{L_p t^{-a}}{r(a-1)} \left((1 - r/2)^{1-a} - 1 \right) \tag{A.23}$$

$$\int_0^{L_p/2} \left(h(x)\right)^a dx = \left[\frac{L_p}{tr(a+1)} h(x)^{a+1} \right]_0^{L_p/2}$$

$$= \frac{L_p t^a}{r(a+1)} \left((1 - r/2)^a - (1 - r)^a \right) \tag{A.24}$$

Substituting Equations A.23 and A.24 into Equation A.22 gives the form of Equation 2.18 applicable to Case I.

For Case II, the pressure distribution is given by Equation 2.12 for $0 \leq X \leq X_2$ and $X_1 \leq X \leq L_p$ and by Equation 2.17 for $X_2 < X < X_1$. The relevent expression for f_p must thus be composed of two parts:

$$f_p = f_{stick} + f_{slip} \tag{A.25}$$

where

$$f_{stick} = \int_{x_2}^{x_n} p_o(x)dx + \int_{x_n}^{x_1} p_i(x)dx \tag{A.26}$$

($P_o(X)$, $P_i(X)$ given by Equation 2.17)

$$f_{slip} = \int_{0}^{x_2} p_o(x)dx + \int_{x_1}^{L_p} p_i(x)dx \tag{A.27}$$

($P_o(X)$, $P_i(X)$ given by Equation 2.12)

Before evaluating the necessary integrals, practical approximations must be made. Equation 2.12 gives, for the slipping region,

$$p_i(x) = \Theta_e\left[1/a + (1 - 1/a)\left(\frac{\epsilon}{h(x)}\right)^a\right]$$

$$\approx \Theta_e\left(\frac{\epsilon}{h(x)}\right)^a \tag{A.28}$$

and similarly

$$p_o(x) \simeq \sigma_c \left(\frac{h(x)}{t(1-r)}\right)^a \qquad (A.29)$$

From Equation 2.16, the bounds of the slipping region are given by

$$h(x_1) = t\left[\left(\frac{1}{(1-1/a)}\right)\left(\frac{1}{2\mu} - \frac{1}{a}\right)\right]^{-1/a}$$

$$\simeq t(2\mu)^{1/a} \qquad (A.30)$$

and $$h(x_2) \simeq t(1-r)(2\mu)^{-1/a} \qquad (A.31)$$

The position of the neutral plane is determined by equation 2.17 and the condition $P_i(X_n) = P_o(X_n)$:

$$\left(1 - \frac{a}{2\mu}\right)\ln\left(\frac{h(x_n)}{t}\right) = \left(1 + \frac{a}{2\mu}\right)\ln\left(\frac{h(x_n)}{t(1-r)}\right)$$

or

$$\ln h(x_n) = -\left(\frac{rt}{2L_p}\right)\left[\left(1 - \frac{a}{2\mu}\right)\ln t - \left(1 + \frac{a}{2\mu}\right)\ln\left(t(1-r)\right)\right] \qquad (A.32)$$

Although it is not obvious, this expression invariably gives $X_n = L_p/2$. Returning to Equations A.26 and A.27, the relevant integrals can now be evaluated. In the slipping region,

$$\int_0^{x_2} p_o(x)dx \simeq \sigma_c \int_0^{x_2} \left(\frac{h(x)}{t(1-r)}\right)^a dx$$

$$= \frac{\sigma_c L_p (1-r)}{(1+a)r}\left(\frac{h(x)}{t(1-r)}\right)^a \Bigg]_0^{x_2}$$

$$= \frac{\sigma_c L_p (1-r)}{(a+1)r}\left[\left(2\mu\right)^{-(a+1)/a} - 1\right] \qquad (A.33)$$

$$\int_{x_1}^{L_p} p_i(x)dx \simeq \sigma_c \int_{x_1}^{L_p} \left(\frac{t}{h(x)}\right)^a dx$$

$$= \frac{\sigma_c L_p}{r(1-a)}\left(\frac{h(x)}{t}\right)^{1-a} \Bigg]_{x_1}^{L_p}$$

$$= \frac{\sigma_c L_p}{r(a-1)}\left[\left(2\mu\right)^{(1-a)/a} - 1\right] \qquad (A.34)$$

note that, since $a >> 1$ in rolling rolling, $a+1 \approx a - 1 \approx a$. Equations A.27, A.33, and A.34 thus give

$$f_{slip} \simeq \frac{\sigma_c L_p (2-r)}{ra}\left[\frac{1}{2\mu} - 1\right] \qquad (A.35)$$

We can avoid evaluating the integrals in Equation A.26 explicity by noticing that $\frac{dp(X)}{dX}$ is nearly constant in the sticking region:

$$\frac{dp_o(x)}{dx} = \frac{(1 + L_p/2\mu)tr}{L_p h(x)} \qquad (A.36)$$

where h(X), and thus $\frac{dp(X)}{dX}$, varies by roughly 100r/2 percent. The average pressure in the sticking region is therefore roughly $\frac{1}{2} P_1\left(\frac{L_p}{2} + \frac{\sigma_c}{2\mu}\right)$. Since the length of this region is $X_1 - X_2$, Equation A.27 gives

$$f_{stick} \approx \left(\frac{x_1 - x_2}{2}\right)\left[p_1(L_p/2) + \theta_o/2\mu\right] \qquad (A.37)$$

From Equations A.30 and A.31

$$\frac{x_1 - x_2}{2} \approx \frac{L_p}{2r}\left[(2\mu)^{1/n} - \frac{1 - r}{(2\mu)^{1/n}}\right] \qquad (A.38)$$

From Equations 2.17 and A.30

$$\frac{\theta_o}{2\mu} + p_1(L_p/2) \approx \theta_o\left\{\frac{1}{\mu} + \left(1 - \frac{n}{2\mu}\right)\ln\left(\frac{1 - r/2}{(2\mu)^{1/n}}\right)\right\} \qquad (A.39)$$

Combination of Equations A.25, A.35, A.37, A.38, and A.39 give the form of Equation 2.18 applicable to Case II.

Appendix II

Mill Data

The following data was obtained on the No. 7 84-inch sheet-temper mill at U. S. Steel's Irvin Works. Two sets of dry-temper rolling tests were conducted over a two-week period. In the first set appliance skirt stock (coils 1 through 5) was rolled; autobody sheet (coils 6 through 8) was used in the second set. Physical data for the coils is given in Table A.1; data for the rolls used is given in Table A.2. Table A.3 lists mechanical and surface-transfer data (when available) for all points sampled in these coils. Transfer levels were calculated using the surface properties of the top roll only, since only the top side of the strip could be profiled after rolling. The probable errors in this data are assessed in Section IV.3.

Table A.1

Physical Data for Coils

Coil	Total Footage	Width, (inches)	Initial Thickness, (inches)	0.2% Yield Strength, (psi)	Initial Surface Properties	
					R_a (μ in.)	ppi_{50}
1	4745	36.5	0.0294	39,470	30	65
2	4714	36.5	0.0294	44,600	30	65
3	4106	36.5	0.0294	38,169	30	65
4	4723	36.5	0.0294	38,169	30	65
5	4549	36.5	0.0294	38,578	30	65
6	6752	47.0625	0.032	~39,500	~35	~75
7	4678	47.125	0.032	~36,000	~35	~75
8	5013	47.125	0.032	~36,000	~35	~75

Table A.2

Work-Roll Properties

Set 1 was used for coils 1 through 5;

Set 2 was used for coils 6 through 8.

Roll	Diameter, (inches)	Type Surface	Rockwell C Hardness	Surface Properties* R_a (μin.)	Surface Properties* ppi_{50}
I (top)	25.504	Chrome plated, shot blasted	102	~82.5	~185
I (bottom)	24.795	Chrome Plated, shot blasted	95	~82.5	~185
II (top)	24.165	Steel, shot blasted	-	Coil 6: 59 Coil 7: 57 Coil 8: 56	122 119 116
II (bottom)	24.378	Steel, shot blasted	-	Coil 6: 58 Coil 7: 56 Coil 8: 55	102 98 95

*Linearly corrected for wear (based on linear footage measurements) in the case of steel-surfaced rolls.

Table A.3

Mechanical and Surface-Transfer Data From Production Dry-Temper Mill

Roughness transfer = final strip roughness/roll roughness

Peak count transfer = final strip peak count/roll peak count

Coil Specimen	Footage From Beginning of Coil	Mill Speed ft/min	Extension, %	Specific Rolling Force, lb/in.	Strip Tensions, psi			Roughness Transfer	Peak Count Transfer
					Entry	Exit	Average		
1/1	700	1,209	0.806	19,430	5,691	5,665	5,678	0.86	0.69
1/2	1,600	2,204	0.698	21,205	5,342	6,310	5,826	0.90	0.71
1/3	3,000	2,939	0.693	21,567	5,931	6,919	6,425	0.90	0.66
1/4	4,300	2,136	0.752	21,151	4,680	5,144	4,912	0.86	0.76
2/1	280	1,193	0.781	19,036	1,952	8,279	5,116	-	-
2/2	1,300	2,714	0.687	20,679	3,967	7,658	5,813	-	-
2/3	2,650	2,645	0.677	20,603	5,088	5,161	5,125	-	-
2/4	4,100	2,646	0.687	21,227	2,980	5,841	4,411	-	-
3/1	200	1,207	0.787	21,918	3,317	10,715	7,016	-	-
3/2	1,400	3,163	0.610	23,879	4,412	7,314	5,863	-	-
3/3	2,800	3,171	0.610	23,912	3,606	6,353	4,980	-	-
3/4	4,040	812	0.619	20,778	5,626	3,958	4,792	-	-
4/1	400	2,398	0.666	22,915	1,251	11,351	6,301	0.81	0.64
4/2	1.900	3,168	0.629	23,923	3,865	6,745	5,305	0.84	0.59
4/3	3,400	2,883	0.629	23,770	3,795	5,517	4,656	0.80	0.52
4/4	4,450	1,318	0.725	21,710	6,672	3,596	5,134	0.81	0.64
5/1	300	1,776	0.655	23,753	0	12,173	6,087	-	-
5/2	1,550	3,431	0.526	24,427	3,266	5,852	4,559	-	-
5/3	3,150	3,392	0.500	24,077	4,322	6,725	5,524	-	-
5/4	4,500	1,879	0.526	22,530	5,554	3,397	4,476	-	-

(Continued)

Table A.3

Mechanical and Surface-Transfer Data From Production Dry-Temper Mill
(Continued)

Roughness transfer = final strip roughness/roll roughness

Peak count transfer = final strip peak count/roll peak count

Coil Specimen	Footage From Beginning of Coil	Mill Speed ft/min	Extension, %	Specific Rolling Force, lb/in.	Strip Tensions, psi			Roughness Transfer	Peak Count Transfer
					Entry	Exit	Average		
6/1	200	1,391	0.620	16,985	8,066	23,296	15,681	0.72	0.54
6/2	1,450	2,785	0.467	19,839	9,824	14,254	12,039	0.65	0.47
6/3	2,950	2,767	0.618	19,786	8,672	14,712	11,692	0.73	0.57
6/4	4,250	2,689	0.642	19,513	6,914	14,342	10,628	0.64	0.56
6/5	5,480	1,720	0.582	18,536	8,828	5,057	6,943	0.66	0.56
6/6	6,250	1,664	0.419	18,550	11,953	10,045	10,999	0.72	0.61
7/1	900	2,158	0.703	18,877	8,110	12,944	10,527	0.76	0.63
7/2	2,100	2,477	0.740	20,506	9,543	12,021	10,782	0.78	0.67
7/3	3,400	2,200	0.729	20,011	11,811	11,239	11,525	0.78	0.59
7/4	4,310	1,124	0.752	18,766	11,140	12,209	11,674	0.82	0.71
8/1	1,400	3,231	0.694	22,210	8,945	12,540	10,742	0.77	0.60
8/2	2,900	3,212	0.752	22,267	9,543	10,966	10,255	0.81	0.62
8/3	4,250	1,930	0.881	21,305	6,169	10,925	8,547	0.78	0.55
8/4	4,940	1,251	0.939	20,230	12,954	8,843	10,898	0.71	0.53